TECHNICAL
LIBRARY

CONTRACTOR REPORT ARLCD-CR-81001

BLAST-RESISTANT CAPACITIES OF COLD-FORMED STEEL PANELS

WILLIAM STEA
FREDRICK E. SOCK
AMMANN AND WHITNEY
TWO WORLD TRADE CENTER
NEW YORK, NY 10048

JOSEPH P. CALTAGIRONE
ARRADCOM

MAY 1981

US ARMY ARMAMENT RESEARCH AND DEVELOPMENT COMMAND
LARGE CALIBER
WEAPON SYSTEMS LABORATORY
DOVER, NEW JERSEY

APPROVED FOR PUBLIC RELEASE; DISTRIBUTION UNLIMITED.

AD-A101915

DEPARTMENT OF THE ARMY
US ARMY ARMAMENT RESEARCH AND DEVELOPMENT COMMAND
DOVER, NEW JERSEY 07801

Mr. Caltagirone/ag/AV880-3662

JUL 1 6 1982

REPLY TO
ATTENTION OF:

DRDAR-LCM-SP

SUBJECT: Errata for ARRADCOM Report ARLCD-CR-81001, "Blast-Resistant
Capacities of Cold-Formed Steel Panels"

SEE DISTRIBUTION

Inclosed is an Errata Sheet for the subject report. Please incorporate these

changes in your copy of the report dated May 1981.

FOR THE COMMANDER:

1 Incl
as

LEON. W. SAFFIAN, P.E.
C, Energetic Systems Process Div
for Cdr/Dir, LCWSL

DISTRIBUTION:

Chairman, Department of Defense Explosive Safety Board, Hoffman Building, No. 1,
  Room 856C, 2461 Eisenhower Avenue, Alexandria, VA 22331
Administrator, Defense Documentation Center, ATTN: Accessions Division,
  Cameron Station, Alexandria, VA 22314
Commander, Department of the Army, Office, Chief Research Development and Acqui-
  sition, ATTN: DAMA-CSM-P, Washington, DC 20310
Office, Chief of Engineers, ATTN: DAEN-MCZ, Washington, DC 20314
Commander, US Army Materiel Development and Readiness Command, ATTN: DRCSF,
  DRCDE, DRCRP, DRCIS, 5001 Eisenhower Avenue, Alexandria, VA 22333
Commander, DARCOM Installations and Services Agency, ATTN: DRCIS-RI, Rock
  Island, IL 61299
Director, Industrial Base Engineering Activity, ATTN: DRXIB-MT, DRXIB-EN,
  Rock Island, IL 61299
Commander, US Army Munitions Production Base Modernization Agency, ATTN:
  SARPM-PBM, SARPM-PBM-S, SARPM-PBM-L, SARPM-PBM-E, Dover, NJ 07801
Commander, US Army Armament Materiel Readiness Command, ATTN: DRSAR-SF, DRSAR-SC,
  DRSAR-EN, DRSAR-PPI, DRSAR-PPI-C, DRSAR-RD, DRSAR-IS, DRSAR-ASF, DRSAR-LEP-L,
  Rock Island, IL 61299
Director, DARCOM Field Safety Activity, ATTN: DRXOS-ES, Charlestown, IN 47111
Commander, US Army Engineer Division, ATTN: HNDED, P.O. Box 1600, West Station,
  Huntsville, AL 35809

ARLCD-CR-81001

BLAST RESISTANT CAPACITIES

OF

COLD-FORMED STEEL PANELS

JULY 12, 1982

E R R A T A

P. 67: Eq. (A.5) should be:

$$r_u = 4(M_{un} + 2M_{up})/L^2$$

P. 68: Line 7 should be:

I_{20} is defined as the moment of inertia of

P. 69: Eq (A-9) should be:

$$T_N = 2\pi \sqrt{0.74mL/K_E}$$

P. 76: Lines 3 and 4 should be:

$$Q_u = 1.5t^2 F_y(4.44 + 0.558 \sqrt{N/t})$$

$$= 90t^2(4.44 + 0.558 \sqrt{N/t}) \text{ ksi}$$

P. 77: Lines 3 and 4 should be :

$$Q_u = 1.5t^2 F_y(6.66 + 1.446 \sqrt{N/t})$$

$$= 90t^2(6.66 + 1.446 \sqrt{N/t}) \text{ ksi}$$

P. 78: Lines 3 and 4 should be:

$$Q_u = 1.5t^2 F_y(4.44 + 0.558 \sqrt{N/t})$$

$$= 120t^2(4.44 + 0.558 \sqrt{N/t}) \text{ ksi}$$

P. 79: Lines 3 and 4 should be:

$$Q_u = 1.5t^2 F_y(6.66 + 1.446\sqrt{N/t})$$

$$= 120t^2(6.66 + 1.446 \sqrt{N/t}) \text{ ksi}$$

P. 91: Step 6 (Equation A.5) Line 6 should be:

$$r_u = (4/L^2) (2M_{up} + M_{un})$$

P. 91: Step 7 (Equation A.6) Line 2 should be:

$$K_E = r_u L/X_E$$

Step 7 (Equation A.6) Line 3 should be:

$$= (EIr_u L)/(0.0062r_u L^4)$$

P. 92: Step 10: Line 5 should be:

$$\tan \theta = X_M/(L/2) = 0.028/2.25 = 0.012$$

Step 10: Line 6 should be:

$$\theta = 0.70^o < 2.0^o \quad OK$$

REPORT DOCUMENTATION PAGE	READ INSTRUCTIONS BEFORE COMPLETING FORM	
1. REPORT NUMBER CONTRACTOR REPORT ARLCD-CR-81001	2. GOVT ACCESSION NO.	3. RECIPIENT'S CATALOG NUMBER
4. TITLE (and Subtitle) BLAST-RESISTANT CAPACITIES OF COLD-FORMED STEEL PANELS	5. TYPE OF REPORT & PERIOD COVERED Final	
	6. PERFORMING ORG. REPORT NUMBER	
7. AUTHOR(s) William Stea and Fredrick E. Sock, Ammann & Whitney Joseph P. Caltagirone, ARRADCOM	8. CONTRACT OR GRANT NUMBER(s) DAAK10-77-C-0134	
9. PERFORMING ORGANIZATION NAME AND ADDRESS Ammann & Whitney, Consulting Engineers Two World Trade Center New York, NY 10048	10. PROGRAM ELEMENT, PROJECT, TASK AREA & WORK UNIT NUMBERS MMT - 5794291	
11. CONTROLLING OFFICE NAME AND ADDRESS ARRADCOM, TSD ATTN: STINFO Div (DRDAR-TSS) Dover, NJ 07801	12. REPORT DATE MAY 1981	
	13. NUMBER OF PAGES 116	
14. MONITORING AGENCY NAME & ADDRESS(if different from Controlling Office) ARRADCOM, LCWSL ATTN: Energetic Systems Process Div (DRDAR-LCM-SP) Dover, NJ 07801	15. SECURITY CLASS. (of this report) Unclassified	
	15a. DECLASSIFICATION/DOWNGRADING SCHEDULE	

16. DISTRIBUTION STATEMENT (of this Report)

Approved for public release; distribution unlimited.

17. DISTRIBUTION STATEMENT (of the abstract entered in Block 20, if different from Report)

18. SUPPLEMENTARY NOTES

This project was accomplished as part of the U.S. Army's Manufacturing Methods and Technology Program. The primary objective of this program is to develop, on a timely basis, manufacturing processes, techniques, and equipment for use in production of Army materiel.

19. KEY WORDS (Continue on reverse side if necessary and identify by block number)

MMT - blast effects	Steel structures
Cold-formed steel panels	Blast resistance
Blast capacity	Pre-engineered buildings
Metal panels and decking	Structural components

20. ABSTRACT (Continue on reverse side if necessary and identify by block number)

Cold-formed steel panels are widely used in the construction of steel structures and pre-engineered buildings at explosives manufacturing and storage facilities. The behavior of these panels differs significantly from that of the hot-rolled structural members due to the large width-to-thickness ratios of the elements that constitute their cross-sections.

(Continued)

DD FORM 1473 EDITION OF 1 NOV 65 IS OBSOLETE

20. ABSTRACT (Cont)

In an earlier project designed criteria were established for cold-formed steel panels. This report documents subsequent tests which were performed to verify or refine these design criteria. The actual tests were conducted at the Dugway Proving Ground, UT.

The accumulated data indicated that the increased strength observed in the test panels was due to the actual static stresses (which exceeded the minimum stress at yield of 227,500 kPa (33,000 psi).

The tests revealed that the maximum ductility ratio criteria of 1.25 for usable structures and 1.75 for non-reusable structures can be increased to 3.0 and 6.0, respectively. Other determinations included: (1) the total moment of inertia should be substituted for the effective moment of inertia when calculating the natural period and elastic deflections (2) open hat shape panels can be used for closed sections in low pressure ranges, and (3) standard screw-type connections performed adequately in blast tests up to 34.5 kPa (5 psi).

SUMMARY

Cold-formed steel panels are widely used in the construction of steel structures and pre-engineered buildings at explosives manufacturing and storage facilities. The behavior of these panels differs significantly from that of the hot-rolled structural members due to the large width-to-thickness and depth-to-thickness ratios of the elements that constitute their cross-sections.

For design purposes, effective utilization of the bending properties of cold-formed sections is obtained by accounting for the post-buckling strength of stiffened compression flanges. This concept, substantiated by numerous tests, is implemented in the AISI Specification for the Design of Cold-Formed Steel Structural Members (ref 1). This specification provides all the necessary guidelines for the design of cold-formed steel panels for static loads. However, additional provisions are required for the blast-resistant design of such panels.

This report was developed as part of the overall effort by the Energetic Systems Process Division of the Large Caliber Weapons Systems Laboratory, ARRADCOM, to verify or refine the design criteria presented in the report titled "Design of Steel Structures to Resist the Effects of HE Explosions" (ref 2). The actual tests were conducted in February 1976 at the White Sage East Test Facility of Dugway Proving Ground, Utah.

The testing program consisted of a series of seven tests that were performed on single-span and three-span continuous panels mounted in four wooden cubic structures. Overpressures produced by detonating 900 kilograms (2,000 pounds) of propellant ranged from 2.07 kPa (0.3 psi) to 103.4 kPa (15 psi) on the panels. Specially mounted transducers measured blast overpressures and two high-speed motion picture cameras recorded any transient motion in the tests.

The program included tests with both types of cold-formed steel panels; specifically, open sections (two flat sheets, one of which was formed into a series of hat sections). The four wooden box-like structures, arranged in two different configurations, were used to support the test panels throughout the program. The explosives used in the tests were M26E1 and T28E1 artillery-type propellants as the primary charges, and Composition C-4 as the booster charge.

The test results are presented in terms of visual observations, photographs of structural damage, measurements of permanent deformations of the test panels, pressure histories recorded by the gages, and overpressures at the four test structures. Tabular arrangements are also presented to further document the results.

The accumulated data indicated that the increase strength observed in the test panels was due to the actual static stresses [which exceeded the minimum stress at yield of 227,500 kPa (33,000 psi)]. It was further determined that the flexural resistances of a simply fixed panel or a continuous panel of equally spaced spans should be computed using the following equation in lieu of equation 3.25 of reference 2:

$$r_u = 4(M_{un} + 2M_{up})/L^2$$

where r_u is the resistance per unit length of the panel, M_{un} is the ultimate negative moment capacity for one-foot width of panel, and M_{up} is the ultimate positive moment capacity for one-foot width of panel.

The tests revealed that the maximum ductility ratio criteria of 1.25 for usable structures and 1.75 for nonreusable structures can be increased to 3.0 and 6.0, respectively. Other determination included: (1) the total moment of inertia should be substituted for the effective moment of inertia when calculating the natural period and elastic deflections (2) open hat shape panels can be used for closed sections in low pressure ranges, and (3) standard screw-type connections performed adequately in blast tests up to 34.5 kPa (5 psi).

CONTENTS

TABLES

FIGURES

INTRODUCTION

Background

Cold-formed steel panels are widely used for roof and floor decking, as well as for wall siding, in the construction of steel structures and pre-engineered buildings at explosives manufacturing and storage facilities. These panels are constructed from thin sheets which are formed into various cross-sections such as those shown in figure 1. Sheet thicknesses utilized for the construction of cold-formed steel panels vary from 12 to 24 gage. The behavior of these panels differs significantly from that of hot-rolled structural members (such as wide flange beams) due to the cross-sectional shapes and to the large width/thickness and depth/thickness ratios of the elements (flanges, webs) which make up the cross-sections. Under static loading, the load deflection curves for a cold-formed steel panel is markedly non-linear and strongly dependent on the extent of local instabilities. For design purposes, effective utilization of the bending properties of cold-formed sections is obtained by accounting for the post-buckling strength of stiffened compression flanges. This concept, substantiated by numerous tests, is implemented in the AISI Specification for the Design of Cold-Formed Steel Structural Members (ref. 1). This specification provides all the necessary guidelines for the design of cold-formed steel panels for static loads. However, additional provisions are required, for the blast-resistant design of such panels.

The economy of blast-resistant design requires that protective structures be designed to perform in the inelastic response range when subjected to blast loads. However, standard plastic design techniques are not directly applicable to cold-formed construction. This is due to the fact that the width/thickness and/or the depth/thickness ratios utilized in cold-formed sections are generally greatly in excess of the limits imposed by the requirements for plastic hinge formation. However, for the purpose of blast design of cold-formed steel panels, it is possible to account for a limited, but definite amount of plastic behavior. The amount of plastic deformation which is acceptable will vary in magnitude depending on the function of a given structure and its intended reusability or non-reusability after an accidental explosion.

ARRADCOM has developed criteria for the inelastic design of cold-formed sections subjected to blast overpressures. This criteria is presented in detail in reference 2 and includes equations for ultimate moment capacities, ultimate resistances,

1

stiffnesses, periods of vibration, shear stresses, support reactions, and rebound effects for single and continuous spans. In order to verify or refine these design criteria and determine the blast load capacities of various panel sections and connection details, a test program was undertaken by the Energetic Systems Process Division of the Large Caliber Weapons Systems Laboratory, ARRADCOM, as part of its overall Safety Engineering Support Program for the Project Manager for Production Base Modernization and Expansion. This report summarizes and evaluates the results and presents recommended changes to more fully utilize the blast capacity of cold-formed steel panels.

Purpose and Objectives

The overall purpose of the test program was to evaluate and refine the criteria and procedures provided in reference 2 for the blast-resistant design of cold-formed steel panels. The objectives of the test program are summarized below:

1. To evaluate the blast capacities of cold-formed steel panels having both closed (hat section with flat sheet) and open hat type cross-sections.

2. To evaluate the dynamic load capacities of various panel connection details.

Format and Scope of Report

The following section describes the test program including the test procedures and results. The next section contains evaluations of the test results and the current procedures (provided in ref. 2) for the blast-resistant design of cold-formed steel panels. Appendix A contains proposed revisions to the methods and procedures of reference 2 pertaining to the blast design of cold-formed steel panels. Utilization of the revised design procedure is illustrated by a sample problem. Appendix B contains reproductions of the test structures, test specimens and testing plans.

Since future standards of measurement in the United States will be based upon the SI Units (International System of Units) rather than the United States System now in use, all measurements presented in this report will conform to those of the SI System. However, for those persons not fully familiar with the SI Units, United States equivalent units of the particular test data are presented in parentheses adjacent to the SI Units.

2

TEST DESCRIPTION

General

Blast tests of cold-formed steel panels were performed as part of the dynamic glass tests (ref. 3) at the White Sage East Test Facility of Dugway Proving Ground (DPG), Utah. The tests were conducted in February 1976 under the direction of ARRADCOM. A total of seven tests were performed on single-span and three-span continuous panels mounted in four wooden box-like structures. The test panels were subjected to overpressures ranging from 2.07 kPa (0.3 psi) to 103.4 kPa (15 psi). The positive phase duration of the overpressure was about 50 milliseconds in each test. The blast loads were produced by detonating 900 kilograms (2,000 pounds) of propellant.

The quantities measured during the testing consisted of the free-field overpressure at various distances from ground zero. In addition, permanent deformations of the test panels were measured when they occurred. Photographic documentation consisted of still photographs to record structural damage after each test as well as high-speed motion pictures to document each shot. Reference 4, which describes the test program, was prepared by Dugway Proving Ground for documentation purposes and was used freely in the preparation of this section of the report.

Test Panels

Cold-formed steel panels are manufactured in either open sections forming continuous corrugations or closed sections consisting of two flat sheets, one of which is formed into a series of hat sections. The formed and flat sheets of the closed section panels are shop-welded together. Both types of panel cross-sections were tested although the provisions of reference 2 specify that only closed-type cross-sections are to be used in blast-resistant construction.

The types and sizes of panels tested are shown in table 1. The Section 3, UKX and NKX sections, are manufactured by the H.R. Robertson Company of Pittsburgh, Pennsylvania. These panel sections are used in conventional buildings as roof and floor decking. The 4-inch ribbed panel, manufactured by the Elwin G. Smith Division of the Cyclops Corporation of Pittsburgh, Pennsylvania, is used for siding. All of these panel types were manufactured from galvanized steel sheet conforming to ASTM A 446, Grade A. This material has a specified minimum yield stress of 227,000 kPa (33 ksi). Similar cold-formed sections are

produced and marketed by companies other than the previously mentioned corporations.

Test Structures

Four wooden box-like structures of two different configurations were used to support the test panels throughout the test program. Engineering drawings showing the framing plans, sections, and details of the test structures are provided in appendix B. A photograph showing the interior framing of one of the test structures is shown in figure 2. The four test structures were fabricated in the shop and towed to the test site by a tractor (fig. 3). At the test site, the structures were labeled for identification and positioned at various locations from the explosives in order to subject them to certain predetermined pressure levels. Once in position, the test structures were anchored by steel rods (fig. 4) driven into the ground.

Two of the test structures (designated as Structures A and B) were 5.18 meters (17 feet) long by 2.13 meters (7 feet) wide and 2.44 meters (8 feet) high. A photograph of Structure B is shown in figure 5. These structures were also utilized to test glass window panes. These structures were designed to withstand approximately 27.6-kPa (4-psi) overpressure. Steel panels were mounted to the roof of each structure. The roof test panels were three-span continuous members 4.57 meters (15 feet) long by 1.22 meters (4 feet) wide. Each span of a roof panel was 1.52 meters (5 feet) long. In addition, single-span test panels each 1.37 meters (4 feet 6 inches) long by 1.22 meters (4 feet) wide, were mounted to the blastward face of Structure B. The blastward face of Structure A was used to test a glass window pane instead of a steel panel.

The other two test structures (designated as Structures C and D) were low wooden support structures which were utilized to test three-span panels at higher overpressures. A photograph of one of these structures is shown in figure 6. The panel sizes utilized with these structures were the same as those mounted on the roof of Structures A and B.

The four wooden test structures were provided with steel beams to support the test panels. The test panels were not attached directly to the support beams; instead, they were connected to support plates which were bolted to the flanges of the support beams.

4

Panel Connections

Each 1.22-meter (4-foot) wide test panel was constructed
from two standard 0.61-meter (2-foot) wide panels which were
fastened together by either seam welds or sheet metal screws.
Attachment of the test panels to the support plates was
accomplished utilizing puddle welds, welded bolts or self-tapping
screws. Table 2 contains a schedule of the connection types used
on the various test panels. A drawing showing the quantities and
locations of the various connections on the test panels is
provided on page 96 of appendix B.

Puddle welding of the test panels to the support plates was
accomplished by drilling or punching a hole in the panel the same
size as the prescribed weld (see fig. 7). The hole was filled
with weld in order to secure the panel to the support plates. A
typical puddle weld connection is shown in figure 8. Weld sizes
utilized are given in table 2. Oblong welds, 15.9 millimeters
(5/8 inch) wide by 25.4 millimeters (1 inch) long, were utilized
at the center seams [laps of 0.61-meter (2-foot) sections] and
along the outer edges of the test panels because the lips
provided at the edges of each panel section (for joining adjacent
sections) reduced the width of the panel valley (bottom of hat
section) to 19 millimeters (3/4 inch).

Details of the bolt and screw connections are shown in
figure 9. The original test plan (see page 98 of appendix B)
provided for the use of Nelson-threaded welded studs to fasten
some of the test panels to the support plates. However, the
studs were not available in time for inclusion into the test plan
and threaded machine bolts were inserted in holes through the
support beams and plates, and spot-welded in position. In
addition, the 15.9-millimeter (5/8-inch) long, No. 14 hexagon
head, self-tapping screws specified in the test plan were not
available for the test and 19-millimeter (3/4-inch), No. 14
panhead self-tapping screws were used in their place.

Propellants

The charges used in this test program were M26E1 and T28E1
artillery-type propellants as the primary charges, and
Composition C-4 as the booster charge. A typical charge is shown
in figure 10. The M26E1 and T28E1 propellants are both
multi-perforated propellants with webs of 0.97 millimeter (0.038
inch) and 1.04 millimeters (0.041 inch), respectively. The
combined weight of the primary charges and the booster in each
test was approximately 900 kilograms (2,000 pounds) with the
booster weighing approximately 20 kilograms (45 pounds). The

5

propellant used was delivered to the site of the fiberboard shipping containers with a net weight of approximately 73 kilograms (160 pounds) each.

The total charge was held in a 1.0-meter (39-inch) cube container (fig. 11) constructed from 19.0-millimeter (3/4-inch) thick plywood, two-by-fours, and strengthened by 13.0-millimeter (1/2-inch) wide steel strips. The Composition C-4 booster was primed with two electric detonators which initiated detonation of the entire charge as illustrated in figure 12.

The location of the test structures was determined on the basis of predictions developed from TNT equivalency tests performed on M26E1 propellant by the IIT Research Institute for ARRACDOM (ref. 5), and on blast pressure data recorded during the test program.

Instrumentation

Blast overpressures were measured with Susquehanna ST-7 transducers housed in integral ballistic probes. Each instrument was mounted in an adjustable pipe stand, as illustrated in figure 13, to facilitate positioning and orientation. Five instruments were used to form a blast line from which the overpressure at each structure was determined. Blast pressure data were recorded on Biomation transient-wave recorders, then transferred to a magnetic tape through a Quad-Systems interface. The magnetic tapes were subsequently reduced by a Hewlett-Packard 2100 computer to obtain the digitized pressure-versus-time history. In addition, the data recorded by the Biomation transient-wave recorders were also photographically recorded. These photographs are provided in appendix A of reference 4.

Photographic Coverage

Two high-speed motion picture cameras operating at speeds up to 1,000 frames per second were used to document any unusual effects or transient motions of the test structures produced by the explosion and the resulting blast loads. In addition, still photographs were taken before and after each test to document the test set-up and to record damage to the test structures and to the panels affixed to those structures.

General Description of Tests

A total of seven tests were conducted to determine the blast-resistant capacities of the test panels. The explosive charge weight and the location of Ground Zero were held constant for all tests, while the four test structures were positioned at predetermined distances from the explosive to achieve the desired blast loading on the test panels. Figures 14 through 20 show the orientations and locations of the test structures and pressure gages with respect to Ground Zero.

After each detonation, the cold-formed panels and the test structure were inspected for damage. Still photographs and physical measurements were taken to document the damage. The explosion area was examined for propellant residue and the crater dimensions were measured and recorded.

Preparation of the site and the test structures for each subsequent test included replacing damaged panels, repairing the test fixtures, filling the crater created by the explosion, and leveling Ground Zero. The blast gages were fixed into new positions and the measuring instruments were checked and calibrated for a new pressure range. The test structures were moved closer to Ground Zero after each test in order to subject the test panels to gradually increasing overpressures.

During Test Series I of the glass tests (ref. 3), it was suspected that an air cushion was developing between each glass pane and the plywood plank behind it when the glass deflected. It was theorized that the effect of the air cushion was to reduce the net loading on the glass, thereby allowing the glass to withstand larger-than-anticipated blast loads. To eliminate the air cushion effect, 0.18-meter (7.0-inch) diameter holes were cut in the plywood planks behind the glass panes in order to vent any pressure build-up behind the glass. Prior to the installation of the first series of test panels, 0.18-meter (7.0-inch) holes were also made in the plywood paneling behind the test panels for the same purpose. However, as the test program progressed, it was determined that venting behind the panels was not required and the holes were boarded over when the first series of test panels were removed from the test structures.

Test Results

General

The test results are presented in terms of visual observations and photographs of structural damage, measurements of permanent deformations of the test panels, pressure histories

recorded by the pressure gages, and overpressures at the four test structures. A summary of the test results is provided in tables 3 through 5. Descriptions of the results are provided below.

Pressure Measurements

Table 3 summarizes the maximum overpressures recorded by the five pressure gages. Included also are the positive phase durations as well as the actual and scaled distances from the charge to each pressure gage. There was some difficulty encountered in achieving the desired blast loads on the test structures. It had been planned to position the test structures and pressure gages on the basis of the data provided in reference 5. However, the pressures measured in test no. 1 were significantly lower than the values expected. Therefore, in subsequent tests, the test structures and pressure gages were positioned using the pressure data generated in the previous tests. Consequently, the positioning of the structures and gages was essentially a trial-and-error procedure until test no. 5 when there was sufficient data available from the previous four tests to yield accurate predictions of the pressures occurring at various distances from Ground Zero.

The measured pressure-versus-time records deviated somewhat from an idealized pressure history (such as the one shown in ref. 6) produced by the detonation of an explosive material. A typical pressure-versus-time history recorded is shown in figure 21. Note that the first half of the record (from 38.4 to 64.0 milliseconds) closely resembles the positive phase of an idealized pressure-versus-time history. However, at 64 milliseconds, there is a disturbance in the record which is characterized by a rapid build-up to a second peak pressure. The disturbance shown in the figure was observed in the recorded pressure histories throughout both the glass and cold-formed panel test programs. In some cases, the second peak pressure equaled and even exceeded the initial peak pressure. It is believed that the occurrence of these "second peaks" can be attributed to the use of artillery-type propellants to produce the blast pressures on the test specimens, and to the use of cubical charges instead of spherical or cylindrical charges.

The overpressures at the four test structures were determined by interpolating the recorded pressure data. The measured pressure data were plotted versus distance to charge, as shown in figure 22. Curves were fitted to the raw data (as shown in the figure) and the pressures at the test structures were read off the curves for the appropriate distance to the charge. The pressures at the test structures are given in tables 4 and 5.

Test No. 1

A 4-inch rib, 24-gage panel was installed on the roof of Structure A while UKX 20-20 gage roof panels were installed on the roof of Structures B and C. Structure D was used to test a NKX 20-20 gage roof panel. In addition, a NKX 16-16 gage was installed on the blastward face of Structure B. The expected pressures were 3.4 kPa (0.5 psi), 13.8 kPa (2.0 psi), 20.7 kPa (3.0 psi) and 27.6 kPa (4.0 psi) at Structures A, B, C and D, respectively. The actual pressures of 2.07 kPa (0.3 psi) at Structure A, 6.89 kPa (1.0 psi) at Structure B, 10.34 kPa (1.5 psi) at Structure C and 13.79 kPa (2.0 psi) at Structure D were considerably lower than the expected values. The positive phase durations were 42.0 ms at Structure A, 48 ms at Structure B and 50 ms at Structures C and D. There was no damage to any of the steel panels.

Test No. 2

The panels used for test no. 1 were left in-place and the four test structures were moved closer to Ground Zero in a second attempt to obtain pressure levels of 3.4 kPa (0.5 psi), 13.8 kPa (2.0 psi), 20.7 kPa (3.0 psi) and 27.6 kPa (4.0 psi) at Structures A, B, C and D, respectively. The recorded overpressures of 2.14 kPa (0.31 psi), 8.27 kPa (1.2 psi) and 19.99 kPa (2.9 psi) for Structures A, B and D, respectively, were significantly lower than the desired values; whereas the overpressure of 13.1 kPa (1.9 psi) recorded for Structure C was nearly equal to the predicted value. Post-test observations revealed that none of the panels had sustained damage.

Test No. 3

Structures A and B, with the same panels utilized in the previous two tests, were relocated closer to Ground Zero where overpressure levels of 4.8 kPa (0.7 psi) at Structure A and 20.7 kPa (3.0 psi) at Structure B were expected. The actual pressures occurring at Structures A and B were 5.38 kPa (0.78 psi) and 15.86 kPa (2.3 psi), respectively. The UKX 20-20 gage panel on the roof of Structure C was replaced with a UKX 18-18 gage panel and the structure was relocated closer to Ground Zero where an overpressure level of 27.6 kPa (4.0 psi) was expected. Structure D, with the NKX 20-20 gage roof panel undamaged from the previous tests, was relocated closer to the charge in order to expose the test panel to an overpressure of approximately 34.5 kPa (5.0 psi). Overpressures recorded for Structures C and D were 21.37 kPa (3.1 psi) and 27.58 kPa (4.0 psi), respectively.

None of the five test panels were damaged when subjected to the pressures recorded in this test.

Test No. 4

Since none of the test panels sustained any damage in test no. 3, they were left in-place and the four test structures were relocated closer to Ground Zero to achieve the following overpressures: 13.8 kPa (2.0 psi) at Structure A, 27.6 kPa (4.0 psi) at Structure B, 34.5 kPa (5.0 psi) at Structure C and 41.4 kPa (6.0 psi) at Structure D.

The overpressures recorded were 8.96 kPa (1.30 psi), 21.37 kPa (3.1 psi), 27.58 kPa (4.0 psi) and 38.61 kPa (5.6 psi) at Structures A, B, C and D, respectively. As was the case with the three prior tests, no damage was inflicted on any of the test panels.

Test No. 5

The five panels tested in the previous trial were left in-place and the four test structures were moved to Ground Zero in order to subject the panels to higher blast loads. After being relocated, the four structures were subjected to the following overpressures in test no. 5: 13.79 kPa (2.0 psi) at Structure A, 31.03 kPa (4.5 psi) at Structure B, 38.61 kPa (5.6 psi) at Structure C and 46.16 kPa (7.0 psi) at Structure D. At these overpressure levels, all of the test panels sustained some damage. Typical panel damage consisted of permanent deflections as well as local buckling at the midspans of the various test sections and kinking at the interior supports of the three-span roof panels. The Cyclops panel on the roof of Structure A suffered a maximum deflection of 19.1 millimeters (0.75 inch) in the exterior span nearest the explosion (fig. 23) as well as kinks at the interior supports (fig. 24). Similar damage was observed on the UKX 20-20 panel and the NKX 20-20 test panels on the roofs of Structure B and D, respectively. Maximum permanent deflections recorded were 19.1 millimeters (0.94 inch) for the NKX panel. The simply-supported UKX 16-16 panel on the blastward face of Structure B sustained a permanent deflection of 12.7 millimeters (0.50 inch) together with considerable local buckling of the raised portion of the hat section as shown in figure 25. The UKX 18-18 panel on Structure C had negligible damage. There was no visible damage to any of the connections. Structures A and B sustained some damage during this test. The plywood backing for the window frame openings were blown inward and the boards covering the 0.18-meter (7.0-inch) vent holes on one of the window frame openings on Structure B were blown off.

Although the damage resulted in some pressure leakage into Structures A and B, it is believed that the peak panel responses would have occurred before a significant internal pressure build-up took place. There was also evidence of movement of Structure B during the test as shown in figure 26.

Test No. 6

The test panels on Structures A, B and D were replaced with new test specimens, while the UKX 18-18 panel remained on Structure C. The Cyclops panel on the roof of Structure A was replaced with a section 3-22 panel. A section 3-18 and a UKX 18-18 were installed on the roof and blastward wall of Structure B, and Structure D was fitted with a new NKX 20-20 panel in place of the one used in test no. 5. The four test structures were moved closer to Ground Zero as shown in figure 19. The overpressures at the four structures were 22.06 kPa (3.2 psi), 31.03 kPa (4.5 psi), 48.95 kPa (7.1 psi) and 65.5 kPa (9.5 psi) at Structures A, B, C and D, respectively. The panels on Structures A, B and D sustained significant damage, while the panel on Structure C received no additional damage. The damage observed was similar to that which occurred in test no. 5. The section 3-22 panel on the roof of Structure A sustained a 33.2-millimeter (1.31-inch) deflection in the blastward span as well as kinks at the interior supports. The section 3-18 panel on the roof of the UKX 18-18 panel on the blastward wall of this structure was severely damaged (fig. 27) and was left with permanent midspan deflections of upwards of 63.5 millimeters (2.5 inches). The NKX 20-20 on Structure D was also severely damaged as shown in figure 28. A maximum permanent deflection of 44.5 millimeters (1.75 inches) was measured in the blastward span. As was the case in test no. 5, there was no damage to any of the connections.

Test No. 7

Structures A, B and D were fitted with new panels for the final test. A Sec. 3-20 panel was installed on the roof of Structure A, while Sec. 3-20 and Sec. 3-18 panels were installed on the roof and blastward wall of Structure B. A NKX 18-18 was installed on Structure D. The four test structures were relocated to the positions shown in figure 20 where overpressures of 31.03 kPa (4.5 psi), 38.61 kPa (5.6 psi), 75.84 kPa (11.0 psi) and 103.35 kPa (15.0 psi) occurred at Structures A, B, C and D, respectively. All of the test panels received damage similar to that which occurred in the previous two tests. The maximum permanent deflections recorded were: 28.6 millimeters (1.13 inches) on the roof panel of Structure A; 47.8

millimeters (1.88 inches) on the roof and wall panels installed on Structure B; 31.8 millimeters (1.25 inches) on the UKX 18-18 panel on Structure C, and 15.9 millimeters (0.63 inch) on the panel mounted on Structure D. Damage to the roof panels of Structures B and C is shown in figures 29 and 30, respectively. All of the panel connections survived the blast pressures undamaged. The plywood backing for one of the window frame openings on Structure A was blown inward.

EVALUATION OF TEST RESULTS

Introduction

An evaluation of the test results indicated that the test panels exhibited considerably greater blast capacities than those predicted by the procedures and criteria provided in reference 2. Specifically, the strengths exhibited by the test panels were significantly greater than their computed strengths. Furthermore, as illustrated in figures 23 through 30, the test panels were able to sustain larger than anticipated plastic deformations without suffering severe damage or complete failure. It is conceivable that the damaged panels may have been able to withstand even greater pressures. It was also apparent that open type cross-sections performed as well under the blast loads as closed type cross-sections. Further discussions of the above conclusions are contained in the remainder of this section. In addition, recommendations are set forth for revising the criteria and procedures of reference 2 for the design of cold-formed steel panels. Details of the modified criteria and procedures are provided in appendix A.

Increased Strength of Test Panels

General

It became apparent during the Test Program that the test panels possessed considerably greater strength, in both flexure and shear, than that predicted by the procedures provided in reference 2, for the design of cold-formed steel panels. In the first four tests, the panels were subjected to pressures considerably greater than their computed blast resistances without sustaining any permanent deformations. In tests nos. 5 through 7, the deformations sustained by the panels were far less than those predicted by current design procedures. To illustrate this point, analyses of the damaged panels were performed to determine their peak responses when subjected to the actual blast pressure acting on them during the tests. These pressures are given in tables 4 and 5. Since there were no measurements of the actual pressure-versus-time histories on the test structures, as well as inconsistencies in the recorded pressure histories, the positive phase durations of the incident pressures had to be extrapolated, utilizing the measured pressure data available together with the methods and data provided in chapter 4, reference 6.

Extrapolation for the blast load durations proceeded in the following manner. First, an equivalent scaled distance, Z_E,

was determined for each test structure (in each of the tests). This quantity was determined by reading off of the appropriate curve in figure 4-12 of reference 6, the value of Z corresponding to the incident pressure at the structure (given in either table 4 or 5). Next, an equivalent charge weight was computed by dividing the actual distance (R) from the test structure to Ground Zero by the equivalent scaled distance, Z_E, and cubing the result [$W_E = (R/Z_E)^3$]. Then, the scaled incident impulse, corresponding to the incident pressure at the structure, was read off the curves in figure 4-12 (ref. 6) and the incident impulse was computed by multiplying this scaled impulse by the cube root of the equivalent charge weight. From this, an estimate of the positive phase duration was computed by assuming a linear decay and then dividing the incident impulse by the peak positive incident pressure and multiplying the result by a factor of two ($2i_s/P_{so}$).

The procedures given in reference 2 were utilized to compute the flexural resistances and equivalent stiffnesses for the analyses of the damaged panels. The loading for the analyses of the roof panels consisted of a linear approximation of the incident pressure waveform that was computed as described above. A piecewise linear (bilinear) waveform was used for analyzing the wall panels. This loading consisted of a linear approximation to the reflected pressure pulse (with a duration equal to the clearing time) superimposed on the incident pressure waveform.

The computed responses of the damage panels are given in table 6, in terms of the permanent deflection in the end span of each roof panel and at the mid-span of each wall panel. Note that in some cases, especially those involving the Section 3 panels, the predicted deflections are excessive and would signify failure of the test panels. The absence of any panel failures, as well as the smaller permanent deflections recorded for the actual test specimens (in tables 4 and 5), support the conclusion that the strength of the test panels greatly exceeded that predicted by the procedures in reference 2. The disparity between exhibited and predicted panel strengths was attributed to two causes. First, from tensile tests it was realized that the actual yield strength of the material used to fabricate the panels was considerably greater than its specified minimum yield strength. Second, the test panels were able to sustain significant yielding of their cross-sections under the dynamic loading. This produced an increase in the ultimate moment capacities of the panels which yielded a corresponding increase in their flexural resistances. Therefore, future selections of panels should consider:

14

1. The actual yield stresses of the materials used to fabricate the panels, and

2. The ability of cold-formed steel panels to sustain yielding of their cross-sections when subjected to short duration dynamic loads.

Effects of Actual Strength of Panel Material

As stated in reference 2, the blast-resistant design of cold-formed steel panels is based on the minimum yield stress of the material used to fabricate them. Since most commercially available panels are fabricated using ASTM A-446, Grade A sheet, the criteria and procedures given in reference 2 are based on the minimum specified yield stress of this material, which is 227,500 kPa (33,000 psi). The test panels were also fabricated from this material. However, it is generally known that the yield stress of the material used in the manufacture of cold-formed panels generally exceeds the specified minimum yield stress by a significant margin. To establish this fact, tensile tests were performed on specimens taken from the test panels. These tests were conducted by the Pittsburgh Testing Laboratory of Salt Lake City, Utah. The report furnish by the laboratory is provided in figures 31 and 32. Specimens taken from the test panels are listed below. The letters "T" and "F" next to some of the panel designations indicated that the specimen was taken from the top hat and flat sheet of the panel, respectively.

Lab Specimen Designation	Test Panel
Sample No. 1	4 inches, ribbed
Sample No. 2	4 inches, ribbed
Sample No. 3	Section 3-22
Sample No. 4	Section 3-22
Sample No. 5	Section 3-20
Sample No. 6	Section 3-20
Sample No. 7	Section 3-18
Sample No. 8	Section 3-18
Sample No. 9	Section 3-16
Sample No. 10	Section 3-16
Sample No. 11	UKX 20-20T
Sample No. 12	UKX 20-20F
Sample No. 13	UKX 20-20T
Sample No. 14	UKX 20-20F
Sample No. 15	UKX 18-18T

```
Sample No. 16          UKX 18-18F
Sample No. 17          UKX 18-18T
Sample No. 18          UKX 18-18F
Sample No. 19          UKX 18-18T
Sample No. 20          UKX 16-16F

Sample No. 21          UKX 16-16T
Sample No. 22          UKX 16-16F
Sample No. 23          NKX 20-20T
Sample No. 24          NKX 20-20F
Sample No. 25          NKX 20-20T

Sample No. 26          NKX 20-20F
Sample No. 27          NKX 18-18F
Sample No. 28          NKX 18-18T
Sample No. 29          NKX 18-18F
Sample No. 30          NKX 18-18T
```

The tensile tests revealed that the sheet stocks used to manufacture the test panels had static yield stresses ranging from a minimum of 296,000 kPa (43,000 psi) to a maximum of 393,000 kPa (57,000 psi) with an average of about 331,000 kPa (48,000 psi). It was also seen that the top hats of panels with closed type cross-sections (UKX and NKX panels) had yield stresses up to 15 percent larger than those recorded for the flat sheets of the same panels. The larger yield stresses recorded for the top hats are probably the result of the cold working of these sheets. It is generally known that cold working can produce increases in the yield stresses of up to 20 percent.

The larger yield stresses measured for the test panel materials have significant effects on the panel responses. Table 6 shows that the fundamental periods of the test panels are relatively short compared to the fictitious durations given for the blast loads. The range of T/T_N (ratio of fictitious duration to natural period of panel) given in table 6 for the damaged test panels varies from a minimum value of 1.37 to a maximum value of 3.00. In this response range, the peak panel responses are extremely sensitive to the magnitudes of the applied loads and the member's resistance. A change in the magnitude of either one of these parameters is magnified into a much greater change in the member's response. To illustrate this point, the test panel responses were recomputed using the actual yield stresses of the material used to fabricate them. In order to provide a more meaningful comparison between the computed and actual resistances of the test panels, the 10 percent increase on the peak pressure, specified in reference 2, was not used in the computation.

A comparison of the calculated permanent deflections given in tables 6 and 7 shows that the utilization of the actual material yield stresses significantly reduces the computed panel responses. Reduction in the calculated deflections range from a minimum value of 51 percent for the Section 3-20 roof panel in test no. 7 to a maximum value of 85 percent for the UKX 20-20 roof panel in test no. 5. The average reduction in the computed deflections is 69 percent. However, in almost all of the cases, the computed permanent deflections in table 7 are still in excess of the measured permanent deflections. In the table, the measured deflections given are the average of the recorded deflections on the span with the most damage. It is apparent, from the discussion above, that the actual resistances of the test panels exceeded their computed resistances, even when the actual material yield stresses were used. In addition, it is concluded that the use of a 10 percent factor on the peak pressure is not required for the blast-resistant design of cold-formed steel panels.

Effect of Dynamic Loads on Hinge Formation Capabilities of Cold-Formed Steel Panels

The special provisions for the blast-resistant design of cold-formed steel panels given in reference 2 were based on the assumption that the behavior of such members is essentially the same under both static and dynamic loadings. Briefly, under static loads, the load-carrying capacity of a cold-formed steel panel is reduced abruptly upon yielding of the most stressed outer fibers. Progressive yielding of the section, resulting in the formation of a plastic hinge, does not occur with cold-formed members due to their large width/thickness, w/t, ratios. The depth/thickness and/or width/thickness ratios are of such magnitudes that the member will buckle locally at stresses below the yield point, if subjected to compression, shear, bending or bearing. As a result, utilization of the full capacity of the section is not considered possible and therefore, for design purposes, the flexural resistance of the member is limited. Also, in continuous members, the inability of cold-formed panels to sustain any appreciable hinge formation (successively) limits the redistribution of moments and consequently the utilization of the full capacity of more cross-sections of the member at ultimate load. Since limited data on the load-deformation responses of cold-formed panels is available, it was considered prudent to utilized the provisions in the AISI Specifications (ref. [1]) as a basis for the blast-resistant design of cold-formed panels and allow for a limited amount of plastic behavior and moment redistribution in the design.

17

However, the test results demonstrated that cold-formed panels exhibit a greater ability to sustain yielding of their cross-sections than was assumed in the formulation of the design criteria. This conclusion is based on the comparison of the measured and calculated wall panel deflections given in table 7. The smaller measured deflections, for two out of three panels, indicate that the actual resistances of these panels were somewhat greater than the values computed using those provisions listed in reference 2. Since the wall panels were simply supported members, the increase in their resistances over the calculated values could only be produced by the development of moments in these members. These moments were greater than those producing yielding of the highest-stressed outer fibers of the cross-sections of the members. Hence, some yielding of the cross-section must have occurred.

The ability of the test panels to sustain yielding of their cross-sections (demonstrated by test results) produced significant moment re-distribution in the continuous panels which had the effect of increasing their resistances over the values computed using the provisions of reference 2. This becomes apparent by comparing the computed and measured deflections for the roof panels in table 7. For nine out of eleven roof panels, the computed permanent deflections exceed the measured deflections. The average of the ratios of the calculated to the measured deflections for these nine panels is 4.4. Even under static loads, cold-formed panels exhibit significant moment re-distribution capabilities.

Recommended Changes in Methods of Computing Resistances and Stiffnesses of Cold-Formed Steel Panels

Tables 8 and 9 list those parameters required for the analysis of the test results. The values of the peak pressure, fictitious duration (t), and permanent deflection (X_p) were obtained from the test data. The values of the natural period (T_n), elastic deflection (X_E), and the actual resistance (r_a) were determined from modified procedures given in reference 2. These modifications include the calculation of the natural period and the elastic deflection using the total rather than the effective moment of inertia and using the actual yield stress (average of several specimens) rather than the minimum stress. The required resistances (r_u) for the continuous members (table 8) were calculated using the modified formula

$$r_u = 4\ (M_{un} + 2\ M_{up})/L^2$$

18

where M_{un} is the ultimate negative moment capacity for one-foot width of panel, and M_{up} is the ultimate positive moment capacity for one-foot width of panel. It is seen from table 8 that the average of the ratio of the required resistance (using the modified formula above) to the actual resistance is equal to 1.1 and the root mean square is equal to 0.209, indicating that this formula provides slightly conservative results. The conclusions and recommendations reached as a result of the test results and analyses are presented in the following section.

CONCLUSIONS AND RECOMMENDATIONS

On the basis of the discussions in the preceding sections, the following conclusions and recommendations for revised criteria of reference 2 are offered:

1. The increased strength observed in the tests are due, in part, to the actual static yield stresses which exceeded the minimum stress at yield of 227,500 kPa (33,000 psi). The actual static yield stresses were found to range from 296,000 kPa (43,000 psi) to 393,000 kPa (57,000 psi) with an average of about 331,000 kPa (48,000 psi). Thus, this represents an average increase of about 40 percent over the minimum yield stress. Although this average increase cannot be expected in all cold-formed members, some increase in strength of the steel above the minimum should be considered in design. A static yield stress of 276,000 kPa (40,000 psi) should be utilized for the design or evaluation of all cold-formed panels fabricated from ASTM A-446, Grade A sheet, unless the actual yield stress of the material is known. When higher strength steels are used, the specified minimum yield stress of the material should be used, unless the actual yield stress is known.

2. The flexural resistances of a simply fixed panel or a continuous panel of equally spaced spans should be computed using the equation below in lieu of equation 3.25 of reference 2:

$$r_u = 4(M_{un} + 2M_{up})/L^2$$

3. The 10 percent factor on the peak pressure stated in reference 2 is not required and, therefore, should be left out.

4. Where the maximum shear forces and dynamic reactions exceed the ultimate load-carrying capacity of the web of the panel, the design of the member must be based on the resistance computed as a function of either the shear or crippling capacities of the web, as the case may be.

5. The maximum ductility ratio criteria of 1.25 for reusable structures and 1.75 for non-reusable structures (ref. 2) can be increased to 3.0 and 6.0, respectively.

6. The maximum support ratio criteria of 0.9 degree and 1.8 degrees for reusable and non-reusable structures (ref. 2) can be increased to 2.0 and 4.0, respectively. However, it should be realized that with the use of these larger rotations, permanent displacements similar to those of figures 25 and 28 may be expected.

7. Future calculations for the natural period and for elastic deflections should utilize the total moment of inertia rather the effective moment of inertia of reference 2.

8. Tests up to 5 psi have indicated that open hat shapes (Section 3 and 4-inch ribbed panels shown in figure 10) can be used for applications in the low pressure range rather than only closed sections (UKX and NKX) as recommended in reference 2.

9. Standard screw-type connections performed satisfactorily in blast tests up to 5 psi.

REFERENCES

1.   American Iron and Steel Institute, "Cold-Formed Steel Design Manual (1977 Edition) Specifications and Commentary," New York, NY, 1968.

2.   J. J. Healey, et al., "Design of Steel Structures to Resist the Effects of HE Explosions," Picatinny Arsenal Technical Report 4837, Picatinny Arsenal, Dover, NJ, August 1975.

3.   S. Weissman, et al., "Blast Capacity Evaluation of Glass Windows and Aluminum Window Frames," Report ARLCD-CR-78016, U.S. Army Armament Research and Development Command, Dover, NJ, June 1978.

4.   A. K. Keetch, "Blast Load Capacity of Tempered Plate Glass," Document No. DPG-LR-C985A-2, U.S. Army Dugway Proving Ground, Dugway, UT, January 1976.

5.   J. J. Swatosh, et al., "Blast Parameters of M26E1 Propellant," Picatinny Arsenal Technical Report 4901, Picatinny Arsenal, Dover, NJ, December 1976.

6.   Department of the Army, "Structures to Resist the Effects of Accidental Explosions (with Addenda)," Technical Manual TM5-1300, Washington, D.C., June 1969.

Table 1

Types and sizes of panels tested

Sizes					
Length		Width		Section and gage	Number of panels
m	(ft-in)	m	(ft-in)		
4.6	(15-1)	0.6	(2-0)	Section 3-22	2
4.6	(15-1)	0.6	(2-0)	Section 3-20	4
4.6	(15-1)	0.6	(2-0)	Section 3-18	2
1.4	(4-6)	0.6	(2-0)	Section 3-16	2
4.6	(15-1)	0.6	(2-0)	UKX 20-20	4
1.4	(4-6)	0.6	(2-0)	UKX 18-18	2
4.6	(15-1)	0.6	(2-0)	UKX 18-18	2
1.4	(4-6)	0.6	(2-0)	UKX 16-16	3[a]
4.6	(15-1)	0.6	(2-0)	NKX 20-20	4
4.6	(15-1)	0.6	(2-0)	NKX 18-18	2
4.6	(15-1)	0.6[b]	(2-0)	Cyclops, 24-gage, 4-inch ribbed	2

[a]One panel damaged in transit.
[b]Panel cut from 0.95-m (37.5-in) width.

Table 2

Schedule of cold-formed steel test panels and types of connection

Test No.	STRUCTURE A Roof[a] Panel	Connection[b] Type	Size[c]	STRUCTURE B Roof[a] Panel	Connection[b] Type	Size[c]	Wall[a] Panel	Connection[b] Type	Size[c]	STRUCTURE C Roof[a] Panel	Connection[b] Type	Size[c]	STRUCTURE D Roof[a] Panel	Connection[b] Type	Size[c]
1	4-in rib 24 gage	S	#14	UKX 20-20 gage	W	19 (3/4)	UKX 16-16 gage	W	19 (3/4)	UKX 20-20 gage	W	19 (3/4)	NKX 20-20 gage	W	25 (1)
2	4-in rib 24 gage	S	#14	UKX 20-20 gage	W	19 (3/4)	UKX 16-16 gage	W	19 (3/4)	UKX 20-20 gage	W	19 (3/4)	NKX 20-20 gage	W	25 (1)
3	4-in rib 24 gage	S	#14	UKX 20-20 gage	W	19 (3/4)	UKX 16-16 gage	W	19 (3/4)	UKX 18-18 gage	TMB[d]	10 (3/8)	NKX 20-20 gage	W	25 (1)
4	4-in rib 24 gage	S	#14	UKX 20-20 gage	W	19 (3/4)	UKX 16-16 gage	W	19 (3/4)	UKX 18-18 gage	TMB	10 (3/8)	NKX 20-20 gage	W	25 (1)
5	4-in rib 24 gage	S	#14	UKX 20-20 gage	W	19 (3/4)	UKX 16-16 gage	W	19 (3/4)	UKX 18-18 gage	TMB	10 (3/8)	NKX 20-20 gage	W	25 (1)
6	Sec 3 22 gage	W	19 (3/4)	Sec 3 18 gage	W	19 (3/4)	UKX 18-18 gage	W	19 (3/4)	UKX 18-18 gage	TMB	10 (3/8)	NKX 20-20 gage	W	38 (1-1/2)
7	Sec 3 22 gage	S	#14	Sec 3 20 gage	S	#14	Sec 3 16 gage	W	19 (3/4)	UKX 18-18 gage	TMB	10 (3/8)	NKX 18-18 gage	W	19 (3/4)

[a]See Table 1 for panel profiles.

[b]S - Self-tapping screw
W - Puddle weld

[c]Quantities given for threaded machine bolts (TMB) and puddle welds (W) are diameters in millimeters. Quantities in parentheses are diameters in inches.

[d]TMB - Threaded Machine Bolt

24

Table 3

Summary of blast overpressure and duration data - Tests Nos. 1 through 7

Test No.	Charge weight kg (lb)	Gage No.	Distance from charge m (ft)	Scale distance Z m/kg$^{1/3}$ (ft/lb$^{1/3}$)	Blast pressure kPa (psi)	Positive-phase duration msec
1	893 (1,969)	1	53 (175)	5.50 (13.97)	26.4 (3.83)	31.2
		2	79 (260)	8.20 (20.75)	a	a
		3	108 (355)	11.21 (28.33)	a	a
		4	165 (540)	17.13 (43.10)	a	a
		5	244 (800)	25.34 (63.85)	1.7	b
2	893 (1,969)	1	43 (140)	4.47 (11.17)	44.8 (6.50)	47.5
		2	69 (225)	7.17 (17.96)	13.1 (1.90)	44.0
		3	98 (320)	10.18 (25.54)	5.0 (0.72)	47.0
		4	154 (505)	16.00 (40.30)	2.6 (0.38)	45.0
		5	233 (765)	24.20 (61.05)	1.7 (0.24)	42.0
3	888 (1,958)	1	53 (175)	5.52 (13.99)	16.7 (2.42)	44.0
		2	79 (260)	8.22 (20.78)	11.9 (1.73)	41.0
		3	108 (355)	11.24 (28.38)	7.3 (1.06)	44.0
		4	165 (540)	17.17 (43.17)	3.9 (0.57)	43.0
		5	244 (800)	25.39 (63.95)	2.4 (0.35)	41.0
4	891 (1,964)	1	38 (125)	3.95 (9.98)	54.1 (7.84)	46.0
		2	49 (160)	5.09 (12.78)	23.4 (3.40)	53.0
		3	61 (200)	6.34 (15.97)	12.2 (1.77)	51.0
		4	79 (260)	8.21 (20.77)	7.9 (1.15)	49.0
		5	130 (425)	13.51 (33.95)	4.3 (0.63)	43.0

aNo data - Instrument failure.
bNo data - Sweeptime too short.

Table 3
(concluded)

Summary of blast overpressure and duration data - Tests Nos. 1 through 7

Test No.	Charge weight kg (lb)	Gage No.	Distance from charge m (ft)	Scale distance Z m/kg$^{1/3}$ (ft/lb$^{1/3}$)	Blast pressure kPa (psi)	Positive-phase duration msec
5	917 (2,021)	1	38 (125)	25.12 (9.89)	62.2 (9.02)	c
		2	45 (150)	30.12 (11.86)	34.0 (4.93)	49
		3	53 (175)	35.15 (13.84)	20.0 (2.90)	46
		4	66 (215)	43.21 (17.01)	12.6 (1.83)	48
		5	79 (260)	52.22 (20.56)	9.6 (1.39)	46
6	914 (2,016)	1	35 (115)	23.11 (9.10)	73.7 (10.69)	d
		2	41 (135)	27.15 (10.69)	46.2 (6.99)	e
		3	50 (165)	33.17 (13.06)	11.5 (1.67)	61
		4	63 (205)	41.22 (16.23)	10.8 (1.57)	58
		5	76 (250)	50.27 (19.79)	8.9 (1.29)	55
7	930 (2,050)	1	31 (100)	19.99 (7.87)	162.2 (23.52)	d
		2	35 (115)	22.99 (9.05)	93.2 (13.52)	e
		3	40 (130)	25.98 (10.23)	39.4 (5.71)	57
		4	46 (150)	29.99 (11.81)	33.1 (4.8)	56
		5	55 (180)	35.99 (14.17)	18.4 (2.67)	54

cNo data - Measurement exceeded calibration level.
dNo data - Measurement exceeded negative level; gage blown over.
eNo data - Measurement exceeded negative leve; interference from Gage No. 1.

26

Table 4

Summary of test results for panels on Structures A and B

| | STRUCTURE A | | | | STRUCTURE B | | | | | |
| | | | Roof panels | | | | Roof panels | | Blastward wall panels | |
Test No.	Blast[a] Pressure kPa (psi)	Positive Phase Duration (ms)	Type	Damage[b]	Blast[a] Pressure kPa (psi)	Positive Phase Duration (ms)	Type	Damage[b]	Type	Damage[b]
1	2.07 (0.30)	42.0	4-in rib 24 gage	None	6.89 (1.0)	48.0	UKX 2D-20 gage	None	UKX 16-16 gage	None
2	2.14 (0.31)	43.0	4-in rib 24 gage	None	8.27 (1.2)	50.0	UKX 20-20 gage	None	UKX 16-16 gage	None
3	5.38 (0.78)	44.0	4-in rib 24 gage	None	15.86 (2.3)	50.0	UKX 2D-20 gage	None	UKX 16-16 gage	None
4	8.36 (1.3)	50.0	2-in rib 24 gage	None	21.37 (3.1)	52.0	UKX 2D-20 gage	None	UKX 16-16 gage	None
5	13.79 (2.00)	50.0	4-in rib 24 gage	2 spans MD 19 mm (0.75 in)	31.03 (4.5)	52.0	UKX 2D-20 gage	1 span MD 6 mm (0.25 in)	UKX 16-16 gage	MD 13 mm (0.50 in)
6	22.06 (3.2)	52.0	Sec. 3 22 gage	2 spans MD 33 mm (1.31 in)	31.03 (4.5)	52.0	Sec. 3 18 gage	1 span MD 5 mm (0.19 in)	UKX 18-18 gage	MD 6 mm (0.25 in)
7	31.03 (4.50)	52.0	Sec. 3 2D gage	1 span MD 29 mm (1.13 in)	38.61 (5.6)	52.0	Sec. 3 20 gage	3 spans MD 48 mm (1.88 in)	Sec. 3 16 gage	MD 48 mm (1.88 in)

aData interpolated from Figure 13.
bMD - Maximum Deflection of panel.

27

Table 5

Summary of test results for panels on Structures C and D

	STRUCTURE C				STRUCTURE D			
Test No.	Blast[a] Pressure kPa (psi)	Positive Phase Duration (ms)	Roof Panels Type	Damage[b]	Blast[a] Pressure kPa (psi)	Positive Phase Duration (ms)	Roof Panels Type	Damage[b]
1	10.34 (1.5)	50.0	UKX 20-20 gage	None	13.79 (2.0)	50.0	NKX 20-20 gage	None
2	13.10 (1.9)	50.0	UKX 20-20 gage	None	19.99 (2.9)	52.0	NKX 20-20 gage	None
3	21.37 (3.1)	52.0	UKX 18-18 gage	None	27.58 (4.0)	52.0	NKX 20-20 gage	None
4	27.56 (4.0)	52.0	UKX 18-18 gage	None	38.61 (5.6)	52.0	NKX 20-20 gage	None
5	38.61 (5.6)	52.0	UKX 18-18 gage	1 span MD 6 mm (0.25 in)	48.26 (7.0)	52.0	NKX	2 spans MD 24 mm (0.94 in)
6	48.95 (7.1)	52.0	UKX	None	65.50 (9.5)	52.0	NKX	3 spans MD 44 mm (1.75 in)
7	75.84 (11.0)	52.0	UKX	2 spans MD 44 mm (1.75 in)	103.41 (15.0)	52.0	NKX	2 spans MD 14 mm (0.56 in)

[a] Data interporated from Figure 13.
[b] MD - Maxium deflection of panels.

28

Table 6

Responses of damaged test panels based on design procedures in reference 2

Test No.	Test structure	Panel Location	Type	Peak pressure kPa (psi)	Fictitious duration (T) (ms)	Natural period (T_N) (ms)	Elastic deflection (X_E) mm (in)	Flexural resistance kPa (psi)	T/T_N	Ductility ratio X_m/X_E	Permanent deflection m (in)
5	A	Roof	4-in rib	13.8 (2.0)	30.0	22.3	18.0 (0.71)	7.0 (1.02)	1.35	22.0	0.33 (12.8)
	B	Roof	UKX 20-20	31.0 (4.5)	26.0	15.2	9.4 (0.37)	21.9 (3.18)	1.71	8.8	0.07 (2.9)
	B	Wall	UKX 16-16	79.3 (11.5)	8.0	15.6	11.2 (0.44)	37.4 (5.43)	c	5.6	0.05 (2.0)
	C	Roof	UKX 18-18	38.6 (5.6)	27.0	14.1	9.7 (0.38)	33.3 (4.84)	1.91	4.6	0.03 (1.4)
	D	Roof	NKX 20-20	48.3 (7.0)	26.0	8.3	4.9 (0.19)	42.4 (6.15)	3.13	7.0	0.03 (1.1)
6	A	Roof	Sec 3-22	22.1 (3.2)	30.0	15.3	11.6 (0.46)	12.8 (1.86)	1.96	22.0	0.24 (9.6)
	B	Roof	Sec 3-18	31.0 (4.5)	28.0	14.2	10.8 (0.42)	18.3 (3.22)	1.97	10.0	0.10 (3.8)
	B	Wall	UKX 18-18	79.3 (11.5)d	8.0e	16.5	10.7 (0.42)	27.8 (3.91)	c	16.2	0.16 (6.4)
	D	Roof	NKX 20-20	65.5 (9.5)	24.0	8.3	4.9 (0.19)	42.4 (6.15)	2.89	30.0	0.14 (5.5)
7	A	Roof	Sec 3-20	31.0 (4.5)	29.0	14.9	11.3 (0.45)	15.9 (2.31)	1.95	35.0	0.39 (15.3)
	B	Roof	Sec 3-20	38.6 (5.6)	27.0	14.9	11.3 (0.45)	15.9 (2.31)	1.81	46.0	0.52 (20.3)
	B	Wall	Sec 3-16	93.1 (13.5)	8.0	15.9	14.7 (0.58)	29.0 (4.21)	c	21.0	0.29 (11.6)
	C	Roof	UKX 18-18	75.8 (11.0)	25.0	14.1	9.7 (0.38)	33.4 (4.84)	1.77	35.0	0.33 (12.9)
	D	Roof	NKX 18-18	103.4 (15.0)	21.0	7.7	4.8 (0.19)	64.2 (9.31)	2.73	27.0	0.13 (5.0)

aPermanent deflection = $(X_m/X_E - 1.0)X_E$.

bX_m = Maximum dynamic deflection.

cResponses for wall panels computed considering both reflected and incident pressures.

dReflected pressure on blastward wall.

eClearing time for relieving reflected pressure on blastward wall.

29

Table 7

Responses of damaged panels using actual yield stresses of material

Test No.	Test structure	Panel Location	Type	Elastic deflection (X_E) mm	(in)	Average yield stress of material[b] mPa	(ksi)	Flexural resistance (kPa)	(psi)	Ductility ratio[c] (X_m/X_E)	Permanent deflections[a] calculated mm	(in)	measured[d] mm	(in)
5	A	Roof	4-in rib	29.0	(1.14)	367	(53.2)	11.3	(1.64)	4.00	86.9	(3.42)	10.9	(0.43)
	B	Roof	UKX 20-20	16.0	(0.63)	390	(56.6)	37.6	(5.46)	1.70	11.1	(0.44)	10.9	(0.43)
	B	Wall	UKX 16-16	15.0	(0.59)	311	(45.1)	51.1	(7.40)	2.62	24.2	(0.96)	9.1	(0.36)
	C	Roof	UKX 18-18	14.7	(0.58)	347	(50.4)	51.0	(7.40)	1.45	16.6	(0.26)	5.1	(0.20)
	0	Roof	NKX 20-20	6.9	(0.27)	325	(47.2)	60.7	(8.81)	1.85	5.9	(0.28)	24.9	(0.98)
6	A	Roof	Sec 3-22	17.3	(0.68)	339	(49.2)	19.1	(2.78)	4.60	62.7	(2.47)	27.7	(1.09)
	8	Roof	Sec 3-18	15.5	(0.60)	321	(46.5)	31.2	(4.53)	2.90	20.0	(1.14)	3.6	(0.14)
	B	Wall	UKX 18-18	16.3	(0.64)	339	(49.1)	40.1	(5.82)	4.18	50.0	(1.97)	61.0	(2.40)
	0	Roof	NKX 20-20	6.9	(0.27)	325	(47.2)	60.7	(8.81)	4.60	29.7	(0.97)	37.6	(1.48)
7	A	Roof	Sec 3-20	17.0	(0.67)	339	(49.2)	23.7	(3.44)	7.50	109.8	(4.32)	19.6	(0.77)
	B	Roof	Sec 3-20	17.0	(0.67)	339	(49.2)	23.7	(3.44)	17.00	254.4	(9.99)	43.7	(1.72)
	B	Wall	Sec 3-16	20.7	(0.81)	321	(46.6)	32.7	(5.91)	7.47	134.0	(5.28)	37.3	(1.47)
	C	Roof	UKX 18-18	14.7	(0.58)	347	(50.4)	51.0	(7.40)	11.50	154.4	(6.08)	29.9	(1.18)
	0	Roof	NKX 18-18	8.4	(0.29)	337	(48.9)	95.1	(13.80)	5.20	30.7	(1.21)	11.4	(0.45)

aAverage of deflections on span with most damage.

bFor UKX and NKX sections, yield stresses given are the average yield stress for the top hat.

cFor values of peak pressures, fictitious durations, natural period and the ratio T/T_N, see table 6.

dFor definition of permanent deflection, see table 6.

Table 8

Responses of damaged continuous panels using the modified procedures

Test No.	Test structure	Panel type	Natural period (ms)	T/T_N	Elastic deflection (mm)	(in)	Measured permanent deflection (mm)	(in)	Maximum dynamic deflection (mm)	(in)	Ductility ratio X_m/X_E	Ultimate unit resistance Calculated r_u kPa	(psi)	Measured r_m kPa	(psi)	r_m/r_c
5	A	4-in rib	19.4	1.55	25.9	(1.02)	10.9	(0.43)	36.8	(1.45)	1.42	13.4	(1.95)	18.4	(2.67)	1.37
	B	UKX 20-20	13.2	1.97	13.0	(0.51)	10.9	(0.43)	23.9	(0.94)	1.85	39.6	(5.74)	36.5	(5.30)	0.92
	C	UKX 18-18	12.2	2.21	11.7	(0.46)	5.1	(0.20)	16.8	(0.66)	1.43	53.8	(7.80)	52.9	(7.67)	0.98
	D	NKX 20-20	7.2	3.61	5.8	(0.23)	18.3	(0.72)	24.1	(0.95)	3.77	68.9	(10.00)	48.3	(7.00)	0.70
6	A	Sec 3-22	13.3	2.26	14.7	(0.58)	27.7	(1.09)	42.4	(1.67)	2.88	21.6	(3.13)	22.6	(3.28)	1.05
	B	Sec 3-18	12.3	2.28	14.0	(0.55)	3.6	(0.14)	17.5	(0.69)	1.25	37.8	(5.48)	47.0	(6.82)	1.24
	D	NKX 20-20	7.2	3.30	5.8	(0.23)	37.6	(1.48)	43.4	(1.71)	7.40	68.9	(10.00)	57.2	(8.30)	0.83
7	A	Sec 3-20	13.0	2.23	15.0	(0.59)	19.6	(0.77)	34.5	(1.36)	2.30	27.7	(4.02)	34.1	(4.95)	1.23
	B	Sec 3-20	13.0	2.08	15.0	(0.59)	43.7	(1.72)	58.7	(2.31)	3.92	27.7	(4.02)	36.1	(5.23)	1.30
	C	UKX 18-18	12.2	2.05	11.7	(0.46)	30.0	(1.18)	41.7	(1.64)	3.57	53.8	(7.80)	71.0	(10.30)	1.32
	D	NKX 18-18	6.7	3.00	5.6	(0.22)	11.4	(0.45)	17.5	(0.69)	2.84	27.6	(4.00)	108.9	(15.80)	1.13

Average = 1.1

Standard Deviation = 0.209

31

Table 9

Responses of damaged simply supported panels using the modified procedures

Test No.	Test structure	Panel type	Natural period (ms)	T/T_N	Elastic deflection (mm)	(in)	Measured permanent deflection (mm)	(in)	Maximum dynamic deflection[a] (mm)	(in)	Ductility ratio[b] X_m/X_E	Ultimate unit resistance Calculated r_u kPa	(psi)	Measured r_m kPa	(psi)	r_m/r_c
5	B	UKX 16-16	13.5	c	11.2	(0.44)	9.1	(0.36)	20.3	(0.80)	1.81	51.0	(7.40)	57.2	(8.30)	1.12
6	B	UKX 18-18	14.3	c	11.9	(0.47)	61.0	(2.40)	72.9	(2.87)	6.10	40.1	(5.82)	37.9	(5.50)	0.95
7	B	Sec 3-16	13.8	c	15.5	(0.61)	37.3	(1.47)	52.8	(2.08)	3.41	40.7	(5.91)	55.2	(8.00)	1.35

Average = 1.14

Standard Deviation = 0.164

[a] Maximum dynamic deflection (X) equals sum of elastic deflection (X) and measured permanent deflection.

[b] For values of peak pressures and fictitious duration, see Table 6.

[c] Responses of wall panels were computed for piecewise linear (bilinear) loading function consisting of both incident and reflected pressure waveforms.

32

4 INCH RIBBED

102mm
(4")

25mm
(1")

0.61 m
(24")

NOTE:
THIS SECTION CUT
FROM A .95m
(3'-1½") PANEL.

SEC. 3

54mm
(2⅛")

60mm

92mm
(3⅝")

38mm
(1½")

0.61 m
(24")

UKX

54mm
(2⅛")

60mm

92mm
(3⅝")

38mm
(1½")

0.61 m
(24")

NKX

54mm
(2⅛")

60mm

143mm
(5⅝")

76mm
(3")

0.61 m
(24")
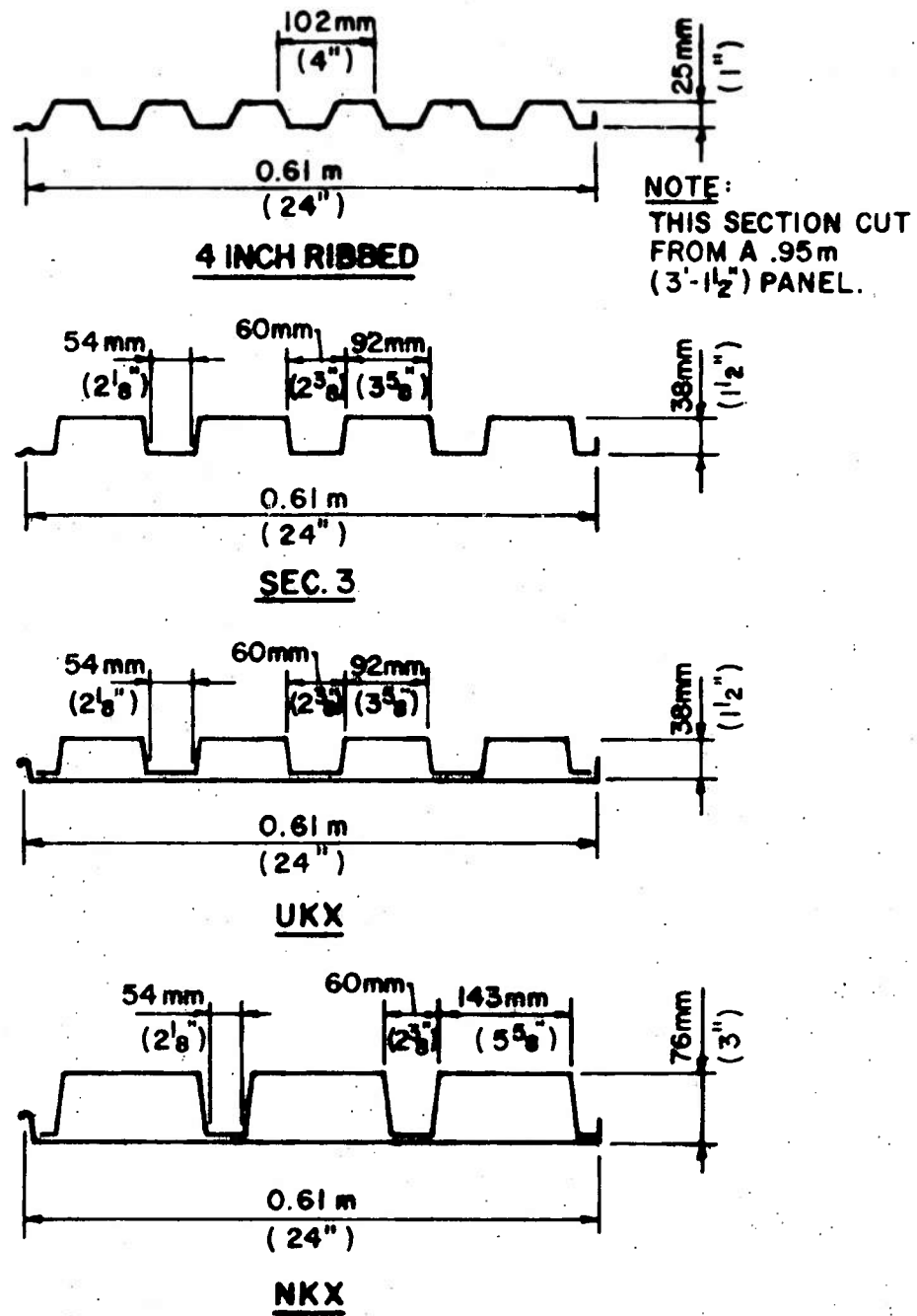
Figure 1. Cross-sections of cold-formed steel panels

33

Figure 2. Interior framing of a test structure

34
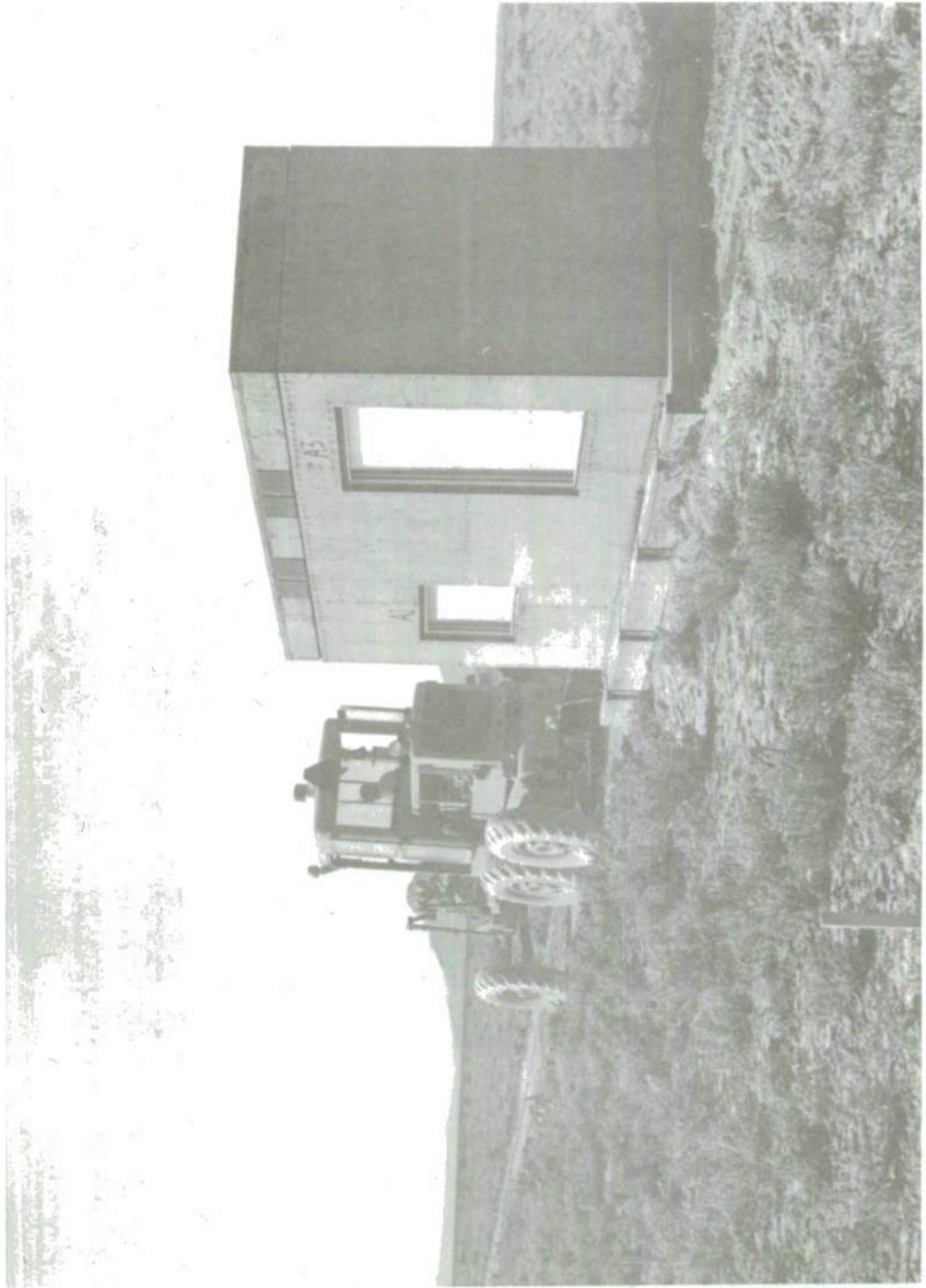
Figure 3. Test structure being towed to test site

ANCHOR RODS
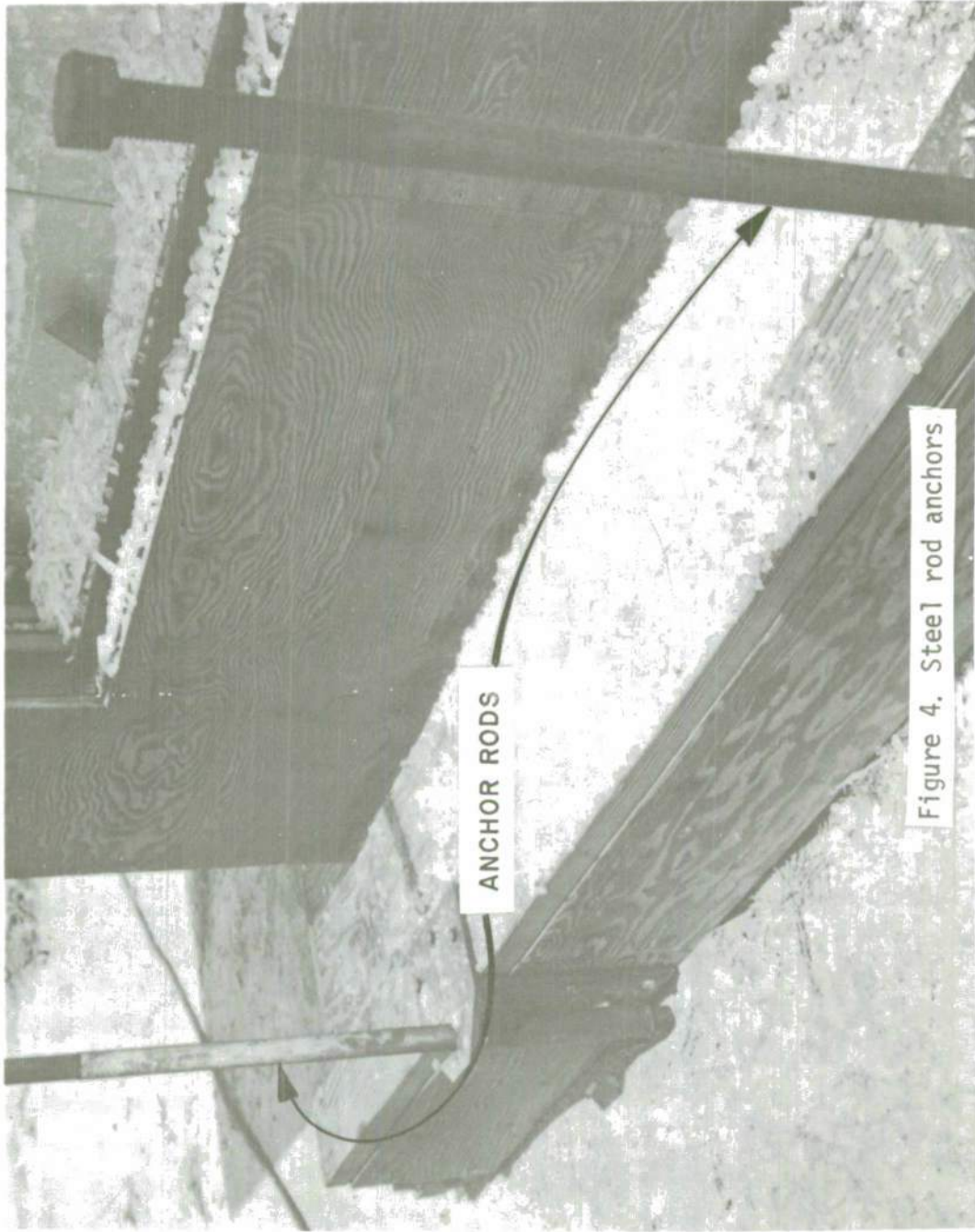
Figure 4. Steel rod anchors

Figure 5. Test Structure B

37
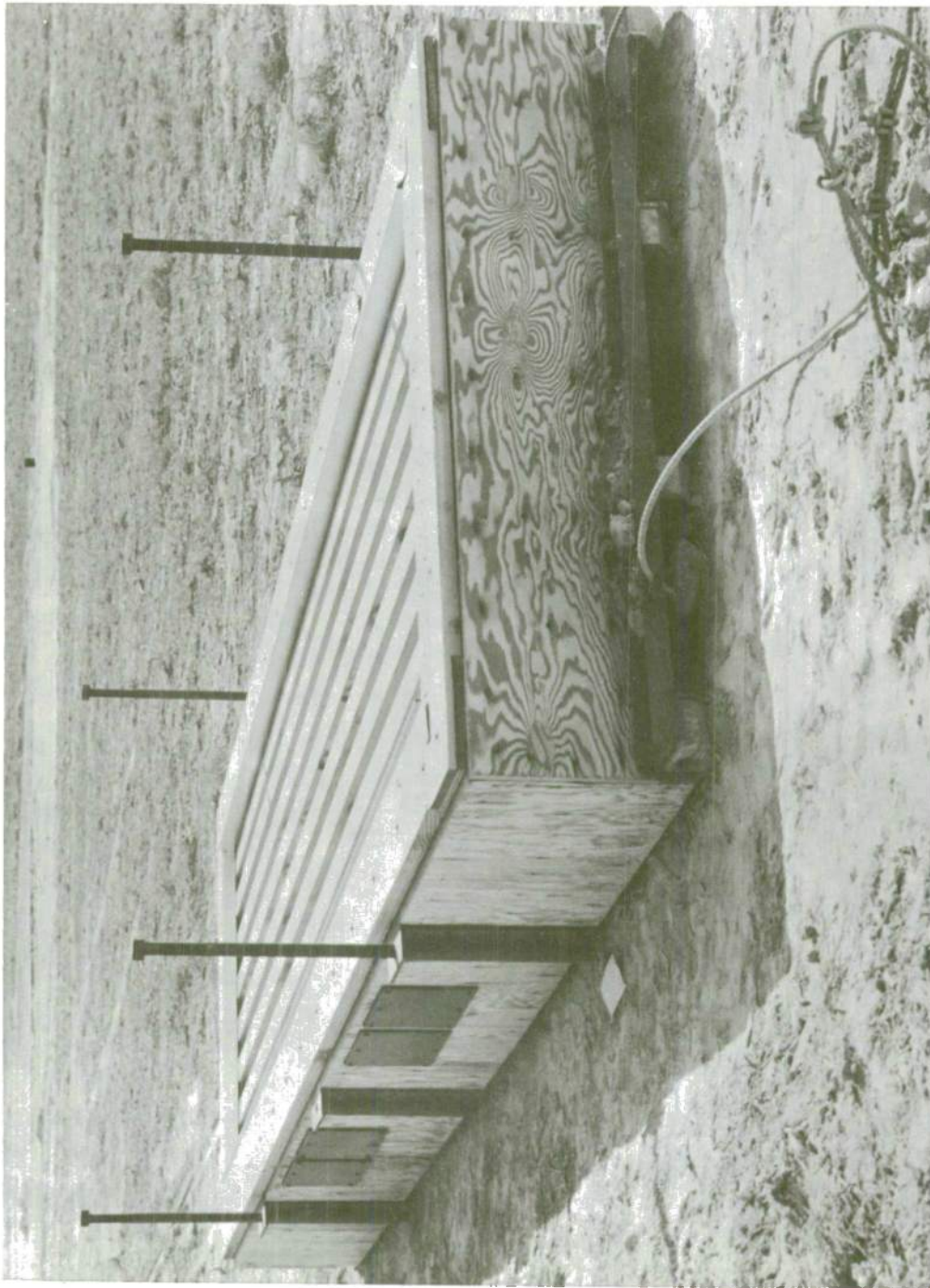
Figure 6. Test Structure C

HOLE FOR PUDDLE WELD

Figure 7. Hole for puddle weld
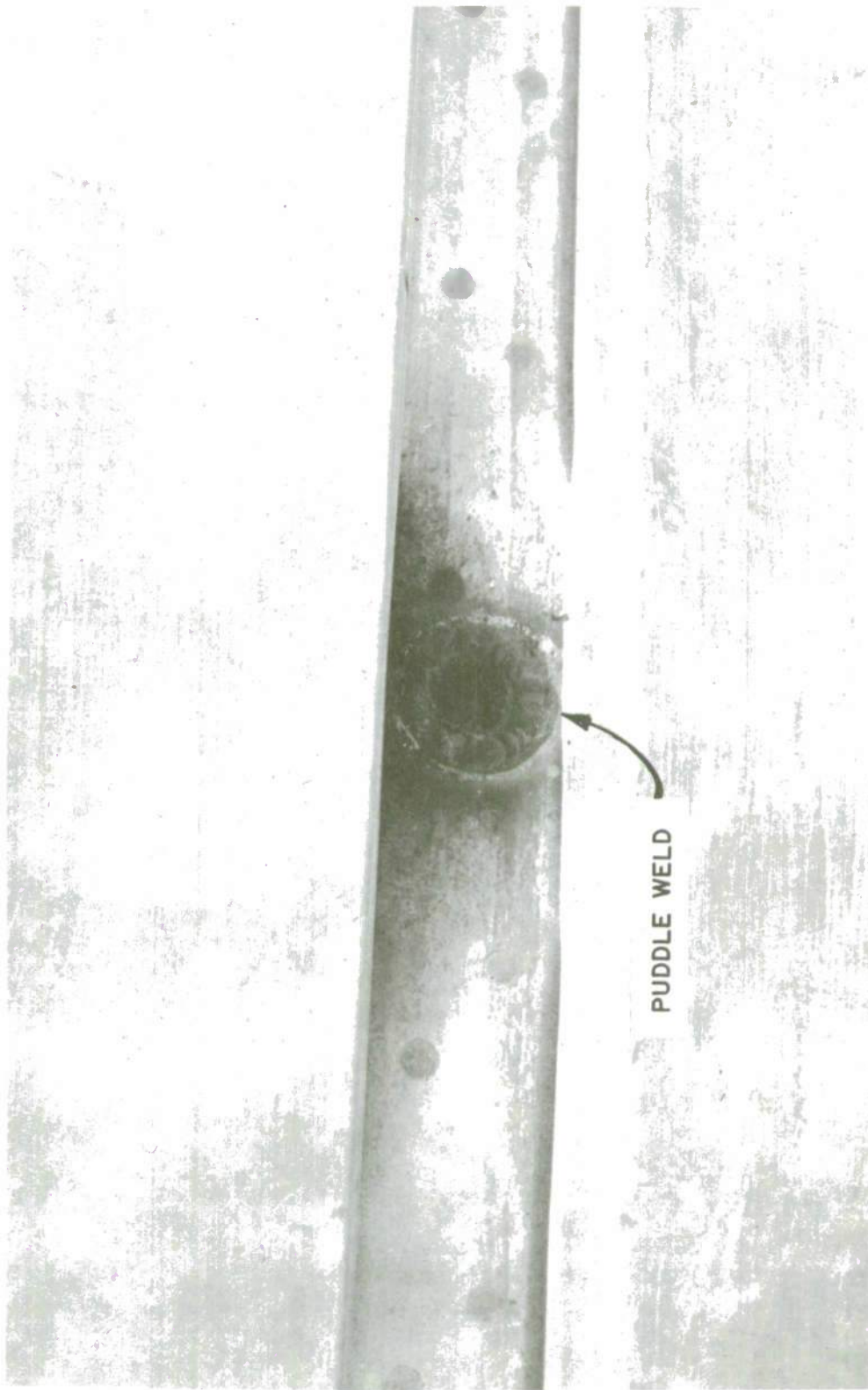
PUDDLE WELD

Figure 8. Typical puddle weld connection
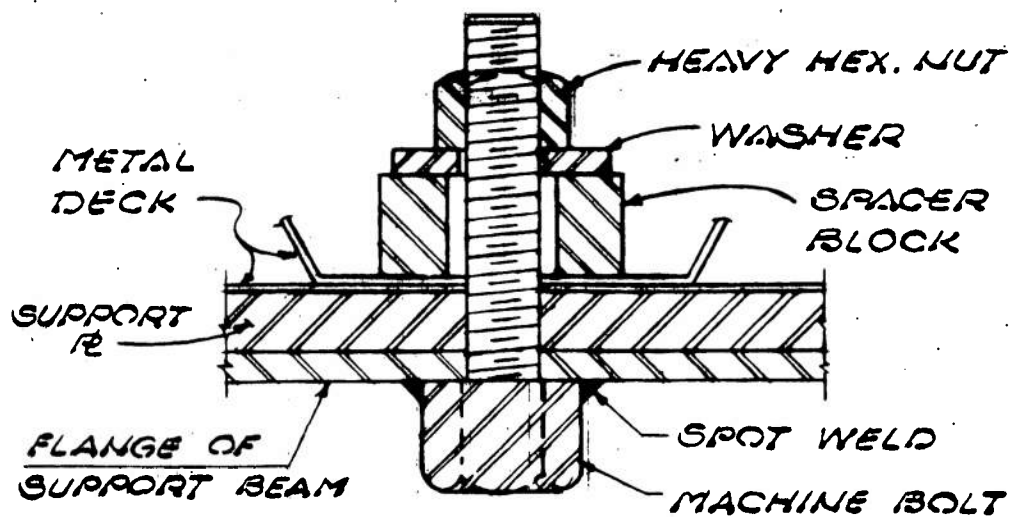
WELDED BOLTED CONNECTION
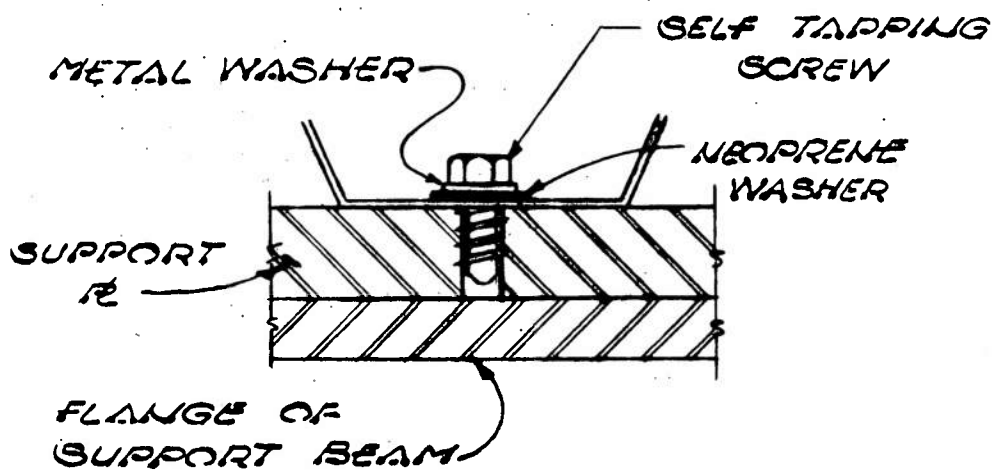
SELF-TAPPING SCREW CONNECTION

Figure 9. Details of bolt and screw connection

41
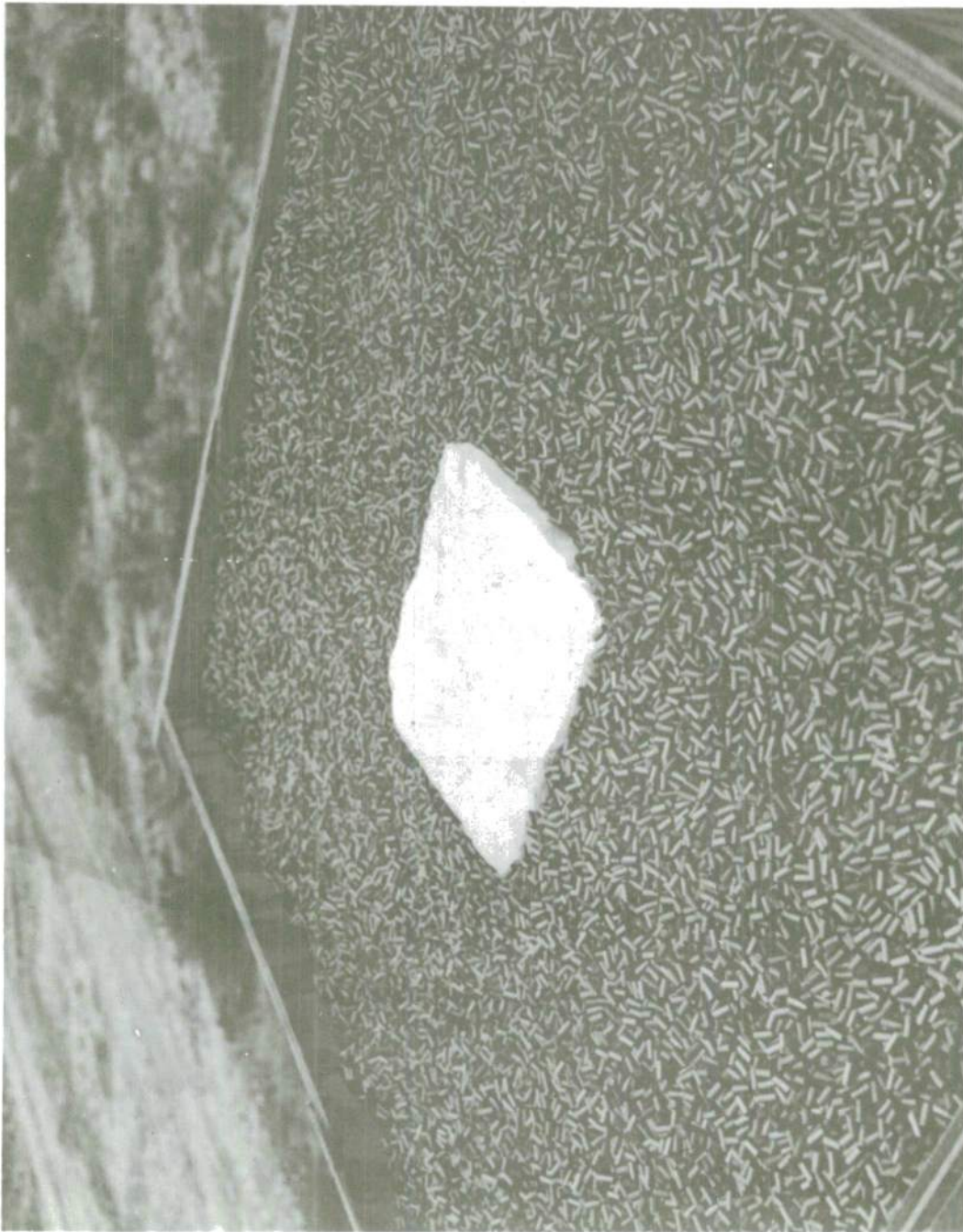
Figure 10 Typical charge
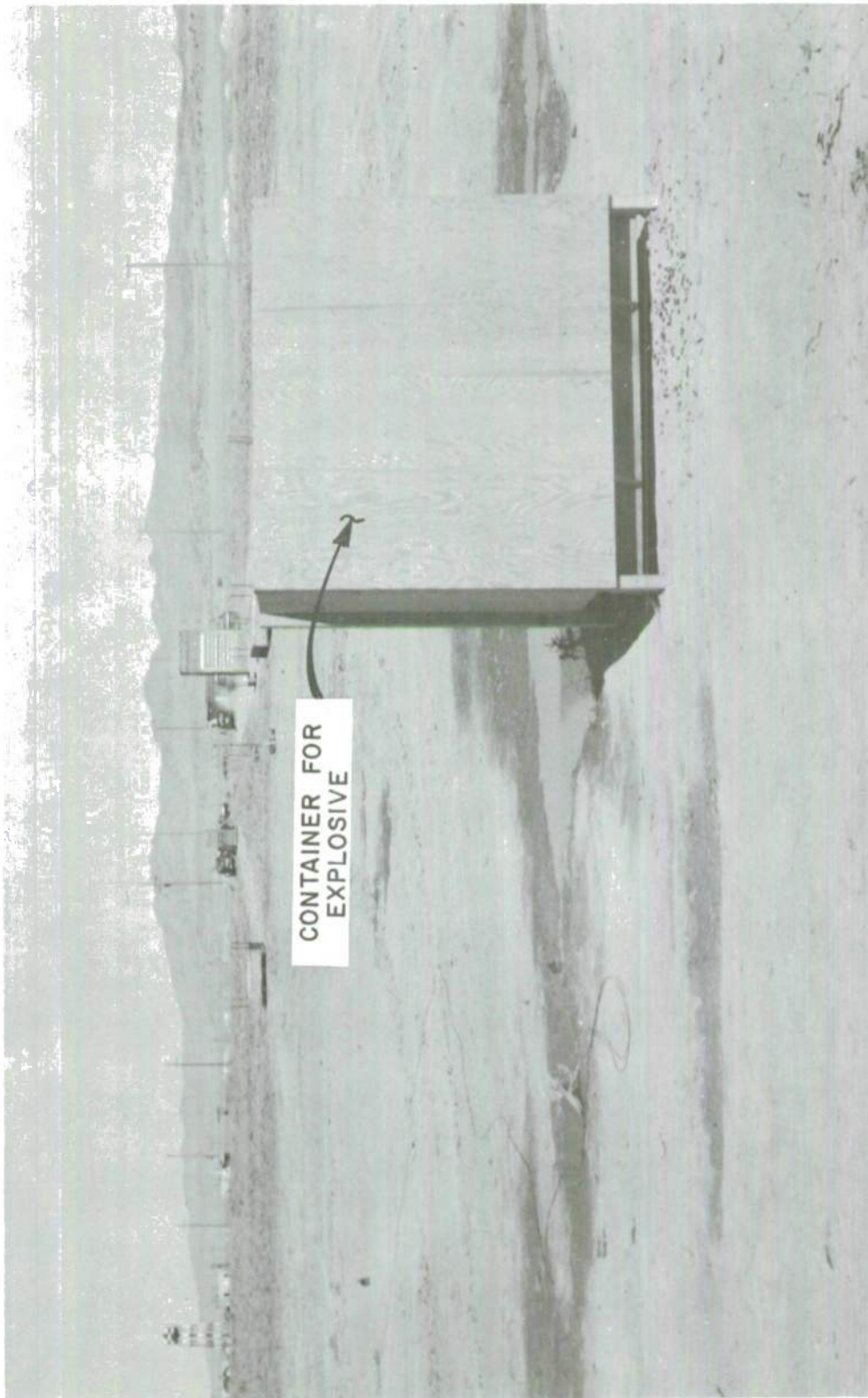
Figure 11. Container with explosive charge

CONTAINER FOR EXPLOSIVE

Figure 12. Detonation of charge

44

PRESSURE GAGE

TEST STRUCTURES A & B
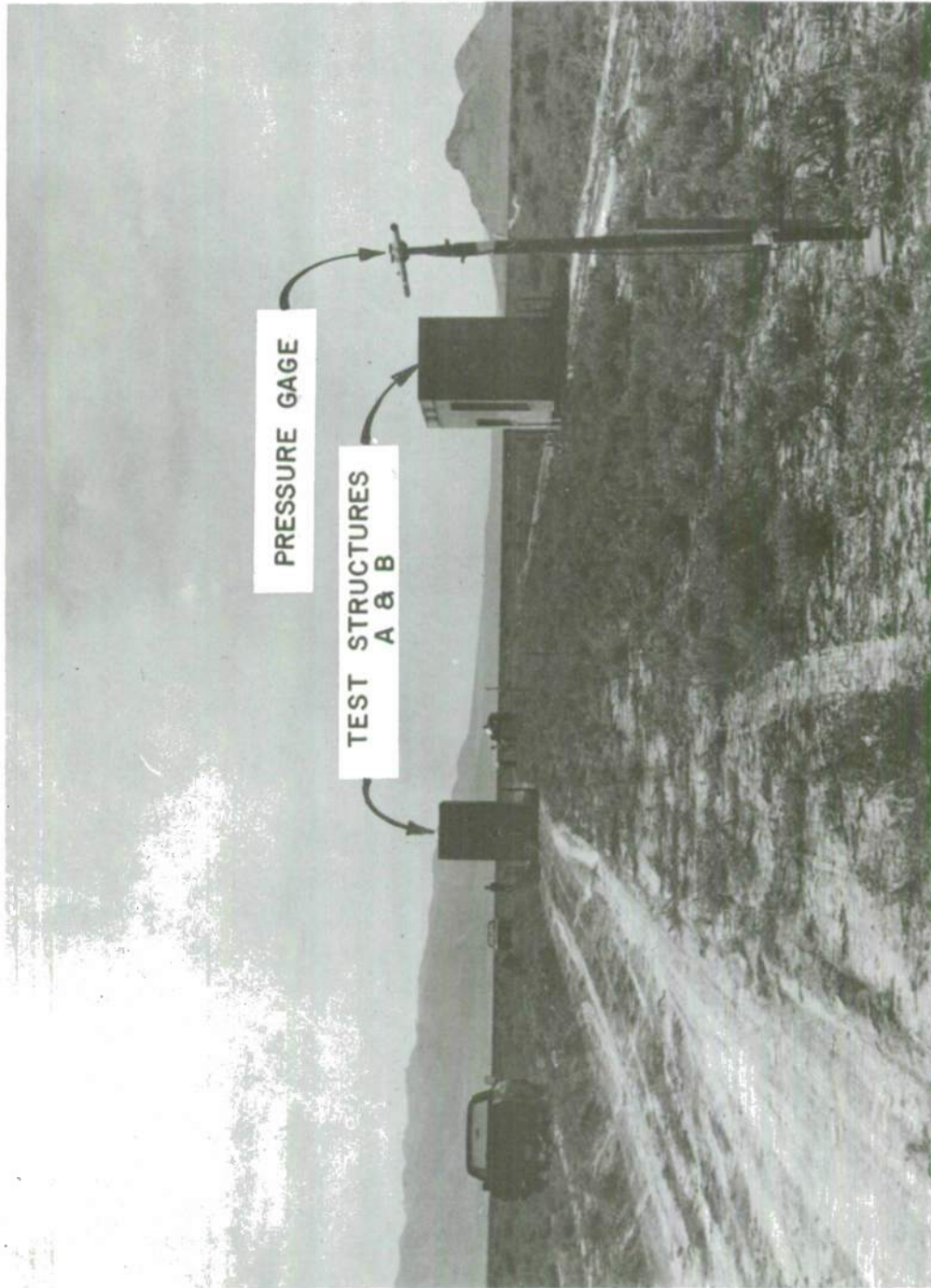
Figure 13. Typical gage mount

45
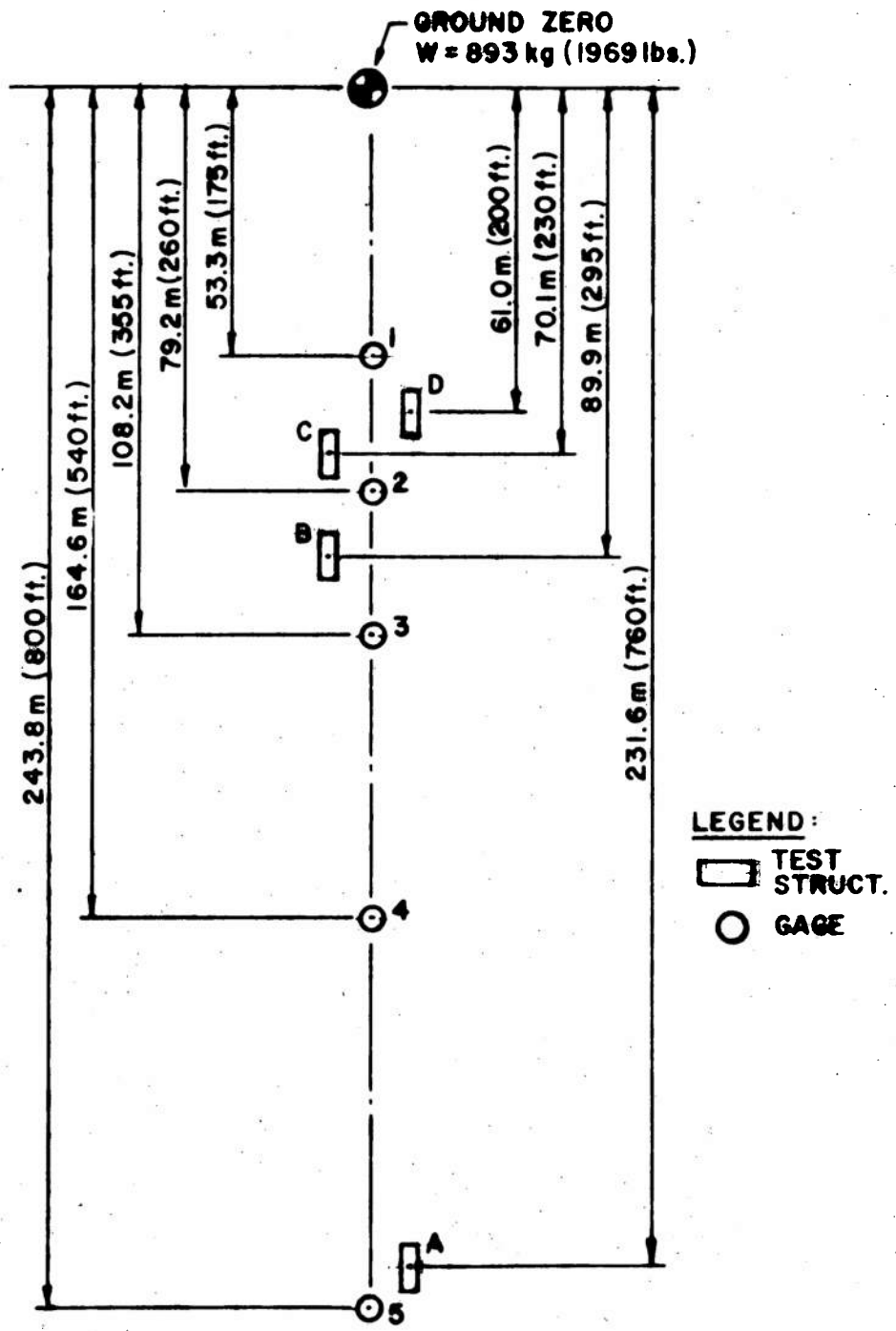
Figure 14. Set-up for Test 1
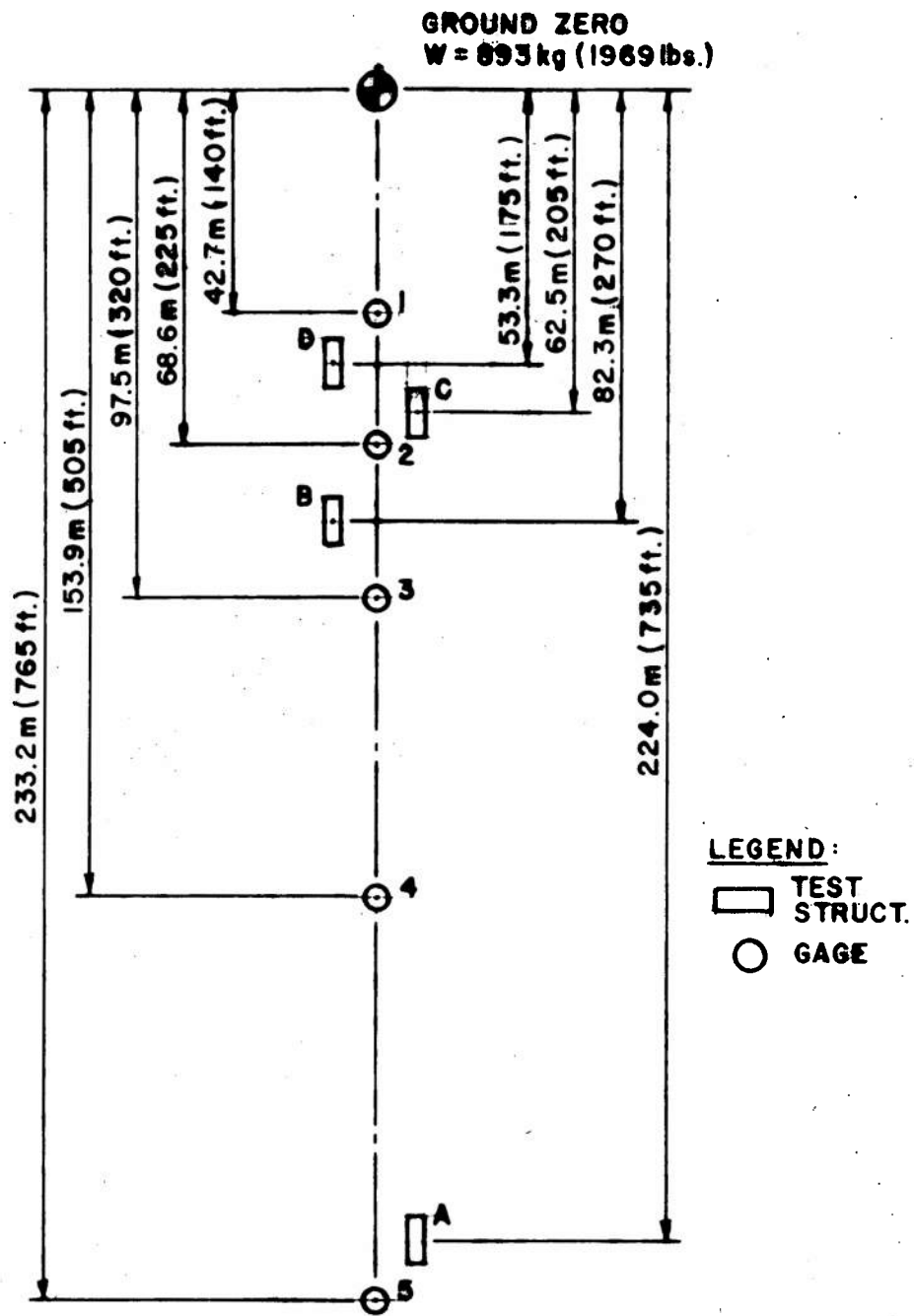
Figure 15. Set-up for Test 2

47
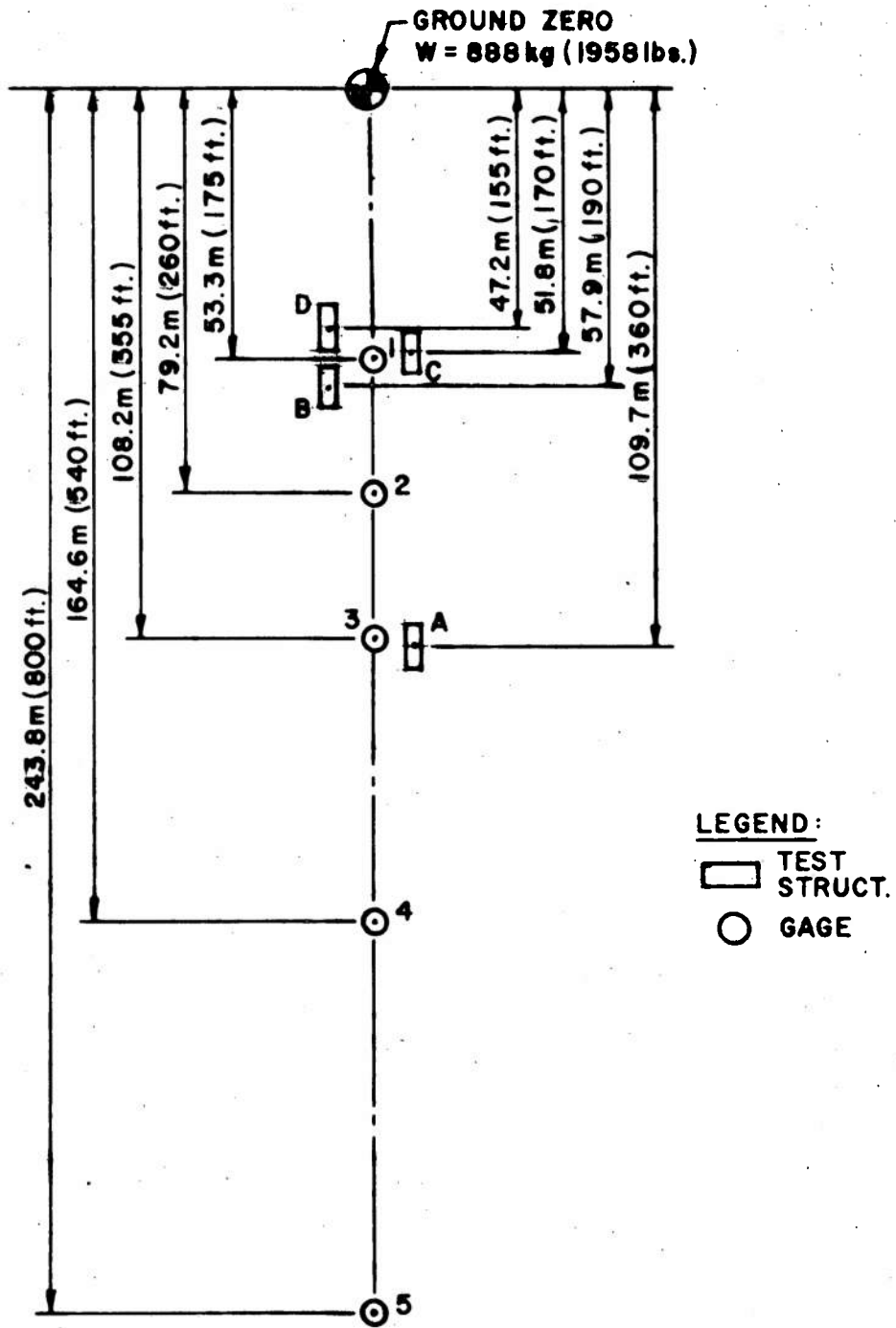
Figure 16. Set-up for Test 3
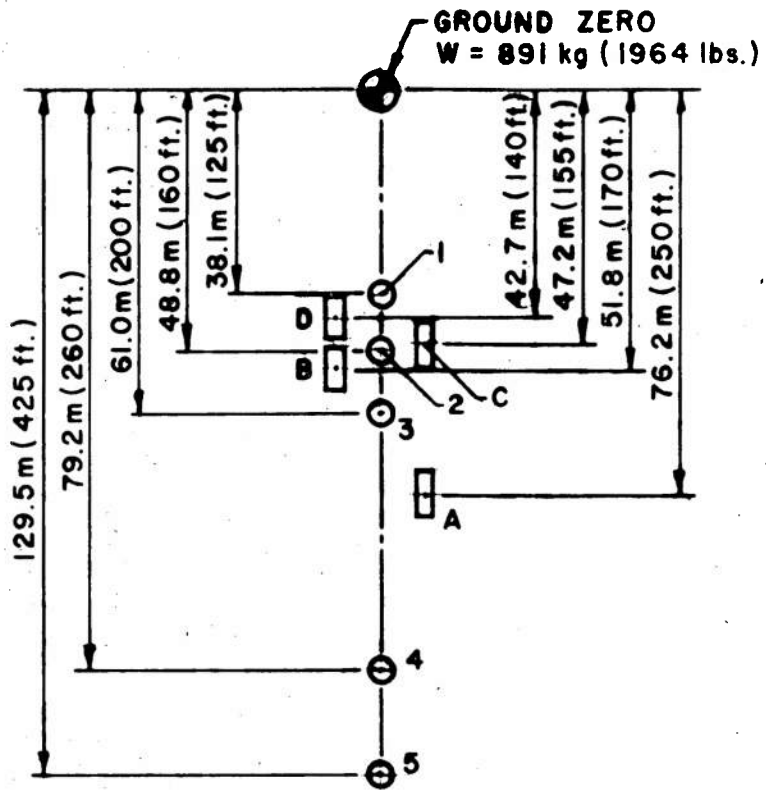
Figure 17. Set-up for Test 4

49
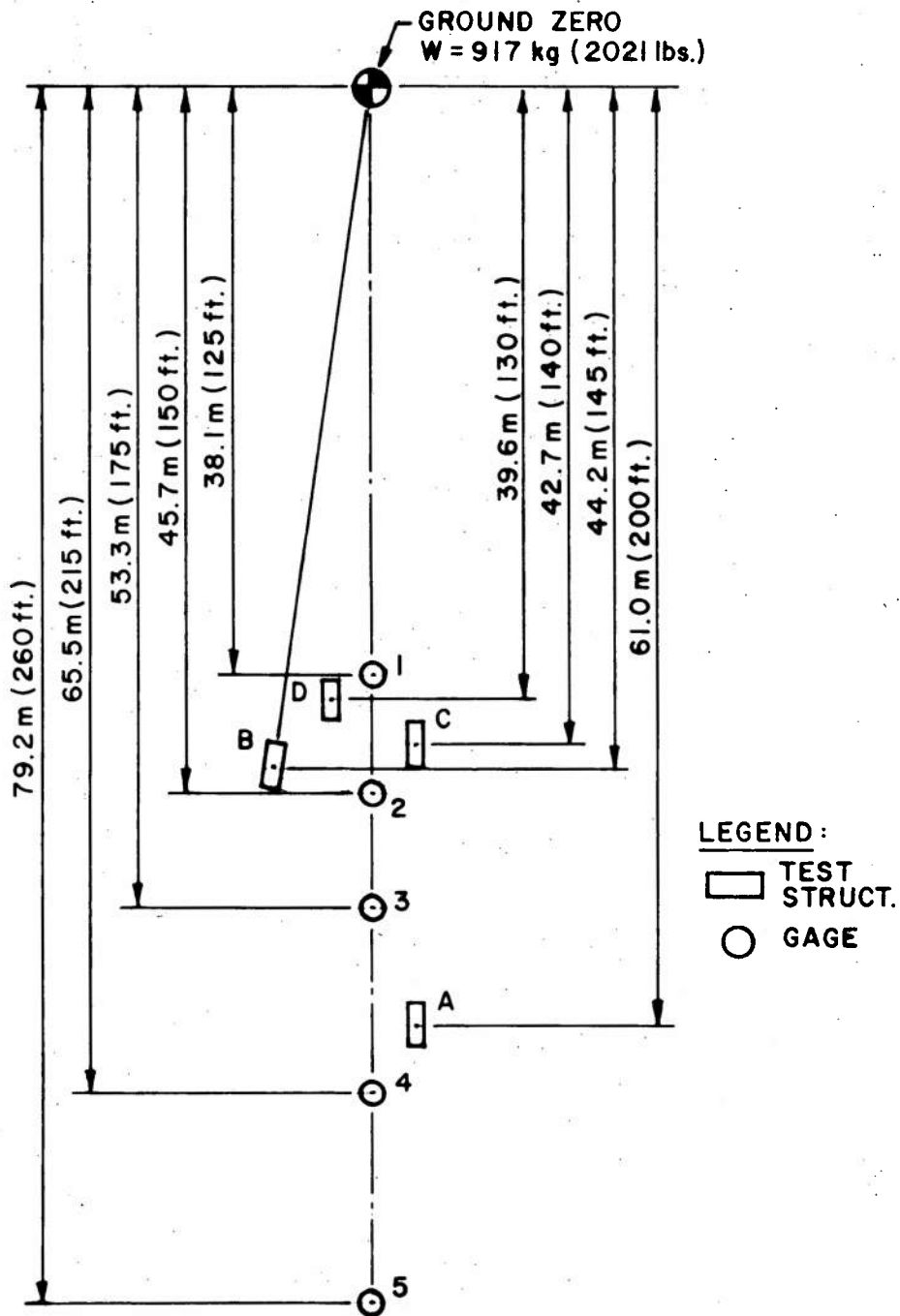
Figure 18. Set-up for Test 5.
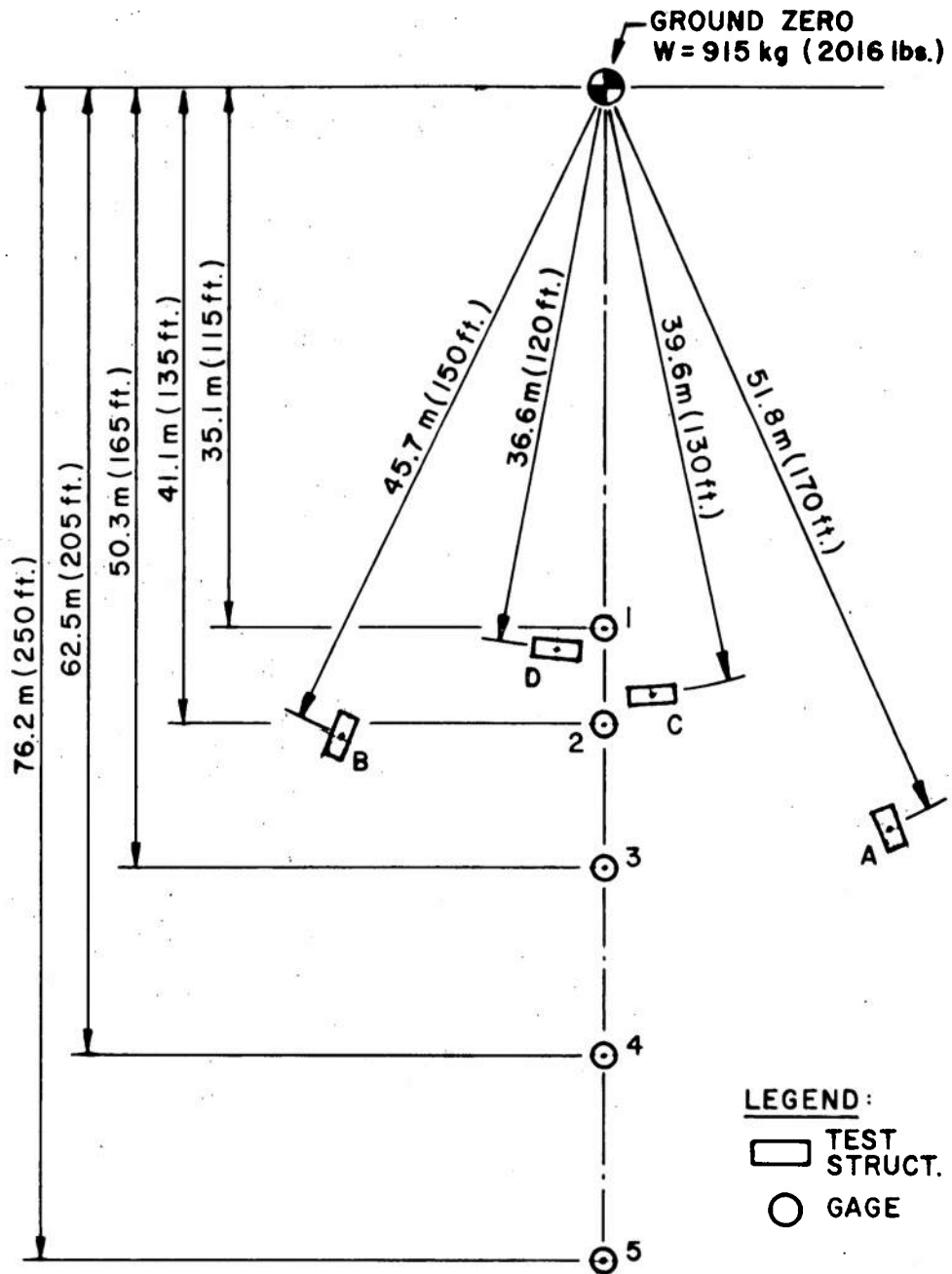
Figure 19. Set-up for Test 6
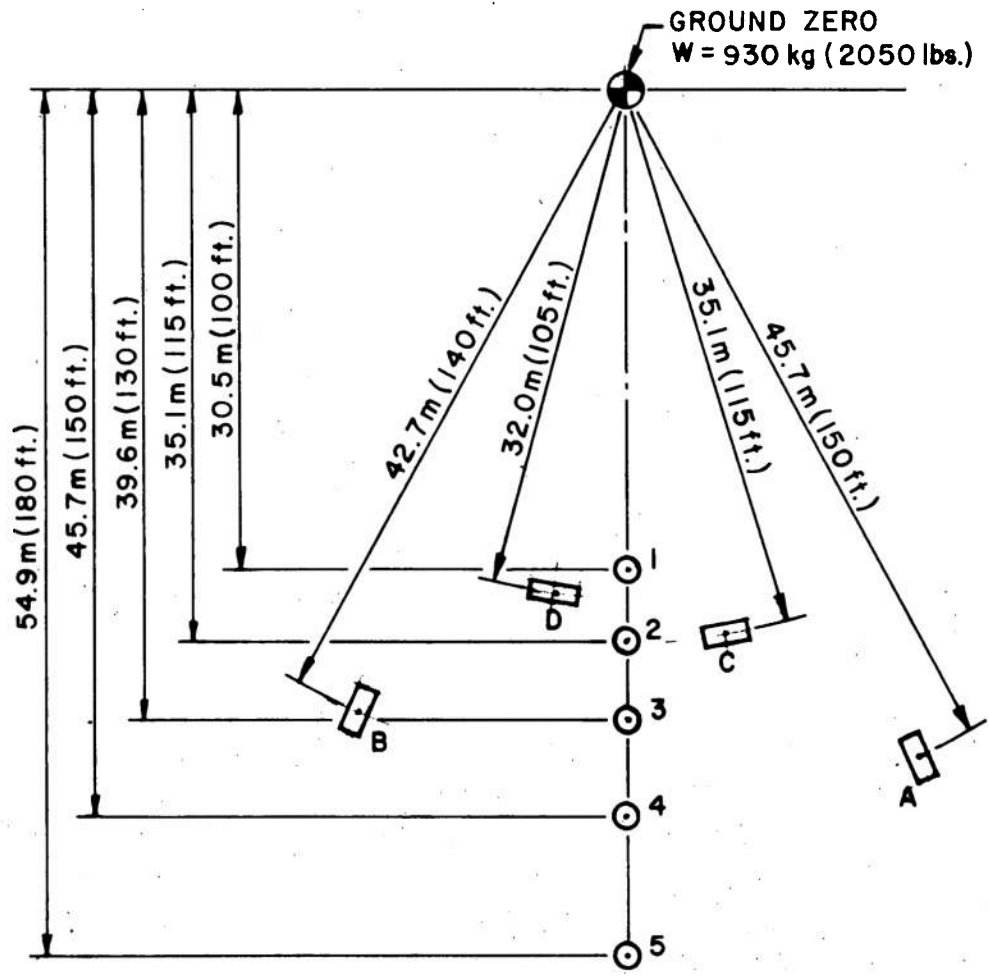
Figure 20. Set-up for Test 7
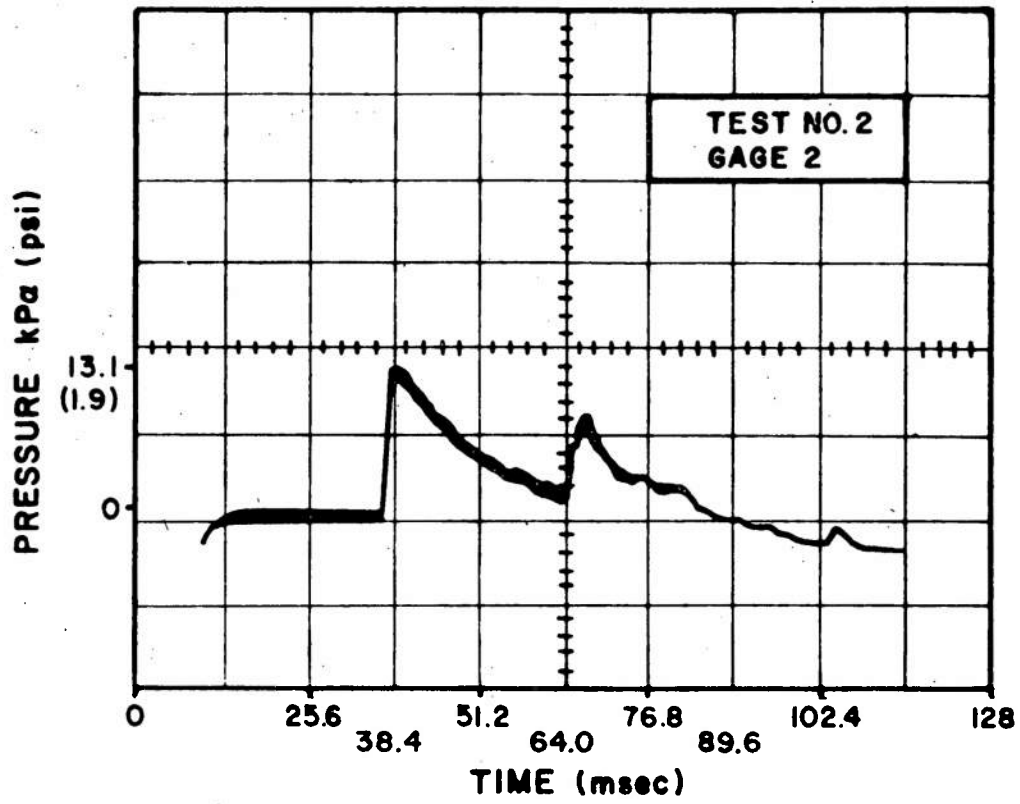
Figure 21. Typical pressure-versus-time history
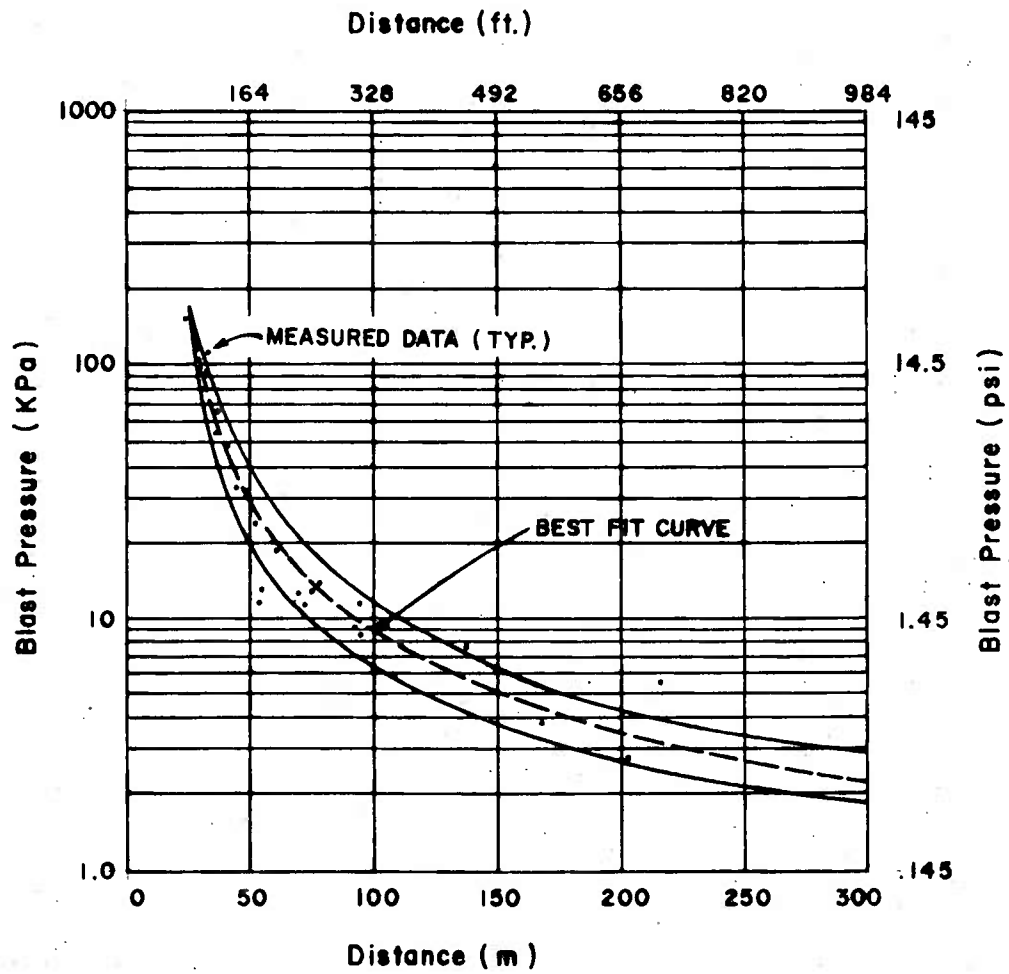
Figure 22. Pressure-versus-distance to charge curves
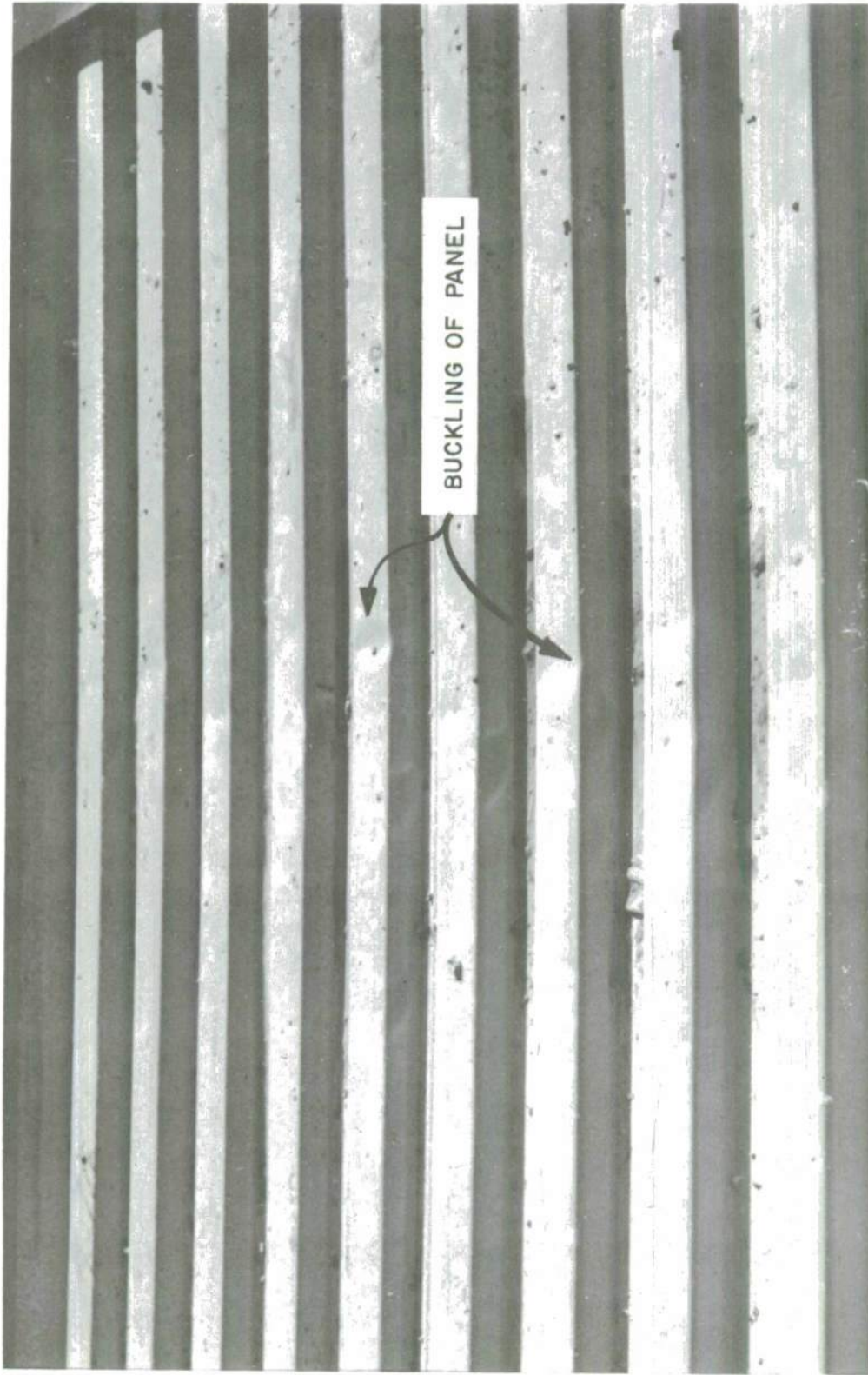
BUCKLING OF PANEL

Figure 23   Buckling of Cyclops panel on roof of Structure A
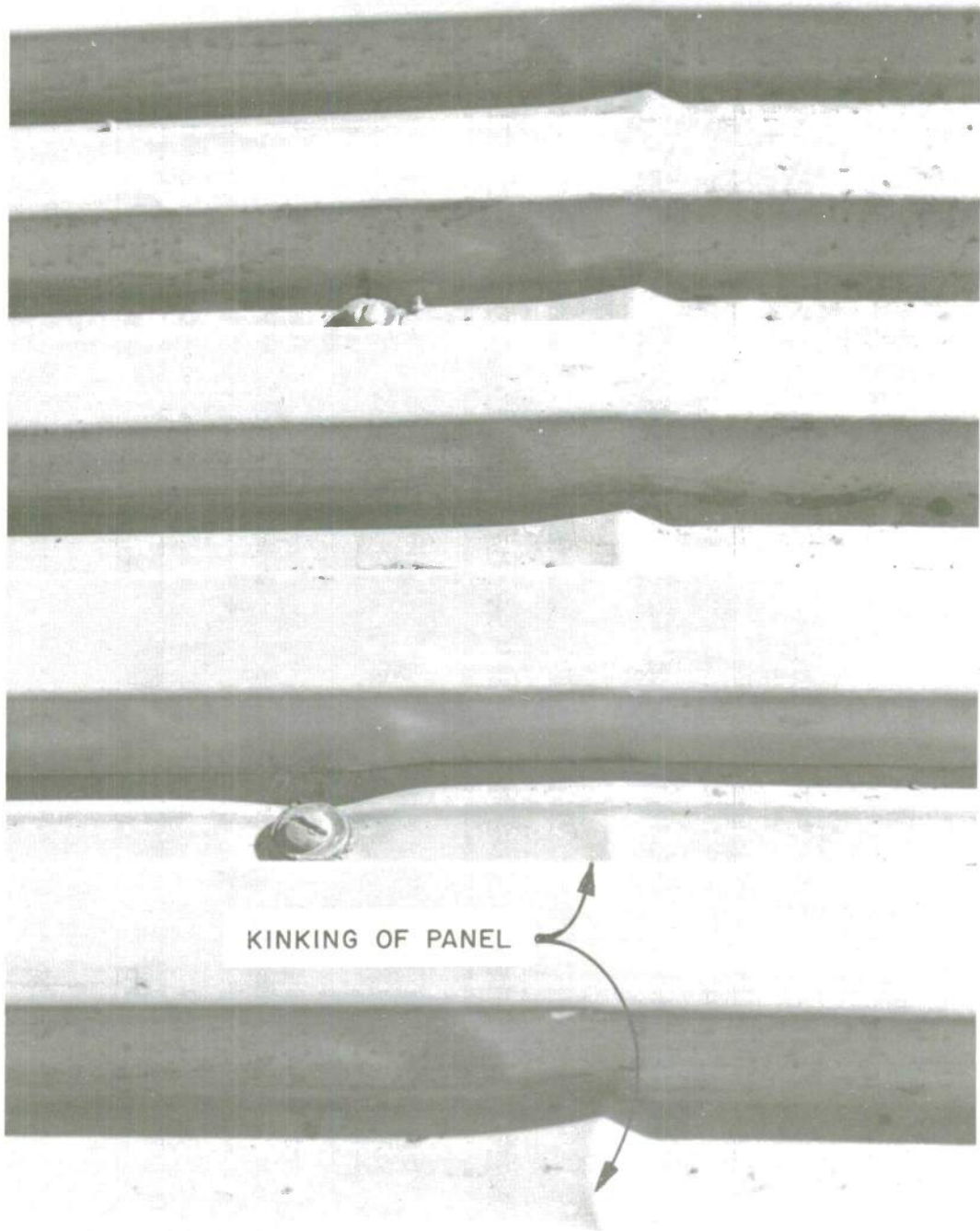
KINKING OF PANEL

Figure 24. Kinks at the interior supports of panel
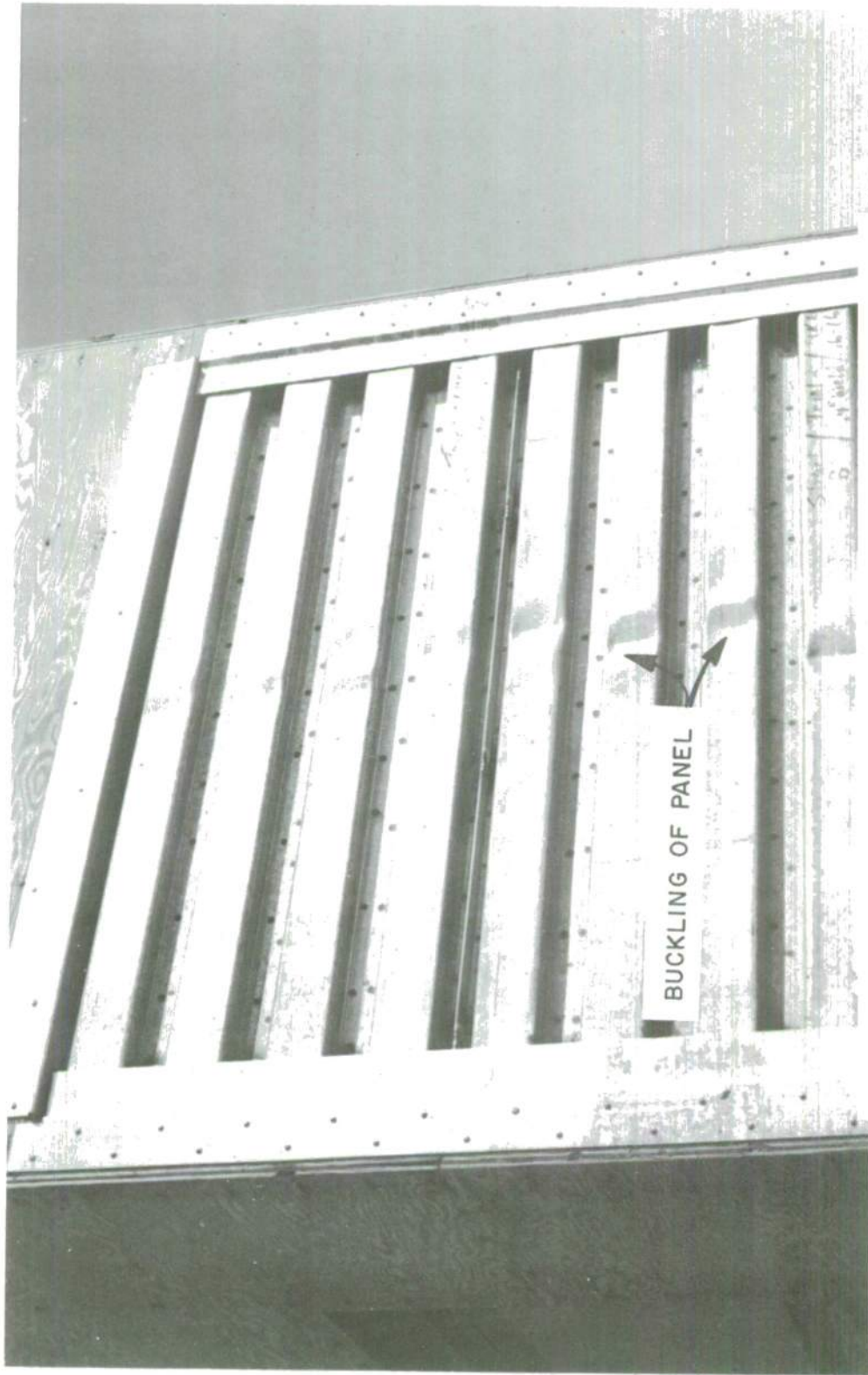
BUCKLING OF PANEL

Figure 25 Permanent deflection in panel on blastward face

Figure 26. Cracked foundation at Structure B
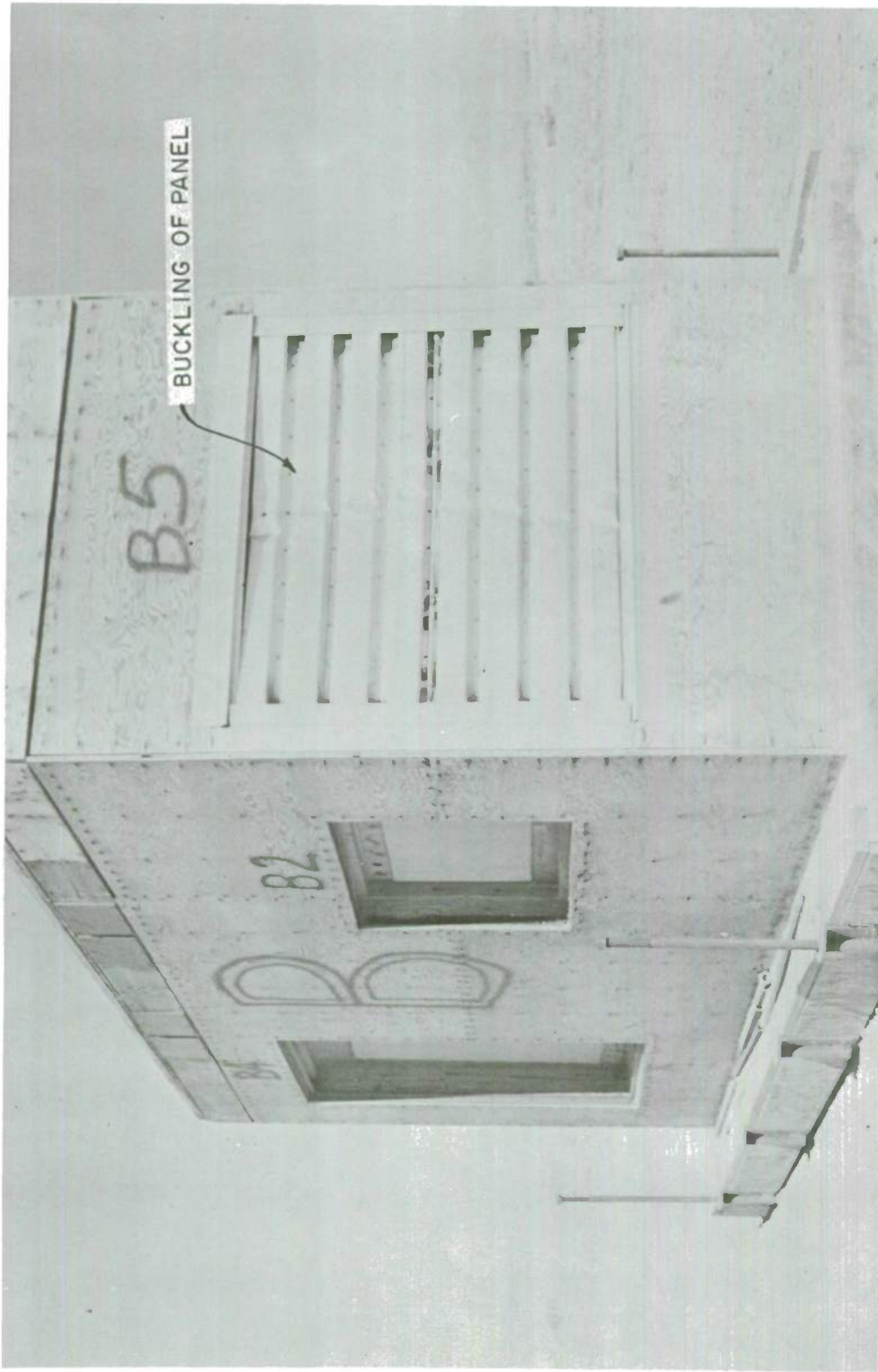
Figure 27. Buckling of the UKX 18-18 panel

BUCKLING OF PANEL

Figure 28. Buckling of the NKX 20-20 panel

BUCKLING OF PANEL

W.O
PIH
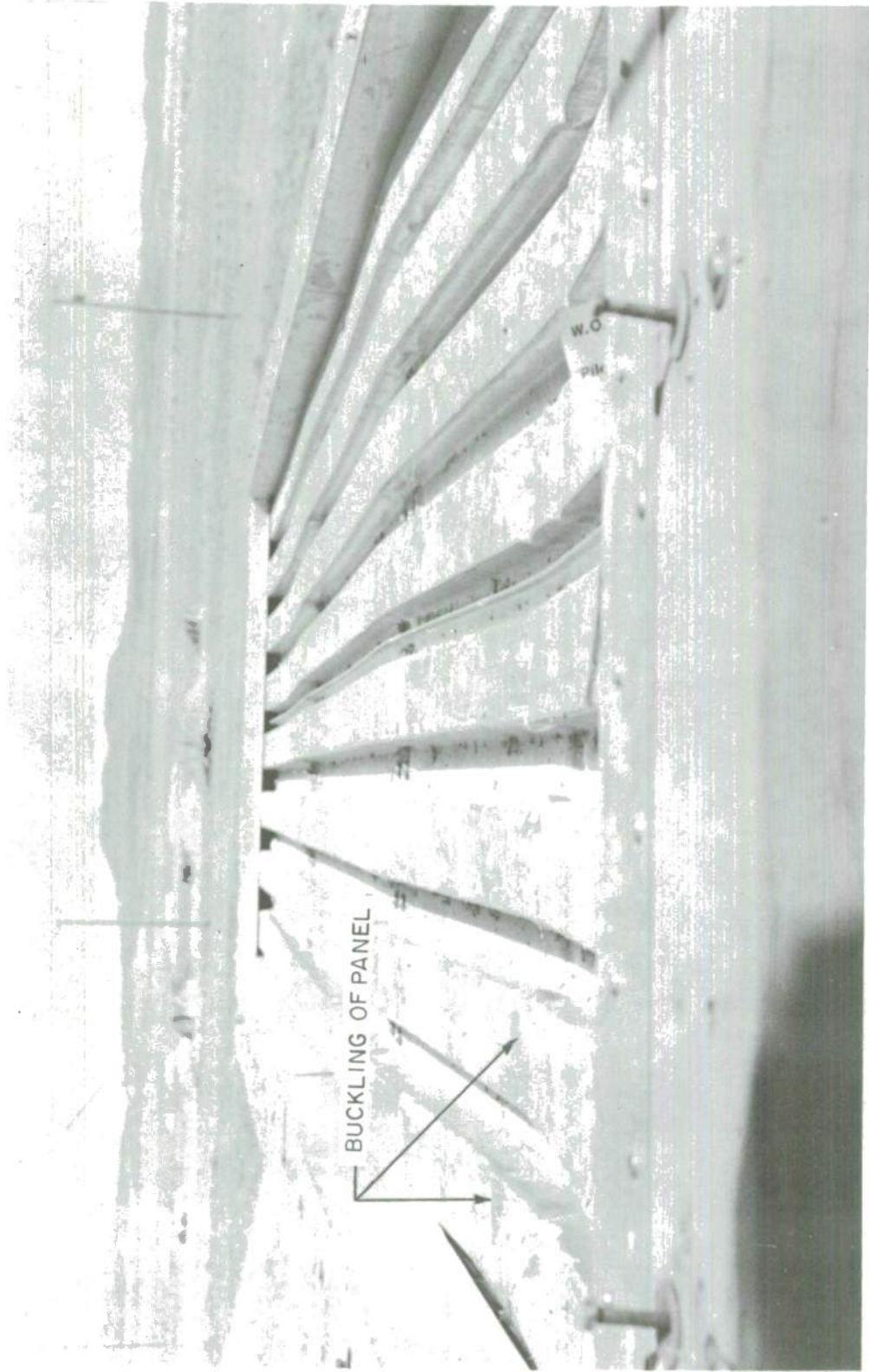
Figure 29. Damage to roof of Structure B

BUCKLING OF PANEL

Figure 30. Damage to roof of Structure C

PITTSBURGH TESTING LABORATORY
2066 SOUTH WEST TEMPLE
SALT LAKE CITY, UTAH 84115

FORM PO 600

ORDER NO. SLC-2471
FILE NO.
LABORATORY NO.
CUSTOMER NO. 6314-4002

U. S. Army Dugway Proving Ground
Procurement Office
P.O. Box 545
Dugway, Utah 84022

January 19, 19 77

REPORT OF TENSILE TEST OF __submitted sheet metal test specimens__

MADE FOR   Contract No. DA&D 09-77-M-0480   page 1 of 2

DESCRIPTION			ORIGINAL AREA SQ. IN.	YIELD POINT POUNDS	MAXIMUM LOAD POUNDS	YIELD POINT LB. PER SQ. IN.	TENSILE STRENGTH LB. PER SQ. IN.	ELONGATION		REDUCTION OF AREA PER CENT	FRACTURE
Sample No.	Width	Thick.						Gage	PER CENT		
1	0.725	0.026	.019	980	1140	51580	60000	2"	21		
2	0.732	0.026	.019	1040	1165	54740	61320	2"	24		
3	0.730	0.026	.019	935	1140	49210	60000	2"	35		
4	0.731	0.026	.019	935	1145	49210	60260	2"	30		
5	0.728	0.032	.023	1160	1375	50430	59780	2"	31		
6	0.726	0.032	.024	1150	1420	47920	59170	2"	30		
7	0.735	0.044	.032	1460	1840	45620	57500	2"	31		
8	0.733	0.043	.032	1470	1845	45940	57660	2"	34		
9	0.735	0.056	.041	1930	2410	47070	58780	2"	34		
10	0.737	0.055	.041	1890	2410	46100	58780	2"	32		
11	0.734	0.032	.023	1330	1530	57830	66520	2"	26		
12	0.734	0.033	.024	1185	1520	49380	63330	2"	28		
13	0.735	0.032	.024	1330	1545	55020	64380	2"	28		
14	0.737	0.032	.024	1140	1450	47500	60420	2"	35		
15	0.735	0.044	.032	1610	1940	50310	60620	2"	29		
16	0.735	0.043	.032	1575	1895	49220	59220	2"	37		
17	0.736	0.043	.032	1615	1925	50470	60160	2"	33		

PITTSBURGH TESTING LABORATORY

Figure 31   Tensile test, laboratory report
(Sheet 1 of 2)

63

FORM PG 800

U.S. Army Ougway Proving Ground

ORDER NO. SLC-2471
FILE NO.
LABORATORY NO.
CUSTOMER NO. 6314-4002

January 19, 19 77

REPORT OF TENSILE TEST OF ___submitted sheet metal test specimens___

MADE FOR Contract No. DAAD 09-77-M-0480

page 2 of 2

DESCRIPTION			ORIGINAL AREA SQ. IN.	YIELD POINT POUNDS	BREAKING LOAD POUNDS	YIELD POINT LB. PER SQ. IN.	TENSILE STRENGTH LB. PER SQ. IN.	ELONGATION		REDUCTION OF AREA PER CENT	FRACTURE
Sample No.	Width	Thick.						Gage	PER CENT		
18	0.735	0.043	.032	1570	1900	49060	59380	2"	37		
19	0.735	0.056	.041	2080	2550	50730	62200	2"	34		
20	0.733	0.054	.040	1810	2410	45250	60250	2"	36		
21	0.735	0.056	.041	2070	2550	50500	62200	2"	33		
22	0.734	0.054	.040	1800	2390	45000	59750	2"	34		
23	0.735	0.032	.024	1130	1390	47080	57920	2"	18*		
24	0.735	0.031	.023	1000	1400	43480	60870	2"	30		
25	0.734	0.031	.023	1090	1415	47390	61520	2"	35		
26	0.735	0.031	.023	1030	1420	44780	61740	2"	34		
27	0.734	0.045	.033	1515	1920	45910	58180	2"	30		
28	0.732	0.043	.031	1540	1830	49670	59030	2"	36		
29	0.731	0.045	.033	1490	1865	45140	56520	2"	30		
30	0.727	0.043	.031	1490	1850	48060	59680	2"	38		
* broke outside gage marks											
Thickness is based on a sheet thickness - coating removed.											

PITTSBURGH TESTING LABORATORY

James L. Munnerlyn, Manager
Salt Lake City District

Figure 31   Tensile test, laboratory report
(Sheet 2 of 2)

APPENDIX A

Introduction

Based upon the discussions presented in the previous section, the methods and procedures of reference 2 pertaining to the blast design of cold-formed steel panels have been revised and portions of section 3.7 of the referenced report are given below.

Special Provisions For Cold-Formed Steel Panels

General

Recent studies on cold-formed panels have shown that the effective width relationships for cold-formed light gage elements under dynamic loading do not differ significantly from the static relationships. Consequently, the recommendations presented in the AISI Specifications are used as the basis for establishing the special provisions needed for the design of cold-formed panels to resist pressure-time loading. Some of the formulas of the Specification have been extended to comply with ultimate load conditions and to permit limited performance in the inelastic range.

Two main modes of failure can be recognized, one governed by flexure and the other by shear. In the case of continuous members, the interaction of the two influences plays a major role in determining the behavior and the ultimate capacity. Due to the relatively thin webs encountered in cold-formed members, special attention must also be paid to crippling problems. Basically, the design will be dictated by the capacity in flexure but subject to the constraints imposed by shear resistance and local stability.

Resistance in Flexure

The material properties of the steel used in the production of cold-formed steel panels conformed to ASTM Specification A 446. This standard covers three grades (a, b, and c) depending on the yield point. Most commonly, panels are made of steel complying with the requirements of grade a, with a minimum yield point of 33 ksi and an elongation of rupture of 20 percent for a 2-inch gage length. However, it is generally known that the yield stress of the material used in the manufacture of cold-formed panels generally exceeds the specified minimum yield

stress by a significant margin; therefore, it is recommended that a minimum yield stress of 40 ksi be used unless the actual yield stress of the material is known.

In calculating the dynamic yield stress of cold-formed steel panels, it is recommended that a dynamic increase factor of 1.1 be applied irrespective of actual strain rate and, consequently, the value to be used in design will be

$$F_{dy} = 1.1 \ F_y \hspace{3cm} (A.1)$$

and hence, F_{dy} equals 44.0 ksi $(0.30 \times 10^6$ kPa) for the particular case of 40-ksi $(0.28 \times 10^6$ kPa) steel.

Ultimate design procedures, combined with the effective width concept, are used in evaluating the strength of cold-formed light gage elements. Thus, a characteristic feature of cold-formed elements is the variation of their section properties with the intensity of the load. As the load increases beyond the level corresponding to the occurrence of local buckling, the effective area of the compression flange is reduced; as a result, the neutral axis moves toward the tension flange with the effective properties of the cross-section such as A, I and S, decreasing with load increase. The properties of the panels, as tabulated by the manufacturer, are related to different stress levels. The value of S referred to that of the effective section modulus at ultimate and the value of I related to a service stress level of 20 ksi. In the case of panels fabricated from hat sections and a flat sheet, two section moduli are tabulated, S^+ and S^-, referring to the effective section modulus for positive and negative moments, respectively. Consequently, the following ultimate moment capacities are obtained:

$$M_{up} = F_{dy} \ S^+ \hspace{3cm} (A.2)$$

$$M_{un} = F_{dy} \ S^- \hspace{3cm} (A.3)$$

where M_{up} = ultimate positive moment capacity for a one-foot width of panel

M_{un} = ultimate negative moment capacity for a one-foot width of panel.

It should be noted that in cases where tabulated section properties are not available, the required properties may be calculated based upon the relationships in the AISI Design Specification.

As for any single-span flexural element, the panel may be subjected to different end conditions, either simply supported or fixed. The fixed-fixed condition is seldom found in practice since this situation is difficult to achieve in actual installations. The simply fixed condition is found because of symmetry in each span of a two-span continuous panel. For multi-span members (three or more), the response is governed by that of the first span which is generally characterized by a simply supported condition at one support and a partial moment restraint at the other. Three typical cases can, therefore, be considered:

1. Simply supported at both ends (single span).

2. Simply supported at one end and fixed at the other (two equal span continuous member).

3. Simply supported at one end and partially fixed at the other (first span of an equally spaced multi-span element).

The resistance of the panel is a function of both the strength of the section and the maximum moment in the member. As demonstrated by recent tests, the ability of the panel to sustain yielding of its cross-section produces significant moment re-distribution in the continuous member which results in an increase of the resistance of the panel.

Consequently, for design purposes, the following resistance formulas are recommended:

1. Simply supported, single-span panel

$$r_u = (8 \ M_{up})/L^2 \qquad\qquad (A.4)$$

2. Simply fixed, single-span panel or first span of an equally spaced continuous panel

$$r_u = 4(M_{un} + 2M_{up})L^2 \qquad\qquad (A.5)$$

where r_u is the resistance per unit length of the panel.

As mentioned in the previous sections, the behavior of cold-formed sections in flexure is non-linear as shown in figures A-1 and A-2. A bilinear approximation of the resistance-deflection curve is assumed for design. The equivalent elastic deflection X_E is obtained by using the following equation:

67

$$X_E = (\beta\, r_u L^4)/EI_{20} \qquad\qquad (A.6)$$

where β is a constant depending on the support conditions as follows:

$\beta = 0.0130$ for a simply supported element

$\beta = 0.0062$ for simply fixed or continuous elements.

I_{20} is defined as the ~~effective~~ moment of inertia of the section at a service stress of 20 ksi (0.14×10^6 kPa). The value of I_{20} is generally tabulated as a section property of the panel.

Figure A-3 illustrates the non-linear character of the resistance-deflection curve and the suggested bilinear approximation. X_1 is defined as the maximum deflection at maximum resistance and X_u is the ultimate deflection after the drop is load-carrying capacity. Based on experimental evidence, the ratio of X_1/X_E has ben estimated to range between 2.0 and 2.5. The amount of plastic deformation which is acceptable in design will vary in magnitude depending on the reusability or non-reusability of the panel after an accidental explosion.

The extent of plastic behavior is expressed in terms of a ductility ratio $\mu = X_m/X_E$. In Figure A-3, $(X_m)_r$ and $(X_m)_n$ designate the maximum deflections for reusable and non-reusable, respectively. Based upon the recommendations the previous section, the criteria have been changed to:

$$\mu = (X_m)_r/X_E = 3.0 \text{ for reusable}$$

and $\qquad\qquad \mu = (X_m)_n/X_E = 6.0$ for non-reusable. $\qquad (A.7)$

The maximum displacements are kept below the deflection, corresponding to maximum resistance, in order to prevent any serious impairment to the element.

In addition, in order to restrict the magnitude of rotation at the supports, limitations are placed on the maximum deflections, namely:

$$(X_m)_r = L/57 \text{ or } \theta_{max} = 2.0^0$$

$$(X_m)_n = L/29 \text{ or } \theta_{max} = 4.0^0$$

$\qquad\qquad (A.8)$

for reusable and non-reusable elements, respectively.

When performing a one-degree-of-freedom analysis of the panel's behavior, the properties of the equivalent system can be evaluated by using a load-mass factor, $K_{LM} = 0.74$, which is an average value applicable to all support conditions. The natural period of vibration for the equivalent single-degree system is thus obtained by

$$T_N = 2\pi\sqrt{0.74mL/K_E} \qquad\qquad (A-9)$$

where $\qquad m = w/g$ is the unit mass of the panel and

$\qquad\qquad K_E = r_uL/X_E$ is the equivalent elastic stiffness of the system.

The problem of rebound should be considered in the design of decking due to the different section properties of the panel, depending on whether the hat section or the flat sheet is in compression. Figure A.4 presents the maximum elastic resistance in rebound as a function of T/T_N. While the behavior of the panel in rebound does not often control, the designer should be aware of the problem; in any event, there is a need for providing connections capable of resisting uplift or pull-out forces due to load reversal in rebound.

In conclusion, due a to limited amount of experimental data available on the performance of cold-formed, light gage elements in the inelastic domain, the overall level of confidence in the design of that type of element should be considered lower than that of hot-rolled sections.

Resistance in Shear

Webs with h/t in excess of 60 are common among cold-formed members and the fabrication process makes it impractical to use stiffners. The design web stresses must therefore be limited to insure adequate stability without the aid of stiffners, thereby preventing premature local web failure and the accompanying loss of load-carrying capacity.

The possibility of web buckling due to bending stresses exists and the critical bending stress is given by

$$F_{cr} = 640,000/ (h/t)^2 \leq F_y \qquad\qquad (A-10)$$

Equating F_{cr} to 32 ksi (a stress close to the yielding of the material), a value $h/t = 141$ is obtained. Since it is known that webs do not actually fail at these theoretical buckling stresses due to the development of post-buckling strength, it can be

safely assumed that webs with h/t $\leq$ 150 will not be susceptible to flexural buckling. Moreover, since the AISI recommendations prescribe a limit of h/t = 150 for unstiffened webs, this type of web instability need not be considered in design.

Panels are generally manufactured in geometrical proportions which preclude web-shear problems when used for recommended spans and minimum support-bearing lengths of 2 to 3 inches. In blast design, however, because of the greater intensity of the loading, the increase in required flexural resistance of the panels calls for shorter spans.

In most cases, the shear capacity of a web is dictated by instability due to either

1. Simple shear stresses or

2. Combined bending and shearing stresses.

For the case of simple shear stresses, as encountered at end supports, it is important to distinguish three ranges of behavior depending on the magnitude of h/t. For large values of h/t, the maximum shear stress is dictated by elastic buckling in shear and for intermediate h/t values, the inelastic buckling of the web governs; whereas for very small values of h/t, local buckling will not occur and failure will be caused by yielding produced by shear stresses. This point is illustrated in figure A.5 for F_y = 40 ksi. The provisions of the AISI Specification in this area are based on a safety factor ranging from 1.44 to 1.67 depending upon h/t. For blast-resistant design, the recommended design stresses for simple shear are based on an extension of the AISI provisions to comply with ultimate load conditions. The specific equations for use in design for F_y = 40, 60 and 80 ksi are summarized in tables A-1 (a), A-2 (a) and A-3 (a), respectively.

At the interior supports of continuous panels, high bending moments combined with large shear forces are present and webs must be checked for buckling due to these forces. The interaction formula presented in the AISI Specification is given in terms of the allowable stresses rather than critical stresses which produce buckling. In order to adapt this interaction formula to ultimate load conditions, the problem of inelastic buckling under combined stresses has been considered in the development of the recommended design data.

In order to minimize the amount and complexity of design calculations, the allowable dynamic design shear stresses

70

at the interior support of a continuous member have been computed for different depth-thickness ratios for F_y = 40, 60 and 80 ksi, and tabulated in tables A-1 (b), A-2 (b) and A-3 (b), respectively.

Web Crippling

In addition to shear problems, concentrated loads or reactions at panel supports, applied over relatively short lengths, can produce load intensities that can cripple unstiffened thin webs. The problem of web crippling is rather complicated for theoretical analysis because it involves:

1. Non-uniform stress distribution under the applied load and the adjacent portions of the web.

2. Elastic and inelastic stability of the web element.

3. Local yielding in the intermediate region of load application.

4. The bending produced by the eccentric load (or reaction) when it is applied on the bearing flange at a distance beyond the curved transition of the web.

The AISI recommendations have been developed by relating extensive experimental data to service loads with a safety factor of 2.2 which was established taking into account the scatter in the data. For blast design of cold-formed panels, it is recommended that the AISI values be multiplied by a factor of 1.50 in order to relate the crippling loads to ultimate conditions with sufficient provisions for scatter in test data.

For those sections that provide a high degree of restraint against rotation of their webs such as I-beams made by welding two angles to a channel, the ultimate crippling loads are given as follows:

1. Acceptable ultimate end support reaction

$$Q_u = 1.5 \ F_y t^2 \ (4.44 + 0.558 \ \sqrt{N/t})$$

2. Acceptable ultimate interior support reaction

$$Q_u = 1.5 \ F_y t^2 \ (6.66 + 1.446 \ \sqrt{N/t}$$

71

where Q_u = ultimate support reaction

                 F_y = yield stress

                 N = bearing length

                 t = web thickness.

The charts in figures A.6 and A.7 present the variation of Q_u as a function of the web thickness for bearing lengths from 1 to 5 inches, for end and interior supports, respectively. tables A.4 through A.7 present the same variation of Q_u for F_y = 60 and 80 ksi, respectively. It should be noted that the values reported in the charts and tables relate to one web only, the total ultimate reaction being obtained by multiplying Q_u by the number of webs in the panel.

In design, the maximum shear forces and dynamic reactions are computed as a function of the maximum resistance in flexure. The ultimate load-carrying capacity of the webs of the panel must then be compared with these forces. As a general comment, the shear capacity is controlled by simple shear buckling or web crippling for simply supported elements and by the allowable design shear stresses at the interior supports for continuous panels.

In addition, it can be shown that the resistance in shear governs only in cases of relatively very short spans. If a design is controlled by shear resistance, it is recommended that another panel be selected since a flexural failure mode is generally preferred. However, for existing installations that are to be checked for their structural strength in a certain pressure range, the maximum resistance of the panel may be determined by either flexure or shear, whichever controls.

Table A-1. Dynamic design shear stress for webs of cold-formed members (F_y = 40 ksi)

(a) Simple Shear

$(h/t) \leq 57$	$F_{dv} = 0.50F_{dy} \leq 22.0$ ksi
$57 < (h/t) \leq 83$	$F_{dv} = 1.26 \times 10^3/(h/t)$
$83 < (h/t) \leq 150$	$F_{dv} = 1.07 \times 10^5/(h/t)$

(b) Combined Bending and Shear

(h/t)	F_{dv} (ksi)
20	10.94
30	10.84
40	10.72
50	10.57
60	10.42
70	10.22
80	9.94
90	9.62
100	9.00
110	8.25
120	7.43

73

Table A-2. Dynamic design shear stress for webs of
cold-formed members (F_y = 60 ksi)

(a) Simple Shear

$(h/t) \leq 47$	$F_{dv} = 0.50F_{dy} \leq 33$ ksi
$47 < (h/t) \leq 67$	$F_{dv} = 1.54 \times 10^3/(h/t)$
$67 < (h/t) \leq 150$	$F_{dv} = 1.07 \times 10^5/(h/t)$

(b) Combined Bending and Shear

(h/t)	F_{dv} (ksi)
20	16.41
30	16.23
40	16.02
50	15.75
60	15.00
70	14.20
80	13.00
90	11.75
100	10.40
110	8.75
120	7.43

Table A-3. Dynamic design shear stress for webs of
cold-formed members (F_y = 80 ksi)

(a) Simple Shear

(h/t) ≤ 41	$F_{dv} = 0.50F_{dy} \leq 44$ ksi
41 < (h/t) ≤ 58	$F_{dv} = 1.78 \times 10^3/(h/t)$
58 < (h/t) ≤ 150	$F_{dv} = 1.07 \times 10^5/(h/t)$

(b) Combined Bending and Shear

(h/t)	F_{dv} (ksi)
20	21.60
30	21.00
40	20.00
50	18.80
60	17.50
70	16.00
80	14.30
90	12.50
100	10.75
110	8.84
120	7.43

75

Table A.4 Maximum end support reaction for cold-formed
steel sections (F_y = 60 ksi)

$$Q_u = 1.5t^2 F_y(4.44 + 0.558 \sqrt{N/t})$$
$$= 90t^2(4.44 + 0.558 \sqrt{N/t}) \text{ ksi}$$

N = Bearing Length (in)

Sheet thickness t (in)	Q_u (ksi)				
	N = 1	N = 2	N = 3	N = 4	N = 5
.02	.30	.36	.41	.45	.48
.04	1.04	1.22	1.34	1.44	1.55
.06	2.18	2.48	2.72	2.91	3.09
.08	3.69	4.17	4.53	4.83	5.10
.10	5.58	6.24	6.75	7.17	7.55
.12	7.85	8.70	9.38	9.93	10.43
.14	10.47	11.55	12.39	13.10	13.71
.16	13.44	14.78	15.80	16.67	17.42
.18	16.79	18.32	19.59	20.61	21.53
.20	20.48	22.34	23.76	24.98	26.03

Table A.5 Maximum interior support reaction for cold-formed
steel sections (F_y = 60 ksi)

$$Q_u = 1.5t^2 F_y (6.66 + 1.446 \sqrt{N/t})$$

$$= 90t^2 (6.66 + 1.446 \sqrt{N/t}) \text{ ksi}$$

N = Bearing Length (in)

Sheet thickness t (in)	Q_u (ksi)				
	N = 1	N = 2	N = 3	N = 4	N = 5
.02	.62	.77	.87	.98	1.07
.04	2.00	2.43	2.76	3.05	3.29
.06	4.07	4.86	5.48	5.99	6.44
.08	6.78	8.00	8.94	9.72	10.43
.10	10.11	11.82	13.13	14.22	15.20
.12	14.04	16.28	18.00	19.46	20.73
.14	18.57	21.39	23.55	25.38	26.99
.16	23.67	27.12	29.78	32.01	33.98
.18	29.36	33.48	36.63	39.30	41.64
.20	35.61	40.44	44.13	47.25	50.01

77

Table A.6   Maximum end support reaction for cold-formed
steel sections (F_y = 80 ksi)

$$Q_u = 1.5t^2 F_y (4.44 + 0.558 \sqrt{N/t})$$

$$= 120t^2 (4.44 + 0.558 \sqrt{N/t}) \text{ ksi}$$

N = Bearing Length (in)

Sheet thickness t (in)	Q_u (ksi)				
	N = 1	N = 2	N = 3	N = 4	N = 5
.02	.40	.48	.54	.60	.64
.04	1.38	1.62	1.78	1.92	2.06
.06	2.90	3.30	3.62	3.88	4.12
.08	4.92	5.56	6.04	6.44	6.80
.10	7.44	8.32	9.00	9.56	10.60
.12	10.46	11.60	12.50	13.24	13.95
.14	13.96	15.40	16.52	17.46	18.28
.16	17.92	19.70	21.06	22.22	23.22
.18	22.38	24.50	26.12	27.48	28.70
.20	27.30	29.78	31.68	33.30	34.70

Table A.7 Maximum interior support reaction for cold-formed
steel sections (F_y = 80 ksi)

$$Q_u = 1.5t^2 F_y(6.66 + 1.446\sqrt{N/t})$$

$$= 120t^2(6.66 + 1.446\sqrt{N/t}) \text{ ksi}$$

N = Bearing Length (in)

Sheet thickness t (in)	Q_u (ksi)				
	N = 1	N = 2	N = 3	N = 4	N = 5
.02	.82	1.02	1.16	1.30	1.42
.04	2.66	3.24	3.68	4.06	4.38
.06	5.42	6.48	7.30	7.98	8.58
.08	9.04	10.66	11.92	12.96	13.90
.10	13.48	15.76	17.50	18.96	20.26
.12	18.72	21.70	24.00	25.94	27.64
.14	24.76	28.52	31.40	33.84	35.98
.16	31.56	36.16	39.70	42.68	45.30
.18	39.14	44.64	48.84	52.40	55.52
.20	47.48	53.92	58.64	63.00	66.68

79
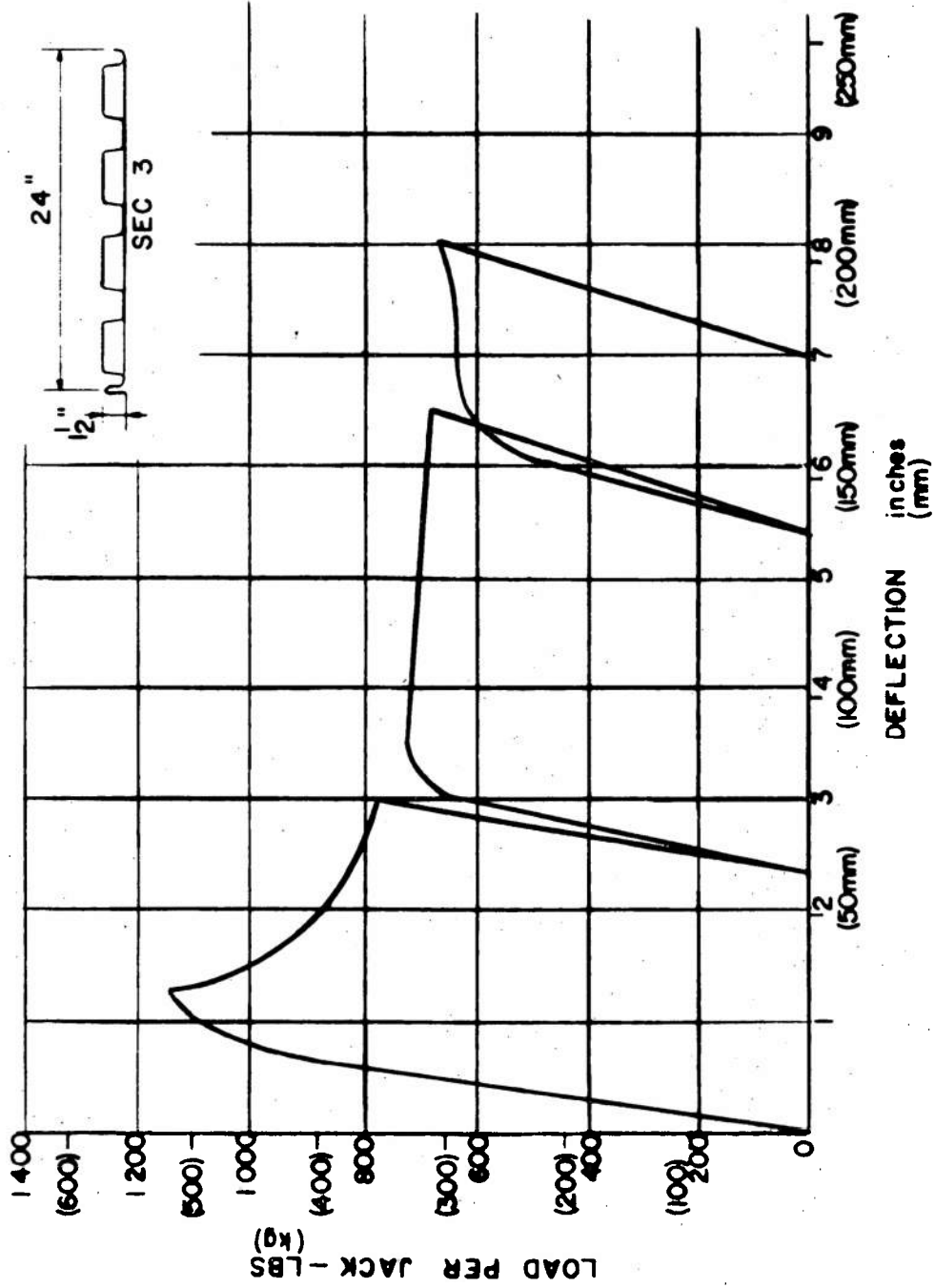
Figure A.1. Behavior of open sections

80
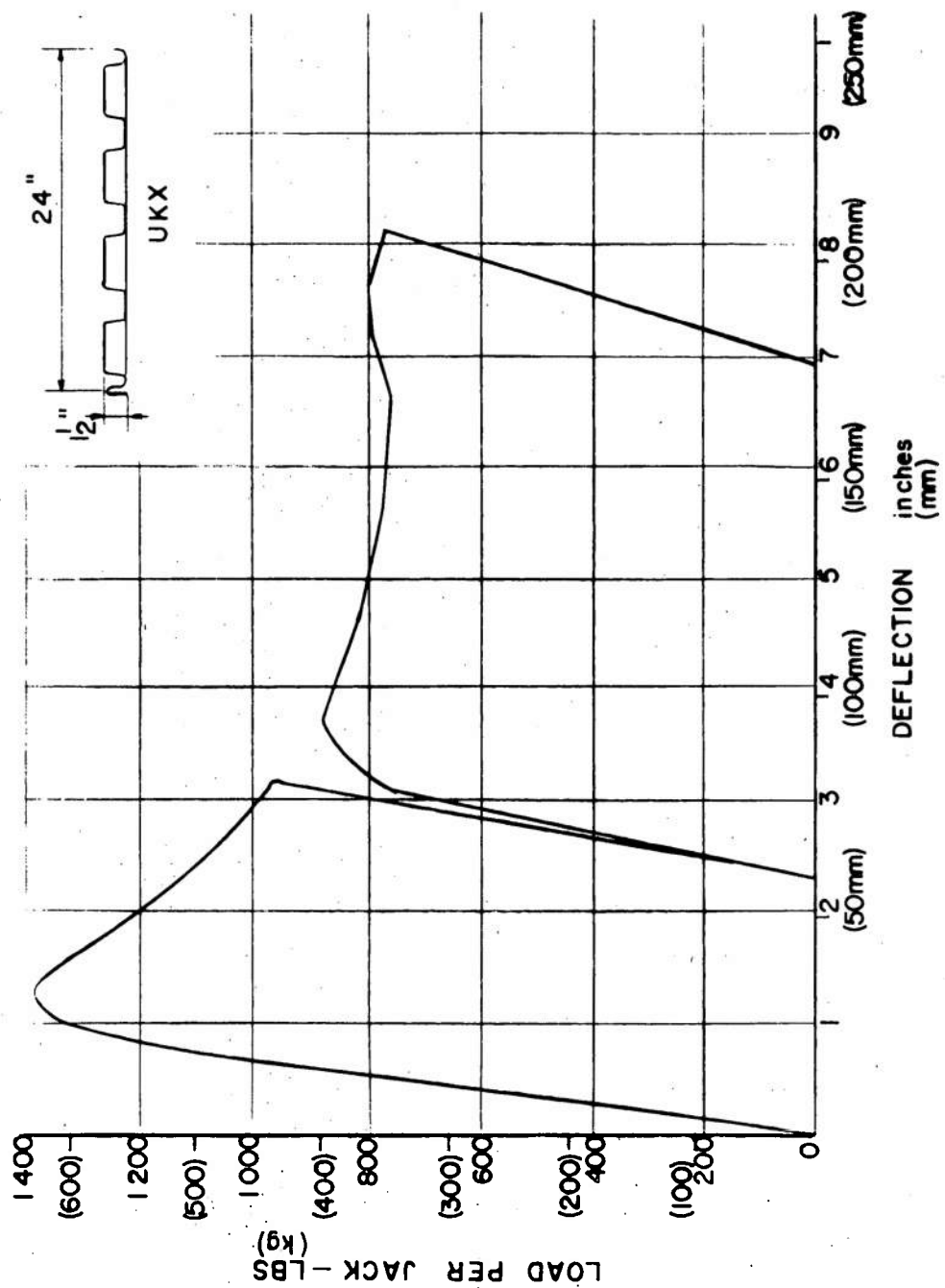
Figure A.2. Behavior of closed sections
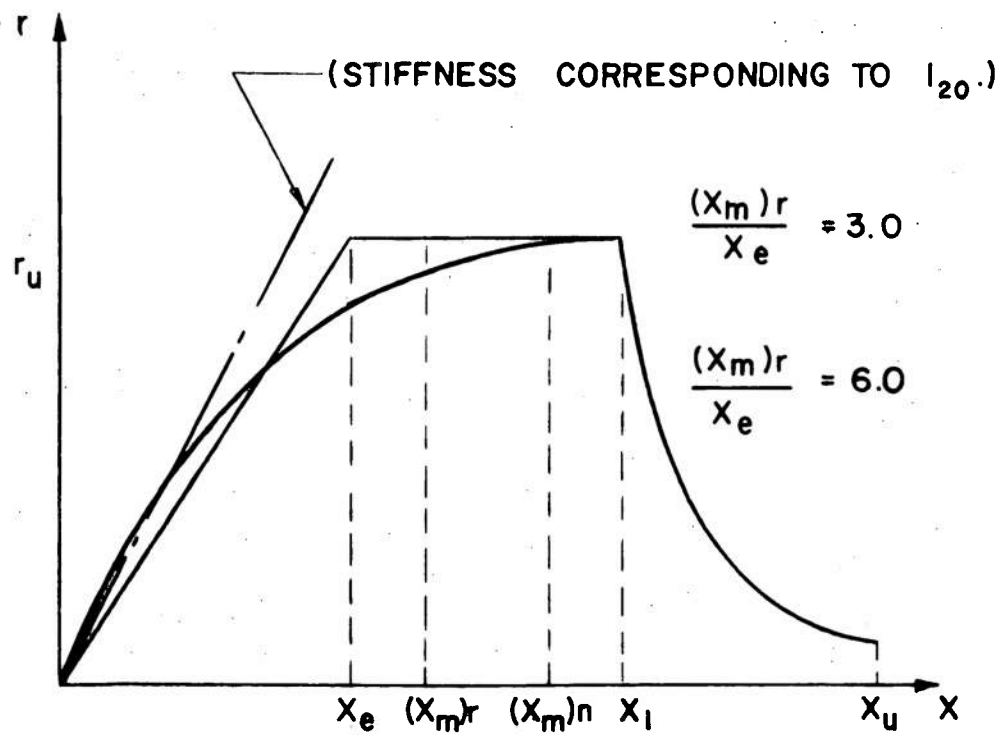
Figure A.3. Bilinear approximation of resistance deflection curve for closed sections
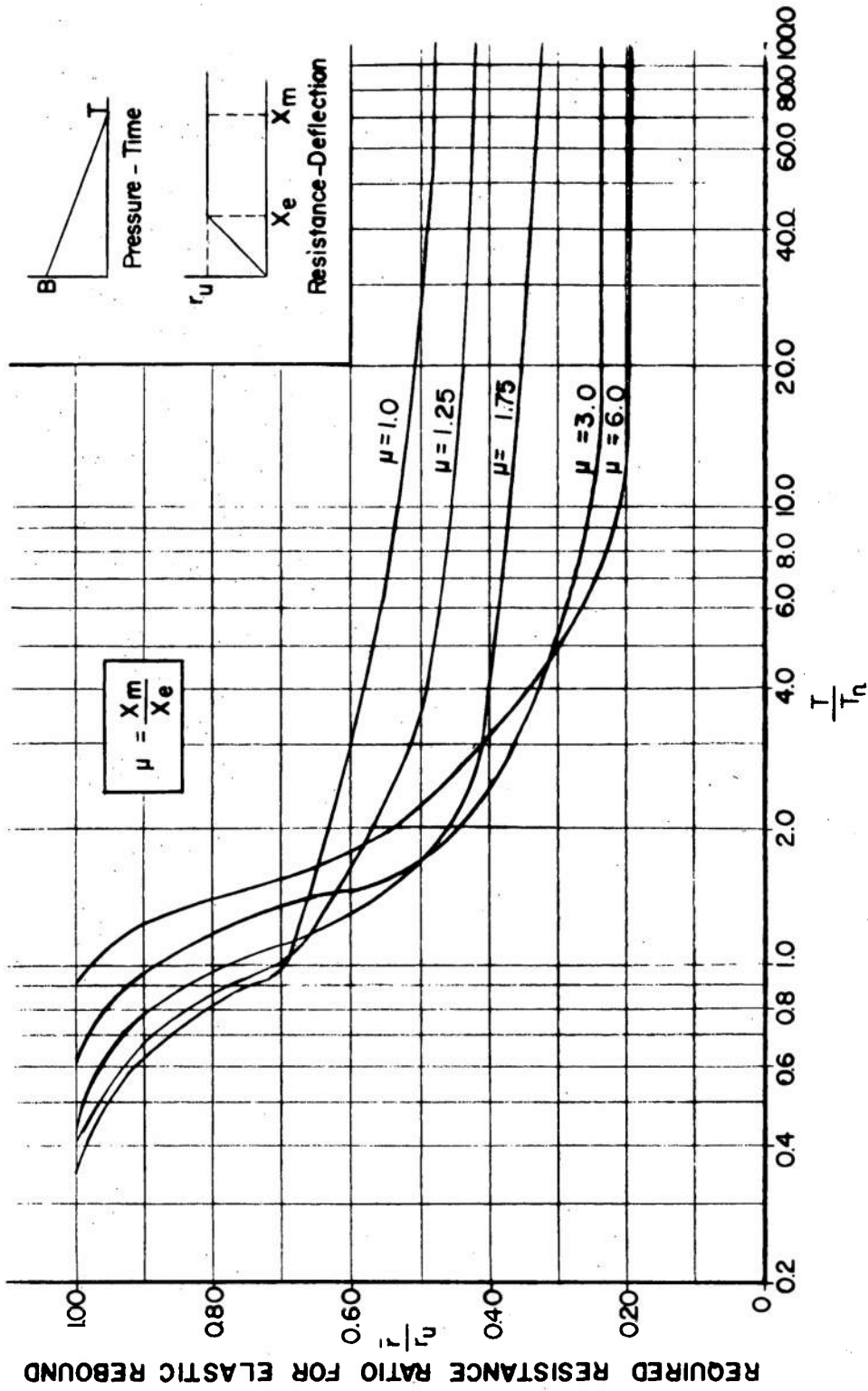
Figure A.4. Elastic rebound of single-degree-of-freedom system

83
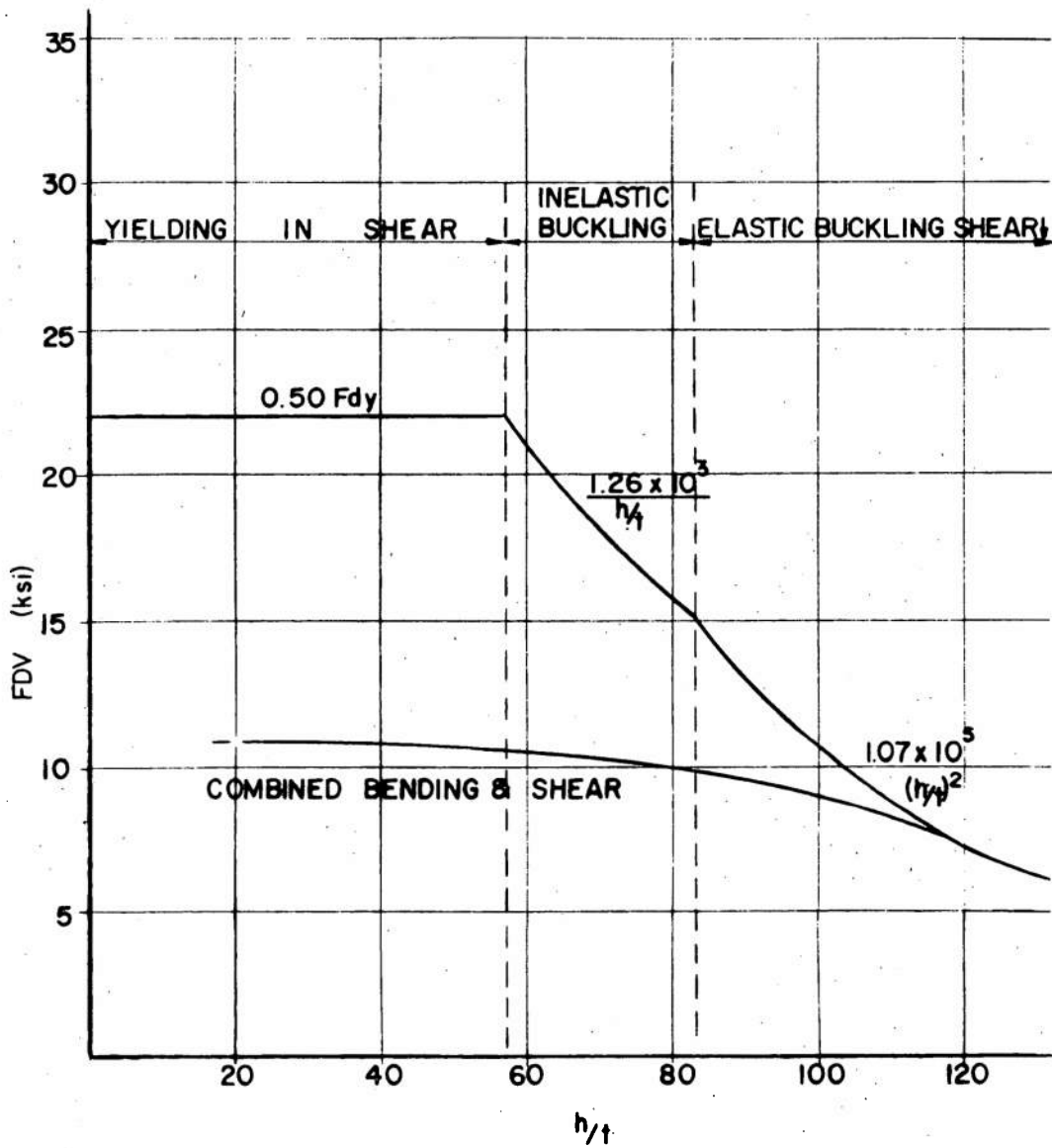
Figure A.5. Allowable dynamic (design) shear stresses
for webs of cold-formed members(F_y=40 ksi)
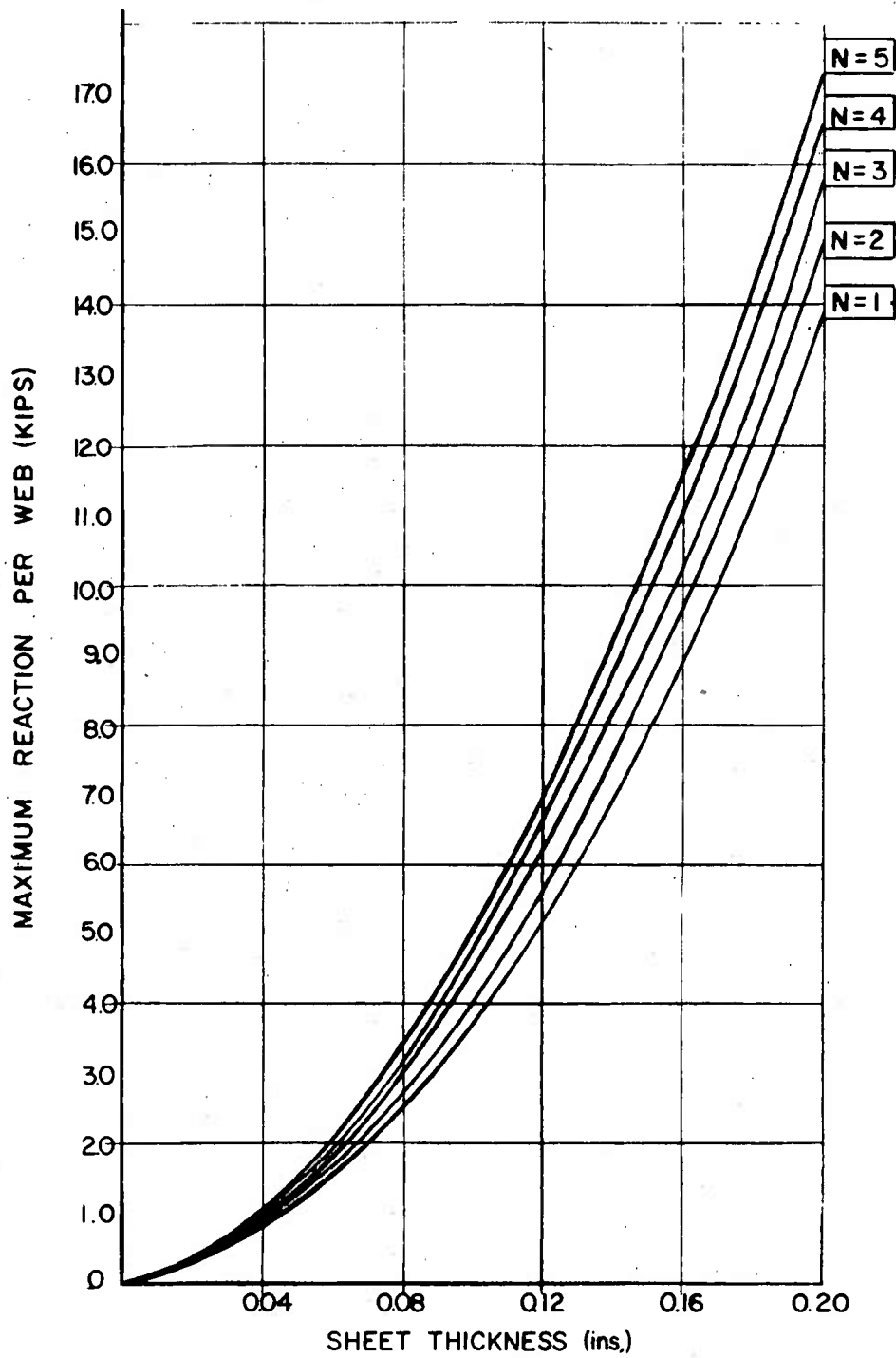
Figure A.6. Maximum end support reaction for cold-formed steel sections (F_y= 40 ksi)
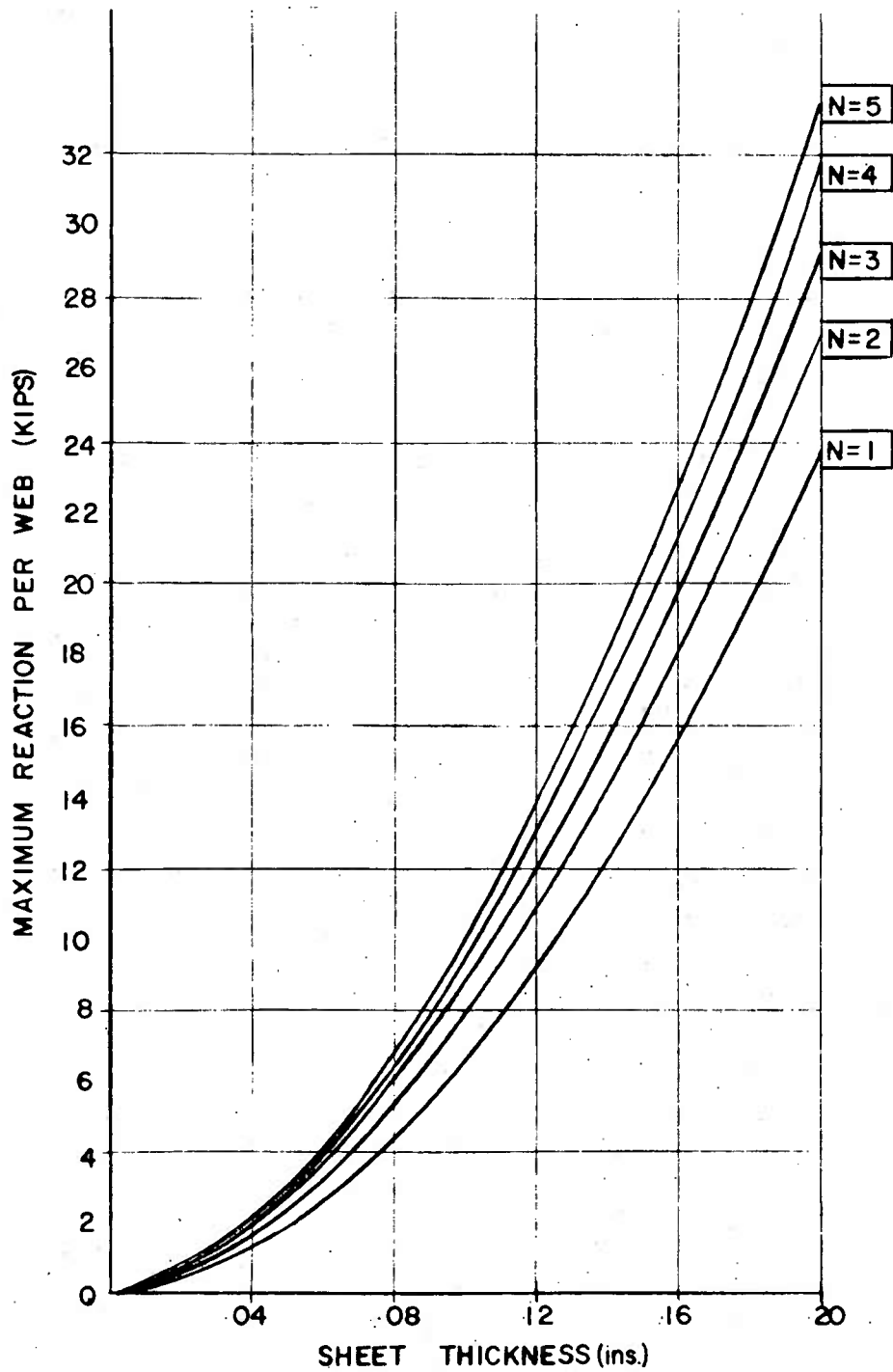
Figure A.7. Maximum interior support reaction for cold-formed steel sections (F_y= 40 ksi)
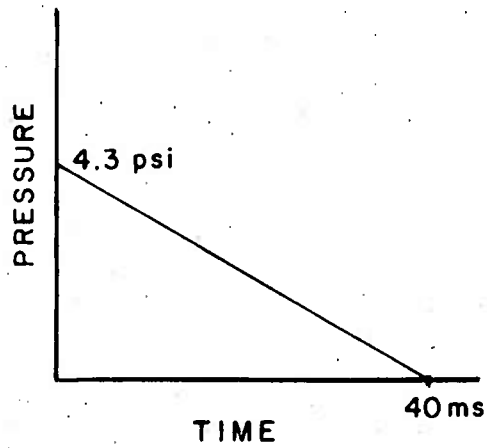
a) PRESSURE LOADING
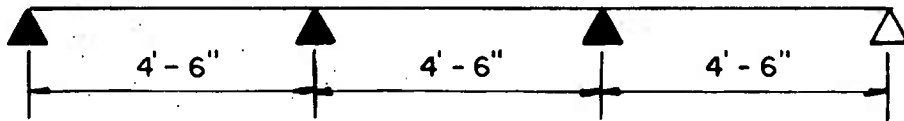
b) ROOF DECKING CONFIGURATION

Figure A.8. Pressure loading and roof decking configuration

Example:

Design of Cold-Formed, Light Gage Steel Panels Subjected to Pressure-Time Loading.

Problem: Design a roof deck as a flexural member which responds to pressure-time transverse loading.

Step 1   Establish the design parameters.

(a)   Pressure-time loading.

(b)   Design criteria (u_{max} and θ_{max} for either a reusable or non-reusable cold-formed panel).

(c)   Span length and support conditions.

(d)   Mechanical properties of steel.

Step 2   Determine an equivalent uniformly distributed static load for a 1-ft width of panel, using the following preliminary dynamic load factors.

	Reusable	Non-Reusable
DLF	1.65	1.40

These load factors are based on an average value of $T/T_N = 10.0$ and the design ductility ratios recommended in equation 3.27. They are derived using figure 6-7 of TM 5-1300.

Equivalent static load w = DLF x p x b

b = 1 ft.

Step 3   Using the equivalent load derived in step 2, determine the ultimate moment capacity (assume positive and negative are the same).

(Section 3.7.2)

Step 4   Determine required section moduli using equation A.2 or A.3.

Select a panel.

88

Step 5   Determine actual section properties of the panel:

              S^+, S^-, I, m = w/g (for 1-ft width of a panel).

Step 6   Compute r_u, the maximum unit resistance per 1-ft width of panel using equation A.4 or A.5.

Step 7   Determine the equivalent elastic stiffness, $K_E = r_u L/X_E$, using equation 3.26.

Step 8   Compute the natural period of vibration.

              $T_N = 2\pi\sqrt{0.74\ mL/K_E}$ (Equation A.9)

Step 9   Calculate B/r_u and T/T_N. Enter figure 6-7 of TM 5-1300 with the ratios B/r_u and T/T_N to establish the actual ductility ratio μ.

              Compare μ with the criteria of section 2.3.3 of reference 2. If μ is larger than the criteria value, repeat steps 4 to 9.

Step 10   Compute the equivalent elastic deflection X_E using $X_E = r_u L/K_E$.

              Evaluate the maximum deflection, $X_m = X_E$.

              Determine maximum panel end rotation.

                    $\tan \theta = X_m/(L/2)$

              Compare θ with the criteria of section 2.3.3 (ref. 2). If θ is larger than specified in the criteria, select another panel and repeat steps 5 to 10.

Step 11   Check resistance in rebound using chart in Figure A.4.

Step 12   Check panel for maximum resistance in shear by applying the criteria relative to:

              (a) Simple shear, table A.1(a), A.2(a) and A.3(a).

              (b) Combined bending and shear, table A.1(b), A.2(b) and A.3(b).

(c) Web crippling, figures A.6 and A.7.

If the panel is inadequate in shear, select a new member and repeat steps 4 to 12.

Solution:

Step 1   Given:

(a) Pressure-time loading [figure A.8(a)].

(b) Criteria:

maximum ductility ratio, μ_{max} = 3.0

maximum rotation θ_{max} = 2.0

(c) Structural configuration [figure A.8(b)].

(d) Steel A 446, grade a, E = 30 x 10^6 psi

$$F_y = 40,000 \text{ psi}$$

$$c = 1.1$$

Step 2   Determine the equivalent static load.

DLF = 1.65 (reusable)

W = DLF x p x b

= 1.65 x 4.30 x 12 x 12 = 1,021.7 lb/ft.

Step 3   Determine required ultimate moment capacities.

$M_{up} = M_{un} = wL^2/12$

= 1,021.7/12 x $(4.5)^2$ = 1,724.1 lb-ft

(Equation A.5)

Step 4   Determine required section moduli.

F_{dy} = 1.1 x 40,000 = 44,000 psi   (Equation A.1)

$S^+ = S^-$ = (1,724.1 x 12)/44,000 = 0.47 in^3

(Select a UKX 18-18, 1-1/2 inches deep)

90

Step 5   Determine actual section properties.

From manufacturer's guide:

$$S^+ = 0.472 \text{ in}^3$$

$$S^- = 0.591 \text{ in}^3$$

$$I = 0.566 \text{ in}^4$$

$$W = 4.8 \text{ psf}$$

Step 6   Compute maximum unit resistance r_u.

$$M_{up} = (44,000 \times 0.472)/12 = 1,730 \text{ lb-ft}$$
(Equation A.2)

$$M_{un} = (44,000 \times 0.591)/12 = 2,167.0 \text{ lb-ft}$$
(Equation A.3)

$$r_u = 4/L^2(2M_{up} + M_{un})$$

$$= (4.5)^2(2 \times 1,730.67 + 2,167.0)$$

$$= 1,111.8 \text{ lb/ft} \qquad \text{(Equation A.5)}$$

Step 7   Determine equivalent static stiffness.

$$K_E r_u L/X_E = (EI r_u L)$$

$$= 0.0062 r_u L^4 \qquad \text{(Equation A.6)}$$

$$= EI/0.0062L^3$$

$$= (30 \times 10^6 \times 0.566)/[0.0062 \times$$

$$(4.5)^3 \times 144] = 208,711.3 \text{ lb/ft.}$$

Step 8   Compute the natural period of vibration for the 1-ft width of panel.

$$mL = w/g = (4.8 \times 10^6 \times 4.5)/32.2$$

$$= 0.67 \times 10^6 \text{ lb-ms}^2/\text{ft.}$$

$$T_N = 2\pi\sqrt{(0.74 \times 0.67 \times 10^6)/208,711.3}$$

$$= 9.68 \text{ msec.}$$

91

Step 9   Calculate B/r_u and T/T_N

$$B = p \times b$$

$$= 4.3 \times 12 \times 12 = 619.2 \text{ lb/ft}$$

$$B/r_u = 619.2/1,111.8 = 0.56$$

$$T/T_N = 40/9.68 = 4.13$$

Entering figure 6-7 in TM 5-1300 with these values

$$= 1.15 < 3.0 \qquad \text{OK}$$

Step 10   Check maximum deflection and rotation.

$$X_E = r_uL/K_E = 1,111.8 \times 4.5/208,711.3$$

$$= 0.024 \text{ ft}$$

$$X_M = X_E = 1.15 \times 0.024 = 0.028 \text{ ft}$$

$$\tan \quad = X_M/(L/2) = 0.028/2.25 = 0.012$$

$$= 0.70^{\circ} < 2.0^{\circ} \qquad \text{OK}$$

Step 11   Check resistance in rebound.

From chart, figure A.4 arequired $\bar{r}/r_u = 0.33$

Available maximum elastic resistance in rebound:

$$(\bar{r}/r_u)_{\text{actual}} = 0.472/0.591 = 0.799 > 0.33 \qquad \text{OK}$$

Step 12   Check resistance in shear.

Interior support (combined shear and bending.

Determine dynamic shear capacity of a 1-ft width of panel:

$$h = (1.500 - 2t) \text{ inches, } t = 0.043 \text{ inch}$$

$$= 1.500 - 0.086 = 1.414 \text{ inches}$$

92

$h/t = 1.414/0.043 = 33 = 30$

$F_{dv} = 10.84$ ksi   (Table 3.4)

Total web area for 1-ft width of panel:

$(8 \times h \times t)/2 = 4 \times 1.414 \times 0.043 = 0.243$ in^2

$V_u = 0.243 \times 10.84 = 2.636$ k = 2,636 lb.

Determine maximum dynamic shear force:

The maximum shear at an interior support of a continuous panel using limit design is:

$V_{max} = 0.55\ r_u L$

$= 0.55 \times 1,111.8 \times 4.5 = 2,751$ lb

$= 2,751.7$ lb $>$ 2,636 lb.   Not Good

Go back to step 4 and choose another section.
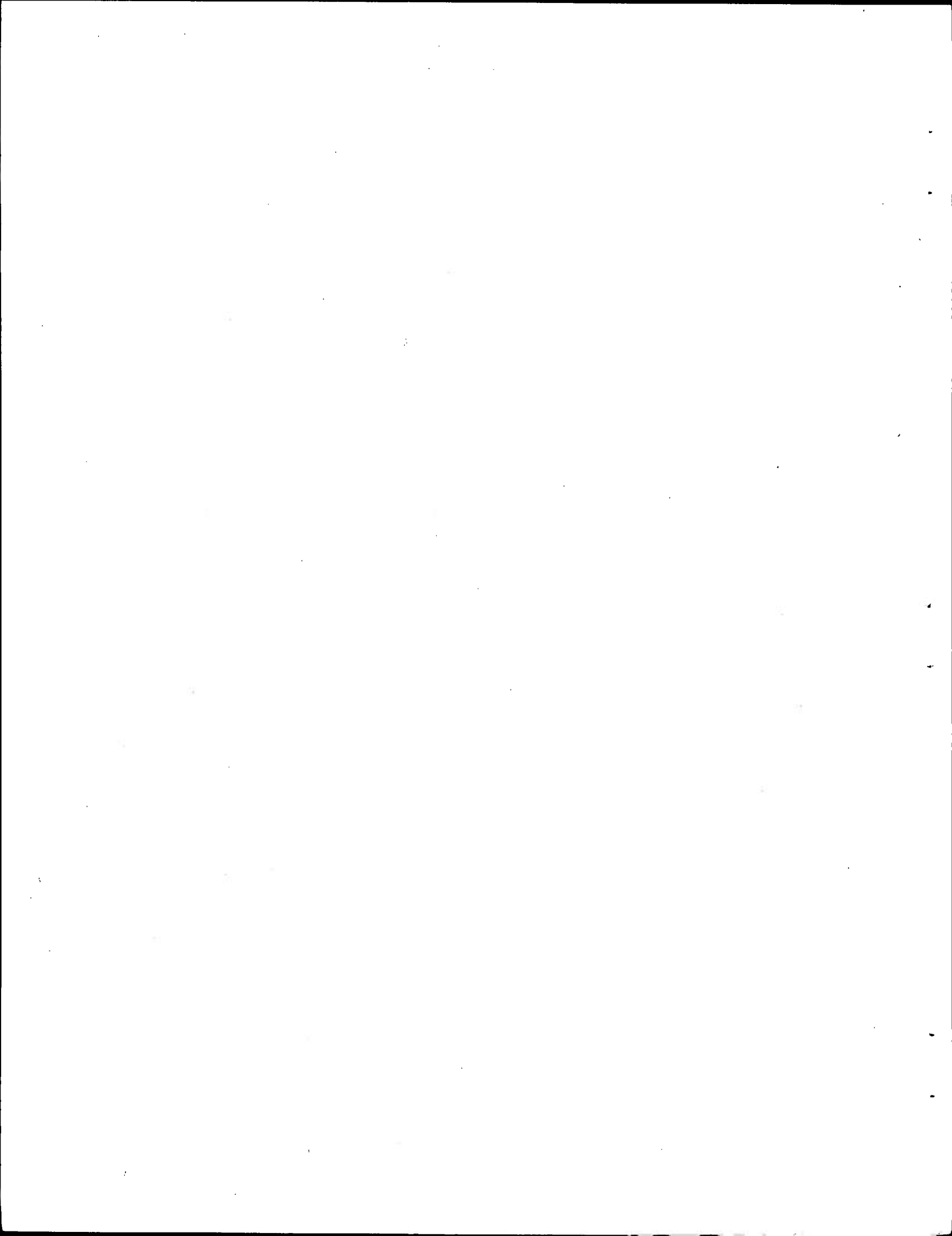
APPENDIX B

ENGINEERING DRAWINGS

TEST STRUCTURE A

TEST SHOT			WINDOW POSITIONS						STEEL DECK @ ROOF				
NO.	CHARGE WEIGHT	PSI	1 SW	2 SW	3 LW	4 LW	5 SW	REMARKS	PANEL SIZE	CONNECTION TYPE	SIZE	DETAIL	REMARKS
1	2,000'	0.5	RS2	RS3	RL2	RL3	RS3	EST. CAPACITY BASED ON STATIC TESTS FOR ½"	4' RIBBED 24 GA.	S	#14	SK10	CYCLOPS PANEL AT 80% ULT. DYN. CAP.
2	2,000'	0.7-1.0	RS2	RS3	RL2	RL3	RS3		4' RIBBED 24 GA.	S	#14	SK10	POSSIBLE FAILURE
3	2,000'	1.0	RS2	RS3	RL2	RL3	RS3		S-22	W	¾"	SK8	REUSABLE
4	2,000'	1.0	FDS2	—	—	—	—		S-22	W	¾"	SK8	SAME DECK AS TEST 3
5	2,000'	1.0	—	—	—	—	—		S-22	S	#14	SK7	SCREW CONNECTION TEST (REBOUND)
6	2,000'							PENDING RESULTS OF PREVIOUS TESTS					PENDING RESULTS OF PREVIOUS TESTS

LEGEND

SW - SMALL WINDOW
LW - LARGE WINDOW
RS2 - REGULAR ⅜" THICK, SMALL WINDOW
RS3 - REGULAR ½" THICK, SMALL WINDOW
RL2 - REGULAR ⅜" THICK, LARGE WINDOW
RL3 - REGULAR ½" THICK, LARGE WINDOW
FDS2 - FRAMED DURASAFE ⅜" THICK, SMALL WINDOW
FFDS2 - FIXED FRAME DURASAFE ⅜" THICK, SMALL WINDOW
S - SELF TAPPING SCREWS
W - PUDDLE WELD
NS - THREADED NELSON STUD

NOTES:
1. SEE SHEET 2 FOR STEEL DECK CONNECTION DETAILS.
2. SEE SHEET 3 FOR FRAMED WINDOW DETAILS.
3. SEE DWG. 123 SHEET 3 FOR DETAILS OF REGULAR GLASS WOOD FRAMES.

TEST STRUCTURE B

TEST SHOT			WINDOW POSITIONS					STEEL DECK @ FRONT FACE					STEEL DECK @ ROOF				
NO.	CHARGE WEIGHT	PSI	1 SW	2 SW	3 LW	4 LW	REMARKS	PANEL SIZE	CONNECTION TYPE	SIZE	DETAIL	REMARKS	PANEL SIZE	CONNECTION TYPE	SIZE	DETAIL	REMARKS
1	2,000'	2.0	FDS2	—	—	—		UKX 18-18	W	¾"	SK4	REUSABLE	UKX 20-20	W	¾"	SK4	REUSABLE
2	2,000'	2.0	—	—	—	—		UKX 18-18	W	¾"	SK4	SAME DECK AS TEST 1	UKX 20-20	W	¾"	SK4	SAME DECK AS TEST 1
3	2,000'	2.0	FFDS2	—	—	—		UKX 18-18	W	¾"	SK4	POSSIBLE FAILURE	S-18	W	¾"	SK6	NON-REUSABLE
4	2,000'	2.0	—	—	—	—		S-18	W	1¾"	SK6	POSSIBLE FAILURE	S-20	S	#14	SK7	SCREW CONNECTION TEST (SHEAR)
5	2,000'	2.0-4.0	FFDS2	—	—	—						PENDING RESULTS OF PREVIOUS TESTS	UKX 18-18	W	½"	SK4	WELDED CONNECTION TEST
6	2,000'						PENDING RESULTS OF PREVIOUS TESTS					PENDING RESULTS OF PREVIOUS TESTS					PENDING RESULTS OF PREVIOUS TESTS

TEST STRUCTURE C / TEST STRUCTURE D

TEST SHOT		TEST STRUCTURE C STEEL DECK					TEST STRUCTURE D STEEL DECK					
NO.	CHARGE WEIGHT	PSI	PANEL SIZE	TYPE	SIZE	DETAIL	REMARKS	PSI	PANEL SIZE	TYPE	SIZE	DETAIL	REMARKS
1	2,000'	3.0	UKX 20-20	W	¾"	SK4	POSSIBLE FAILURE	4.0	UKX 20-20	W	1"	SK3	REUSABLE
2	2,000'	3.5	UKX 18-18	NS	⅞"	SK3	REUSABLE BOLTED CONNECTION TEST	4.0	UKX 20-20	W	1"	SK3	SAME DECK AS TEST 1
3	2,000'	5.0	UKX 18-18	NS	⅞"	SK3	SAME DECK AS TEST 2	5.0	UKX 20-20	W	1½"	SK3	NON-REUSABLE
4	2,000'	7.0	UKX 14-14	NS	½"	SK3	NON-REUSABLE	5.0	UKX 18-18	NS	⅞"	SK3	REUSABLE BOLTED CONNECTION TEST
5	2,000'	7.0	UKX 18-18	W	1"	SK4	PROBABLE FAILURE	7.0	UKX 18-18	NS	½"	SK3	NON-REUSABLE
6	2,000'						PENDING RESULTS OF PREVIOUS TESTS						PENDING RESULTS OF PREVIOUS TESTS

97

- SKETCH NO. 1 — DECK SPLICE & SUPPORT PLATE DETAILS FOR ROOF & PLATFORM DECKS
- SKETCH NO. 2 — DECK SPLICE & SUPPORT PLATE DETAILS FOR FRONT WALL DECKS
- SKETCH NO. 3 — SUPPORT PLATE CONNECTION DETAILS
- SKETCH NO. 4 — WELDED CONNECTION DETAIL FOR UKX DECKS
- SKETCH NO. 5 — WELDED CONNECTION DETAIL FOR NKX DECKS (TYPE II)
- SKETCH NO. 6 — WELDED CONNECTION DETAIL FOR TYPE 3 DECKS
- SKETCH NO. 7 — SCREW CONNECTION DETAIL FOR TYPE 3 DECKS
- SKETCH NO. 8 — WELDED CONNECTION DETAIL FOR NKX DECKS (TYPE II)
- SKETCH NO. 9 — BOLTED CONNECTION DETAIL FOR UKX & NKX DECKS
- SKETCH NO. 10 — SCREW CONNECTION DETAIL FOR 4" RIBBED DECKS
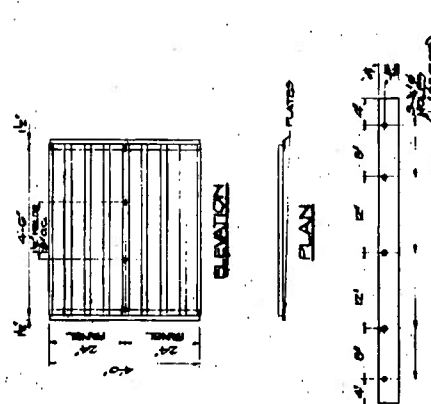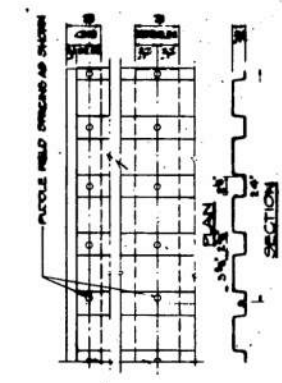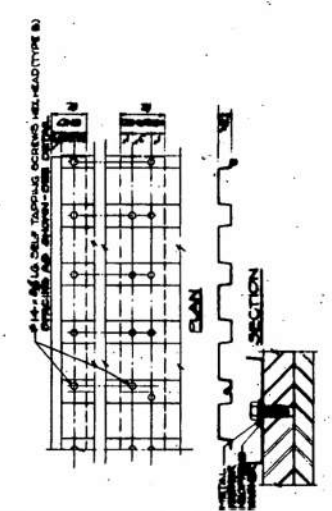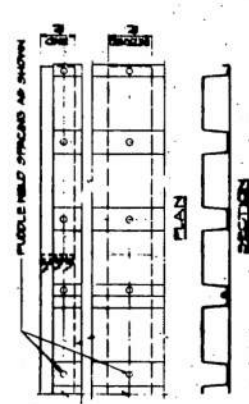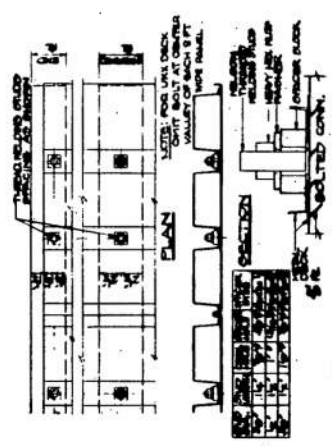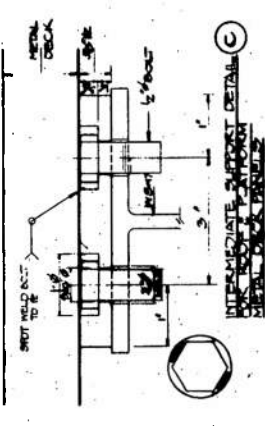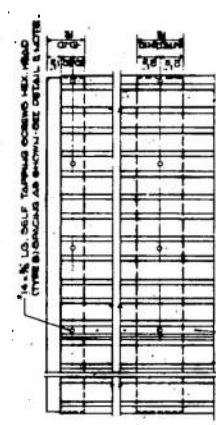
Title block:
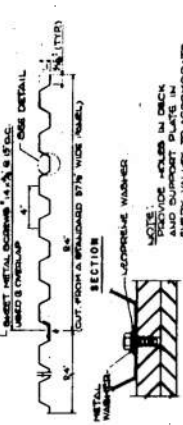
PICATINNY ARSENAL
DOVER, NEW JERSEY

AMMANN & WHITNEY
CONSULTING ENGINEERS
NEW YORK, N.Y.

METAL DECK ATTACHMENT DETAILS

END WALL PLYWOOD LAYOUT
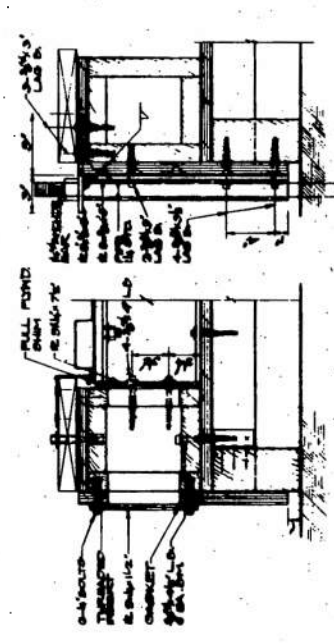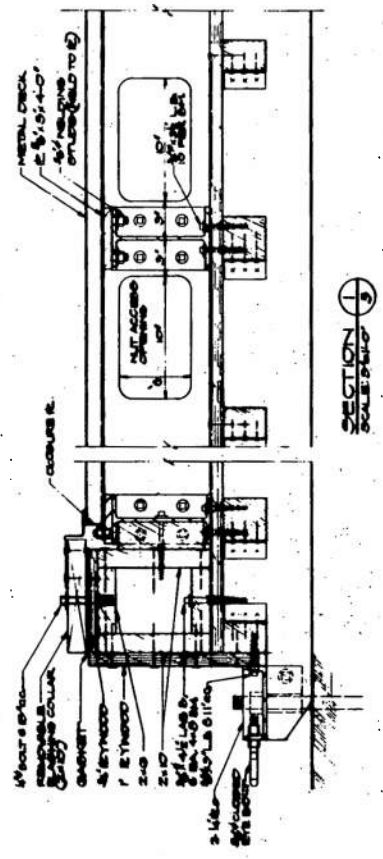WITH GLAZED PANEL

END WALL PLYWOOD LAYOUT
WITHOUT PANEL

FRONT FACE PLYWOOD LAYOUT

ROOF PLYWOOD LAYOUT

BACK PLYWOOD LAYOUT

103

METAL DECK ARRANGEMENT

SAND BAG ARRANGEMENT

PLAN

BASE FRAMING PLAN

Commander
U.S. Army Armament Research and
   Development Command
ATTN: DRDAR-CG
          DRDAR-LCM-M
          DRDR-LCM-SP   (25)
          DRDAR-SF
          DRDAR-TSS   (5)
          DRDAR-GCL
Dover, NJ   07801

Chairman
Department of Defense Explosive
   Safety Board   (2)
Hoffman Building, No. 1, Room 856C
2461 Eisenhower Avenue
Alexandria, VA   22331

Administrator
Defense Documentation Center
ATTN: Accessions Division   (12)
Cameron Station
Alexandria, VA   22314

Commander
Department of the Army
Office, Chief Research Development
   and Acquisition
ATTN: DAMA-CSM-P
Washington, DC   20310

Office, Chief of Engineers
ATTN: DAEN-MCZ
Washington, DC 20314

Commander
U.S. Army Materiel Development and
   Readiness Command
ATTN: DRCSF
          DRCDE
          DRCRP
          DRCIS
5001 Eisenhower Avenue
Alexandria, VA   22333

Commander
DARCOM Installations and Services Agency
ATTN: DRCIS-RI
Rock Island, IL 61299

Director
Industrial Base Engineering Activity
ATTN: DRXIB-MT
       DRXIB-EN
Rock Island, IL 61299

Commander
U.S. Army Munitions Production Base
  Modernization Agency
ATTN: SARPM-PBM
       SARPM-PBM-S
       SARPM-PBM-L   (2)
       SARPM-PBM-E
Dover, NJ 07801

Commander
U.S. Army Armament Materiel
  Readiness Command
ATTN: DRSAR-SF
       DRSAR-SC   (3)
       DRSAR-EN
       DRSAR-PPI
       DRSAR-PPI-C
       DRSAR-RD
       DRSAR-IS
       DRSAR-ASF
       DRSAR-LEP-L
Rock Island, IL 61299

Director
DARCOM Field Safety Activity
ATTN: DRXOS-ES
Charlestown, IN 47111

Commander
U.S. Army Engineer Division
ATTN: HNDED
P.O. Box 1600, West Station
Huntsville, AL 35809

Commander
Radford Army Ammuntion Plant
Radford, VA 24141

Commander
Badger Army Ammunition Plant
Baraboo, WI 53913

Commander
Indiana Army Ammunition Plant
Charlestown, IN 47111

Commander
Holston Army Ammunition Plant
Kingsport, TN 37660

Commander
Lone Star Army Ammunition Plant
Texarkana, TX 75501

Commander
Milan Army Ammunition Plant
Milan, TN 38358

Commander
Iowa Army Ammunition Plant
Middletown, IA 52638

Commander
Joliet Army Ammunition Plant
Joliet, IL 60436

Commander
Longhorn Army Ammunition Plant
Marshall, TX 75670

Commander
Louisiana Army Ammunition Plant
Shreveport, LA 71130

Commander
Cornhusker Army Ammunition Plant
Grand Island, NE 68801

Commander
Ravenna Army Ammunition Plant
Ravenna, OH 44266

Commander
Newport Army Ammunition Plant
Newport, IN 47966

Commander
Volunteer Army Ammunition Plant
Chattanooga, TN 37401

Commander
Kansas Army Ammunition Plant
Parsons, KS 67357

District Engineer
U.S. Army Engineering District, Mobile
Corps of Engineers
P.O. Box 2288
Mobile, AL 36628

District Engineer
U.S. Army Engineer District, Ft Worth
Corps of Engineers
P.O. Box 17300
Fort Worth, TX 76102

District Engineer
U.S. Army Engineering District, Omaha
Corps of Engineers
6014 U.S.P.O. and Courthouse
215 North 17th Street
Omaha, NE 78102

District Engineer
U.S. Army Engineering District, Baltimore
Corps of Engineers
P.O. Box 1715
Baltimore, MD 21203

District Engineer
U.S. Army Engineering District, Norfolk
Corps of Engineers
803 Front Street
Norfolk, VA 23510

Division Engineer
U.S. Army Engineering District, Huntsville
P.O. Box 1600, West Station
Huntsville, AL 35807

Commander
Naval Ordnance Station
Indian Head, MD 20640

Commander
U.S. Army Construction Engineering
    Research Laboratory
Champaign, IL 61820

Commander
Dugway Proving Ground
Dugway, UT 84022

Commander
Savanna Army Depot
Savanna, IL 61704

Civil Engineering Laboratory
Naval Construction Battalion Center
ATTN: L51
Port Hueneme, CA 93043

Commander
Naval Facilities Engineering Command
200 Stovall Street
(Code 04, J. Tyrell)
Alexandria, VA 22322

Commander
Southern Division
Naval Facilities Engineering Command
ATTN: J. Watts
P.O. Box 10068
Charleston, SC 29411

Commander
Western Division
Naval Facilities Engineering Command
ATTN: W. Moore
San Bruno, CA 94066

Officer in Charge
TRIDENT
Washington, DC 20362

Officer in Charge of Construction
TRIDENT
Bangor, WA 98348

Commander
Atlantic Division
Naval Facilities Engineering Command
Norfolk, VA 23511

Commander
Naval Ammunition Depot
Naval Ammunition Production
  Engineering Center
Crane, IN 47522

Director
U.S. Army TRADOC Systems
  Analysis Activity
ATTN: ATAA-SL
White Sands Missile Range, NM 88002

Commander/Director
Chemical Systems Laboratory
U.S. Army Armament Research and
  Development Command
ATTN: DRDAR-CLJ-L
       DRDAR-CLB-PA
Aberdeen Proving Ground, MD 21005

Director
Ballistics Research Laboratory
U.S. Army Armament Research and
  Development Command
ATTN: DRDAR-TSB-S
Aberdeen Proving Ground, MD 21005

Chief
Benet Weapons Laboratory, LCWSL
U.S. Army Armament Research and
  Development Command
ATTN: DRDAR-LCB-TL
Watervliet, NY 12189

Ammann & Whitney
Consulting Engineers
Two World Trade Center
ATTN: N. Dobbs   (5)
New York, NY 10048